

Accelerated Expansion a Fallacy

Gerd Pommerenke*

Retired/Independent Researcher, Germany

*Corresponding Author

Gerd Pommerenke, Retired/Independent Researcher, Germany

Submitted: 2024, Jul 01; Accepted: 2024, Aug 02; Published: 2024, Aug 09

Citation: Pommerenke, G. (2024). Accelerated Expansion a Fallacy. *Adv Theo Comp Phy*, 7(3), 01-62.

Abstract

Due to discrepancies in the SN-Ia-cosmology-project, at the time an increasing expansion was postulated instead of the previously assumed decreasing expansion. At the beginning of this work it is stated that this is a fallacy resulting from mutually contradictory premises, mainly geometric damping with and EM wave propagation without expansion. It is shown that the prevalent propagation function applies locally only, since MAXWELL's equations neither take into account, imply nor condition the expansion of the universe. In succession, an alternative propagation function with expansion is developed, which behaves like the classic MAXWELL solution in the first approximation for $z \leq 0.1$. This repeats the positive comparison I made earlier with the observational data of the SN-Ia-cosmology-project supplementing it by the latest high- z data $z \geq 0.9$, at which point the MLE model is confirmed for this area too. Applying this model consistently, an additional evaluation $mb(r)$ is carried out. A new, unexpected deviation emerges at $r \geq 0.1R$. The observational data there is darker than calculated. The reason is the HUBBLE parameter, which depends on time and distance. Route sections that are further away expand faster than those that are closer. The greater the distance, the greater the value of H and the expansion speed $v = Hr$. With the help of a correction factor m from [29], a function $m_b(r)$ is set up that correctly traces the deviating distribution. This is proof that the expansion rate decreases over time and does not increase.

Keywords: Cosmology, Big Bang Cosmology, Physics, Astronomy, Radio Astronomy, Wave Propagation, Expansion, Statistics, Red-shift, HUBBLE-Parameter

1. Fundamentals

At the beginning of the last century, the world of astronomy was still in order. Only one galaxy was known and the distances to most of the stars in it could be determined by parallax measurements and possibly extended measurements based on them. Then it was discovered that, along with our galaxy, there is a huge number of other galaxies as well as galaxy groups, clusters and superclusters. Determining the distance to these much larger structures or parts thereof using the hitherto existing methods proved to be almost impossible, but was of general interest.

Fortunately, Georges LEMAÎTRE and Edwin HUBBLE discovered the law named after latter, which states that the further away galaxies, the faster they move from us [$v = H_0 r$]. Furthermore, the velocity-dependent frequency shift z of the metallic absorption lines in the spectrum of stars was discovered.

Thus, it would have been so easy to use z to determine the distance to the respective objects. The problem with it is that we don't know the exact value of H_0 respectively, that there was and is a huge number of various values – depending on the model used. Therefore, in order to calibrate the z -method, we need an alternative method to the determination of the distance.

Since starlight is an electromagnetic phenomenon, it was assumed that it propagates in a vacuum according to MAXWELL's equations. What is important here is the so-called geometric damping. If we know the »transmission« power, the luminosity L [W] of the celestial body, we may calculate the Poynting vector [Wm^{-2}] or the astronomical equivalent, the flux F and the associated magnitude class m_b (apparent bolometric brightness) in that we divide it by the spherical surface $4\pi r^2$. This is the value that the astronomer determines. The problem now, is that we don't know the exact value L , or rather that it varies even more than H_0 , depending on the type and size of the celestial body. Therefore, we need a certain type of celestial body which can be easily identified, i.e. differentiated from others which has a defined luminosity L (standard candle). Such objects really exist. These are the so-called supernovae (SN) of type Ia [74].

These are multiple stars in which a certain type, the explosion candidate, pulls matter away from a companion. Thus increases its mass until a critical value is reached. Then the candidate explodes as SN-Ia. The process is already very well described by today's model, so that the maximum luminosity L_{Ia} is known. Since there is a statistical spread of values on hand, we need a series of observations to determine the average. A comparison with the distances determined by z leads to the correct value of H_0 and the world radius R then. Now we are able to create a 3D map of the galaxy distribution in the universe using only the z -values, because not all celestial bodies are SN-Ia and are just in the act of exploding.

For this purpose, the Supernova Ia cosmology project has been initiated since 1988 [45], [72]. From 1994 on, the High- z Supernova Search Team [73] added more observational data. The aim of the investigations [45] was to determine the HUBBLE parameter and, of course, which of the hitherto established world models comes closest to reality. However, the investigation has caused more confusion than it has produced any reasonable results, as we will see.

Comparing the observed (maximum) brightness m_b with the respective value m_z calculated from L_{Ia} on the basis of z , it turned out that the measured brightness is slightly smaller, i.e. the SN is darker than calculated. The deviation is visible from circa $z=0.1$ on increasing more and more over and above. Therefore, the objects were guessed to be further away than assumed, possibly leading to a greater geometric attenuation. As reason one guessed now, that an increasing expansion ($H_0 \sim T^{n>1}$) should exist instead of the previously assumed decreasing ($H_0 \sim T^{-1}$) one. And because thereof further contradictions arise, the whole issue even comes along in a package with fine-tuning, dark energy, dark matter and – oh yes – inflation.

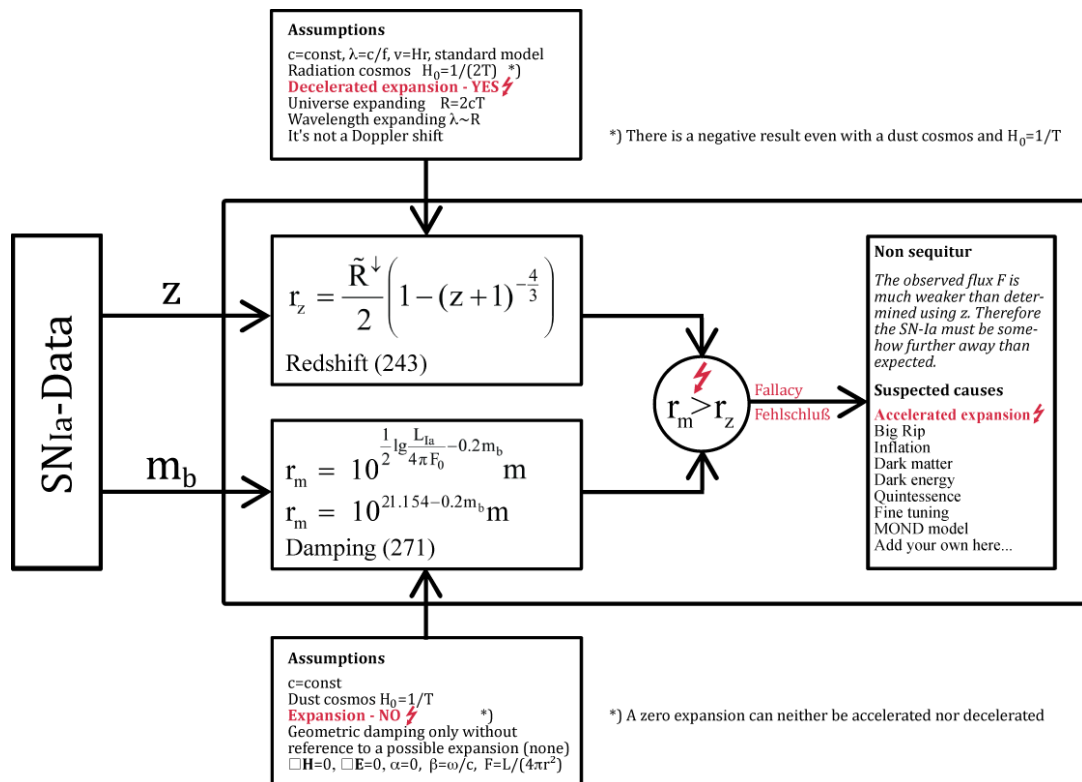


Figure 1:
 Contradictions in Data Analysis of the Supernova Ia Cosmology Project

I depicted the whole thing as a diagram in Figure 1, however as a comparison of the two distances r_z and r_m , what's the same in my view. In principle we are concerned with a kind of proof experiment that has failed. But what could be the cause of the failure? The data itself can be regarded as correct with a clear conscience. The determination of z and m_b is not rocket science, even with the means of 1988. The actual reason is a so-called **informal fallacy**.

In [69] it's stated: Informal fallacies are, as the name suggests, wrong without any formal reason. Your premises are not correct. The derivation itself can be formally correct, but if one of the premises is factually incorrect, the argument will not fit either.

Example *All philosophers find Plato's allegory of the cave convincing.
 Jacques Derrida is a philosopher.
 As a result, he finds Plato's allegory of the cave convincing.*

Formally speaking there is nothing wrong with the argument. The error lies in the first premise, which is factually incorrect. With it, the whole argument lapses.

It looks similar when premises contradict each other. I made the effort to illustrate the premises used as well as the suspected causes in Figure 1. As it can be seen, all the blame is being projected on expansion only. Something can't

be right if the supernovæ are further away than calculated, so \rightarrow *Accelerated expansion*. At the same time however, you can see that we are dealing with two contradictory premises here. Once decreasing expansion at z , the other time no expansion, stationary state at m_b or no matter whether yes or no. On the other hand, it's yet somewhat surprising that there is no increased geometric damping, since the sphere of the wave front is expanding at the same time too. And the surrogate justification *Accelerated expansion* always contradicts one of the premises or the comparison, and is therefore nonsense.

According to [70], the principle “**Ex falso quodlibet** applies, rather *ex falso sequitur quodlibet* (Lat. ‘anything follows from what is wrong’), shortened to ‘e.f.q.’, more clearly *ex contradictione sequitur quodlibet* (Lat. ‘anything follows from a contradiction’), denotes in the narrower sense one of the two laws valid in many logical systems:

1. From a logically – not just factually – incorrect sentence follows each arbitrary statement.
2. From two contradictory sentences follows each arbitrary statement.

[...] According to the ‘ex falso quodlibet’, any statement follows from a contradictory theory. With it however, the theory becomes pointless. A theory from which everything follows cannot be used to make distinctions, cannot give us answers to our questions, and cannot help us make our decisions. Thus, the ‘ex falso quodlibet’ means that a contradictory set of premises is worthless in practice.

Therefore it astonishes all the more if both, [72] and [73] praise the Supernova Ia cosmology project as evidence of an *accelerated expansion*. PERLMUTTER probably deserved his Nobel Prize for organizing and implementing the actual project, but not for its evaluation. The reason is not the investigation itself, but the lack of a correct world model, such as the one in [29], as well as one or more incorrect premises. At all, the case in which we obtain the correct result using two incorrect premises usually works with incorrect data only.

Therefore, let's return to the increased geometric damping caused by the expansion of the spherical surface of the wave front. So it's about the wave propagation itself, i.e. about the MAXWELL expressions and the propagation function. Because it works so pretty in the lab, it's naturally assumed that it also applies to the wave propagation with distances $z \geq 0.1$. What if not?

Such a length definitely expands. In the expressions $\square \mathbf{H}=0$, $\square \mathbf{E}=0$, $\alpha=0$, $\beta=\omega/c$ and in the propagation function $\mathbf{E}=\mathbf{E}e^{i\omega t-\gamma r}$ no extension at all can be found. Therefore, we should endeavour to find a propagation function with expansion that behaves like MAXWELL's solution on a small scale. Furthermore, this should also explain *cosmological redshift*.

In [71] it says: The expansion of the universe must not be interpreted in such a way, that galaxies in space-time are moving away from each other (relative motion). It is space itself that expands, the galaxies are carried along [correct]. Gravitationally bound objects such as galaxies or galaxy clusters do not expand [wrong]. [...] In contrast, an electromagnetic wave that propagates freely through an expanding space-time the expansion motion is being impressed directly: If space-time increases by a factor η during runtime, it also happens with the wavelength of the light [correct].

This cosmological redshift differs fundamentally from the redshift caused by the Doppler effect, which only depends on the relative speed of the galaxies during emission and absorption. Thus, the escape velocities of distant galaxies derived from cosmological redshift are directly attributable to the expansion of space-time (recession velocity). Already at distances from a few 100 megaparsecs on [$z \geq 0.1$] the share of Doppler effect is negligible.

Furthermore, it follows from the GR that the observed escape velocities do not cause relativistic time effects, as described by the SR for motions in space. A cosmological time dilation still occurs because the photons emitted later by an object have to travel a greater distance due to expansion. Therefore, physical processes with redshifted objects appear to proceed [...] increasingly slowly.

You can see that there is a wide variety of models and opinions and the comments [correct] and [wrong] are not necessarily relevant either, as they refer to the model described below, in which data is used, which is primarily in the local area being accessible by present-day technical means. It are in particular the universal natural constants and their relationships with each other as well as the electron's charge, mass and similar values as well as the known physical laws.

As fundamentals therefore serves a cosmologic model based on a lecture, delivered in German language by Prof. Cornelius LANZOS on the occasion of the EINSTEIN-Symposium 1965 in Berlin. See [1] also in English. It's a model with variable natural constants with expansion. That leads to a reduction of commonly known contradictions, such as those between SR and GR with strong curvature, at the redshift in relation to the expression $\hbar\omega=mc^2$ and much more.

Since some of the variable natural constants also affect the observer, i.e. he is affected by them himself, some of the changes cancel out. A *virtual relativity principle* applies. The laws of nature just *seem* to be the same in all frames of reference.

With the help of the electron mass and charge, the relations to the corresponding PLANCK units may be precisely determined. That makes it possible to calculate all natural constants outside the atomic nucleus as a function of the reference system or space and time to at least 10 decimal places, including the HUBBLE parameter and the CMBR temperature. Especially because of this influence I named the line element appearing in the model the *Metric Line*

Element (MLE). Unlike the MINKOVSKIAN line element, it's about a physical object and not a mathematical abstraction.

In contrast to similar models based on the hydrogen atom, where the ratio F_g/F_e is approximately $1:10^{40}$, this model is based on the PLANCK length with a ratio of 1:1. The theoretical electrotechnics custom notation is used in the work (j instead of i). Deviantly, the letter β is used for the Lorentz factor γ , since it is already heavily overused avoiding confusion with the propagation rate $\gamma = \alpha + j\beta$ definitely.

1. Attention, the PLANCK charge q_0 in this model is defined differently than usual.

The following considerations are particularly aimed at the development of an alternative propagation function for EM waves, as well as its application to the observational data of the Supernova Ia cosmology project. See [29] for further information.

2. Cosmological model

2.1. Specification of the model

In his lecture LANZOS the metrics to be built like a (regular) cubic face centred space-lattice of MINKOVSKIAN line-elements, periodically in all directions. For mathematicians, however, these only exist on paper, while LANZOS regards them more as physical objects. Thus, in future, we want to call them Metric Line-Elements with the abbreviation MLE.

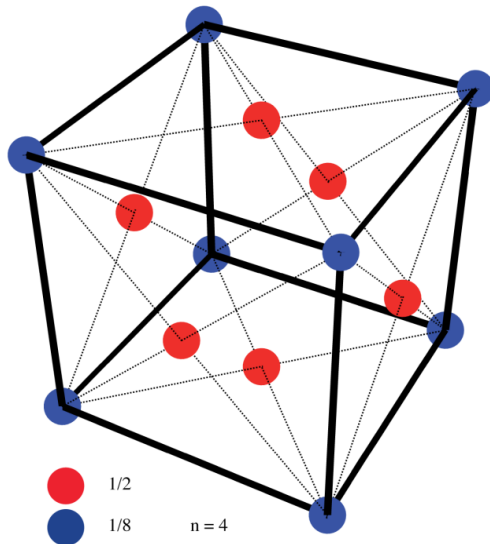


Figure 2:
Cubic Face-Centred Crystal Lattice (fc)

We accept LANZOS' assumption. Such a cubic face-centred space lattice (fc) is shown in Figure 2. According to [48] Such a system behaves isotropically. Simply let's go out from the MAXWELL equations, which in fact, even beside the known methods according to [1], should can be derived on the basis of an infinitesimal interference on the lattice. Now, at first we want to consider these equations less mathematically but more according to their content.

$$\begin{aligned} \operatorname{div} \mathbf{B} &= 0 & \operatorname{div} \mathbf{D} &= \rho \\ \operatorname{curl} \mathbf{E} &= -\dot{\mathbf{B}} & \operatorname{curl} \mathbf{H} &= \mathbf{i} + \dot{\mathbf{D}} \end{aligned} \quad (1)$$

As well for the electric as for the magnetic field-strength the operator curl for rotation (also rot) appears. Let's assume that a rotation would really take place here. Thereto we look at the model figured in Figure 3 that is to imagine three-dimensional however.

2.2. Forces in the model

A ball-capacitor (Figure 3) with the radius r_c and the charge of q_0 moves on an orbit with the angular frequency ω_0 , the radius r_0 and the velocity $c = \text{const}$ (speed of light). The capacity results in $C_0 = 4\pi\epsilon_0 r_c$. the energy stored in this capacitor in

$$W_0 = \frac{1}{2} \frac{q_0^2}{C_0} = \frac{q_0^2}{8\pi\epsilon_0 r_c} \quad (2)$$

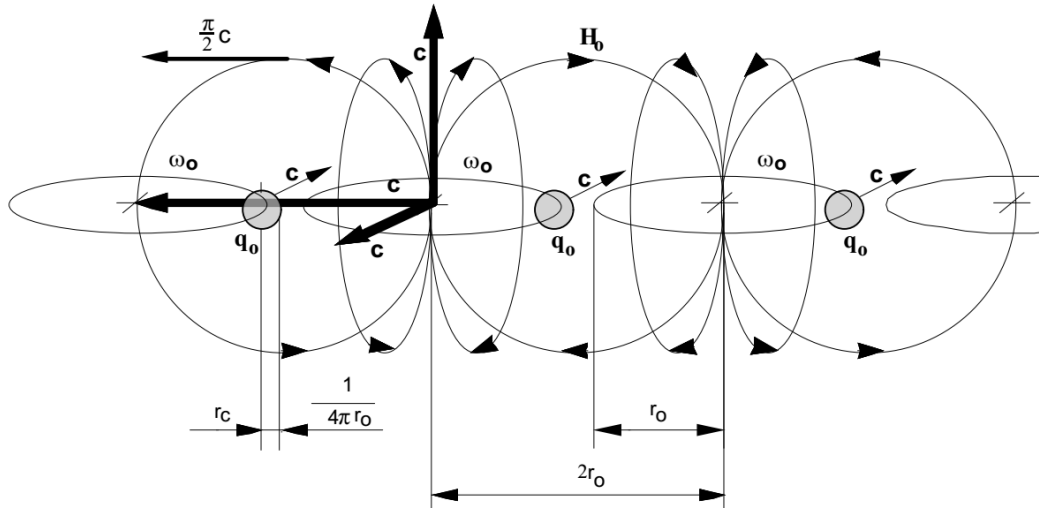


Figure 3:
Metric Line-Elements
Physical Dimensions and Mutual Coupling

and with $r_0 = 4\pi r_c$ and $C_0 = \epsilon_0 r_0$

$$W_0 = \frac{q_0^2}{2\epsilon_0 r_0} \quad (3)$$

Furthermore this energy even should have a mass m_0 . Since it's rotating its mass-moment of inertia results to

$$J_0 = m r_0^2 \quad (\text{point-mass}) \quad (4)$$

According to our formulation, applies $\omega_0 = c/r_0$ and we receive for the kinetic energy, that should be equal to the electric one,

$$W_0 = \frac{1}{2} J_0 \omega_0^2 = \frac{1}{2} m_0 c^2 \quad (5)$$

Since the capacitor does not have any mass itself, the mass m_0 of the charge is given by

$$m_0 = \frac{q_0^2}{\epsilon_0 c^2 r_0} = \frac{\mu_0 q_0^2}{r_0} \quad (6)$$

The 2nd expression of (6) we get from the known relation

$$c = \frac{1}{\sqrt{\mu_0 \epsilon_0}} \quad (7)$$

which has a strong similarity with the formula for the resonance-frequency of a loss-free oscillatory circuit on the first look

$$\omega = \frac{1}{\sqrt{L_0 C_0}} = \frac{1}{r_0 \sqrt{\mu_0 \epsilon_0}} = \frac{c}{r_0} \quad (8)$$

Then for the centrifugal force (amount) $F_Z = m_0 r_0 \omega_0^2$ applies:

$$F_Z = \frac{\omega_0^2 q_0^2}{\epsilon_0 c^2} = \mu_0 \omega_0^2 q_0^2 = \frac{q_0^2}{\epsilon_0 r_0^2} \quad (9)$$

F_Z is directed outwardly. Expression (9;3) represents with the exception of a factor $1/4\pi$ the COULOMB law (repulsion), only that there is no second charge, which could wield a repelling force, here. Centrifugal force and COULOMB-force would just be of same magnitude. To guarantee, that m_0 doesn't vanish in the infinite, a force is required, able to eliminate the appearing centrifugal force. Thereto it must be directed contrarily and of same quantity.

Since we are concerned with the circular motion of a charge here, we can even talk about a current $i_0 = \omega_0 q_0$. This current generates a magnetic field at which point even an inductivity occurs (1 turn). Simplifying, we now assume, that the inductivity should be $L_0 = \mu_0 r_0$. That agrees with the equation for a coil with one turn as well:

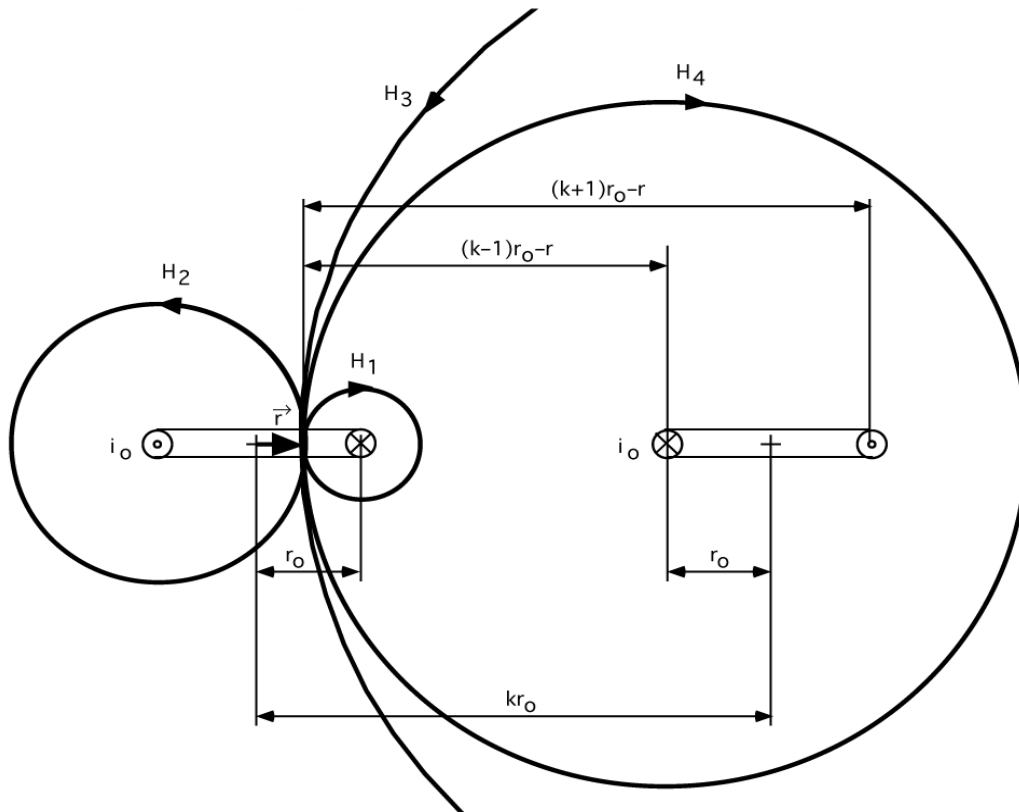


Figure 4:
Magnetic Field-Strength in One and
in Several Conductor Loops

$$L = \mu_0 r \left[\ln \frac{8r}{r'} - \frac{7}{4} \right], \quad (10)$$

in which r represents the inside-radius, r' the wire-radius of one single short-circuited turn ($\mu_r=1$). If $r'=0.5114r$ applies, the bracket-expression yields 1 and we get the aforementioned expression. This is, as said, only a model, since our coil doesn't consist of wire. Rather one should imagine the charge and current something like »spreaded« across the space. According to [20] the magnetic field-strength \mathbf{H}_0 (in future always figured as vector, H is the HUBBLE-parameter) in the centre of the conductor loop (left) amounts to

$$\mathbf{H}_0 = -\frac{i_0}{2r_0} \mathbf{e}_r \quad (11)$$

\mathbf{e}_r is the unit-vector. The negative sign results from the definition of the field-strength as difference between zero-potential ($r=\infty$) and potential in the distance r . Since there are several MLEs in the fc lattice whose magnetic fields are superimposed, we finally get for H_0 :

$$\mathbf{H}_0 = -\frac{i_0}{r_0} \mathbf{e}_r \quad (12)$$

and for the magnetic induction

$$\mathbf{B}_0 = \mu_0 \mathbf{H}_0 = \frac{\mu_0 \omega_0 q_0 \mathbf{e}_r}{r_0} = \frac{\mu_0 c q_0 \mathbf{e}_r}{r_0^2} \quad (13)$$

Simultaneously, we are concerned with a moved charge in the magnetic field. So, a LORENTZ-force $\mathbf{F}_m = q_0(\mathbf{c} \times \mathbf{B}_0)$ will apply. It is directed inside. For the simplification, we want to look at the system along the x -axis again. Therefore, we can set for the amount of the attractive force $F_m = -q_0 c B_0$. We get using

$$F_m = -\frac{\mu_0 c^2 q_0^2}{r_0^2} = -\frac{q_0^2}{\epsilon_0 r_0^2} \quad (14)$$

Expression (9), just with inverse signs. Centrifugal force and LORENTZ-force cancel each other. Now, we can determine even the rest-mass of the magnetic field:

$$W_0 = \frac{1}{2} i_0^2 L_0 = \frac{1}{2} \omega_0^2 q_0^2 \mu_0 r_0 = \frac{1}{2} m_0 c^2 \quad (15)$$

$$m_0 = \frac{\mu_0 q_0^2}{r_0} \quad (16)$$

As it can be proven easily, this expression is identical to (6). Now, we want to determine the gravitative attraction of the magnetic and the electric rest mass (we imagine it as point-masses in the centre of the orbit). We can write on reason of the mass-equality

$$F_g = -G \frac{m_0^2}{r_0^2} = -G \frac{\mu_0^2 q_0^4}{r_0^4}. \quad (17)$$

Let's now look at the energy stored in C_0 once again (3). Since this represents only the half of the total-energy of the MLE, we can write

$$W_0 = \frac{q_0^2}{2\varepsilon_0 r_0} = \frac{1}{2} \hbar \omega_0 \quad (18)$$

Then, following expression arises for the charge:

$$q_0 = \sqrt{\hbar c \varepsilon_0} = \sqrt{\frac{\hbar}{Z_0}} \quad (19)$$

In the following, deviating from the historical definition, this charge is named the PLANCK's charge or even the charge of the MLE. In this connection, Z_0 stands for the vacuum wave-propagation impedance $Z_0 = \sqrt{\mu_0/\varepsilon_0}$. This represents because of equation (7) a similarly invariable quantity like c . Herewith we have already »linked the lattice-oscillations with HEISENBERG's uncertainty principle« by the way, as it LANCZOS demands in his lecture. From (17) and (19) we get:

$$F_g = -G \frac{\hbar c \varepsilon_0 \mu_0^2 q_0^2}{r_0^4} = -\frac{G \hbar}{c} \frac{q_0^2 \mu_0}{r_0^4} \quad (20)$$

and after expansion with c^2

$$F_g = -\frac{G \hbar}{c^3} \frac{q_0^2}{\varepsilon_0 r_0^4} \quad (21)$$

Now let's have a look at the first fraction $G\hbar/c^3$ somewhat more exactly, so it represents, with the exception of a factor of $1/2\pi$, exactly the square of PLANCK's elementary-length, how we already know it from other models. If we now state that

$$r_0 = \sqrt{\frac{G \hbar}{c^3}} \quad (22)$$

should be, we also get for the gravitational-force expression (14) as well as (9)

$$F_g = -\frac{q_0^2}{\varepsilon_0 r_0^2} \quad (23)$$

In brief, we are faced with the PLANCK mass m_0 , which has the PLANCK charge q_0 , moving in its own magnetic field, at which point the centrifugal force and the LORENTZ force cancel each other. *Attention, the PLANCK charge q_0 in this model is defined differently than usual!*

2.3. The Metric line-element as oscillatory circuit

Having considered so far only the case of electric and magnetic mass which are equally large – charge and flux φ_0 would have its effective-values and m_0 would describe an orbit in this case – the MLE doesn't behave quite so simply. So it suffices however to assume an orbit for later contemplations. As already more above suggested, there is an oscillatable system with a capacitor and a coil available, which shall (in the moment) be interconnected via a loss-free medium, namely the vacuum. So, we can make even an equivalent circuit for it (Figure 5), the one of an undamped parallel-oscillatory circuit.

We already have specified the equation for the resonance-frequency in (8). If L_0 and C_0 behave like a parallel-oscillatory circuit however, even all values like q_0 , φ_0 , H_0 , etc. have to change time wise according to harmonic functions. The same even is valid for the distance r_0 . The temporal course of q_0 and B_0 (H_0) in detail of the marked track-points is figured in Figure 6. The exact track-function arises from (33), (35) and (37) of [29] using the following formula:

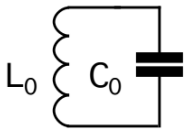


Figure 5:
Equivalent Circuit
of a Static MLE

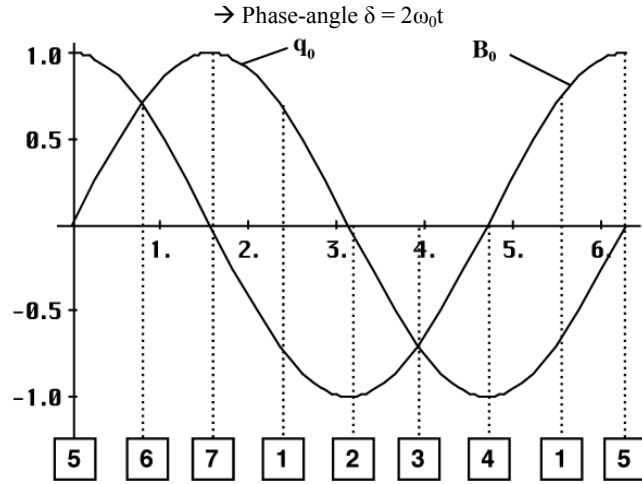


Figure 6:
Courses of Charge and Induction
with Labelling of the Track-Points

$$W_0 = \hbar\omega_0 = \frac{q_0^2}{\epsilon_0 r_0} \sin^2 2\omega_0 t \quad (24)$$

Rearranged to r_0 by neglecting the fixe phase-angle $\pi/2$ with $\delta = 2\omega_0 t$:

$$r(\omega_0 t) = \frac{q_0}{2\epsilon_0 \phi_0 \omega_0} \left(1 + \cos \left(\frac{\pi}{2} + 4\omega_0 t \right) \right) \Rightarrow \frac{c}{2\omega_0} (1 + \cos 4\omega_0 t) \quad (25)$$

$$r(\delta) = \frac{r_0}{2} (1 + \cos 2\delta) \quad \text{or in x and y to} \quad (26)$$

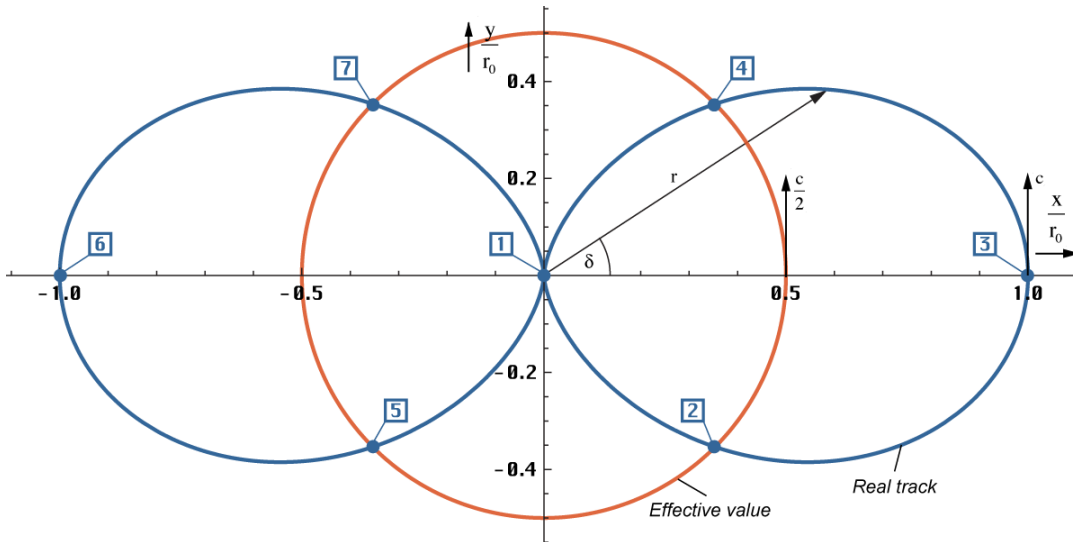


Figure 7:
Real Track-Course in the xy-Plane

$$x(\delta) = \frac{r_0}{2} (1 + \cos 2\delta) \cos \delta \quad (27)$$

$$y(\delta) = \frac{r_0}{2} (1 + \cos 2\delta) \sin \delta \quad (28)$$

The exact course is figured in Figure 7. In the xy-plane it corresponds exactly to the course of the envelope of the POYNTING-vector \mathbf{S} (like r) of a HERTZian dipole [24].

For most further examinations, it suffices to go out from an orbit simplifying by consideration of effective-values only. Significant is the shape of a dipole (vector \mathbf{E}_0) by the true track-course (Figure 7 and 8), since the charge q_0 is equally large at the respective bend points of the track however affected with opposite sign. This dipole may be oriented in all three directions at will and it corresponds in principle to the HERTZian dipole.

A possible expansion of this of model is achieved by the temporal increase of r_0 . The model however is only valid, if the expansion-velocity of r_0 is smaller than $c/2$. If it is larger, so there is no more rotation anyway. The motion proceeds rectilinear as well as curvilinear then. It has no more exact track-function declared. That would be also rather pointless, as we will still see later.

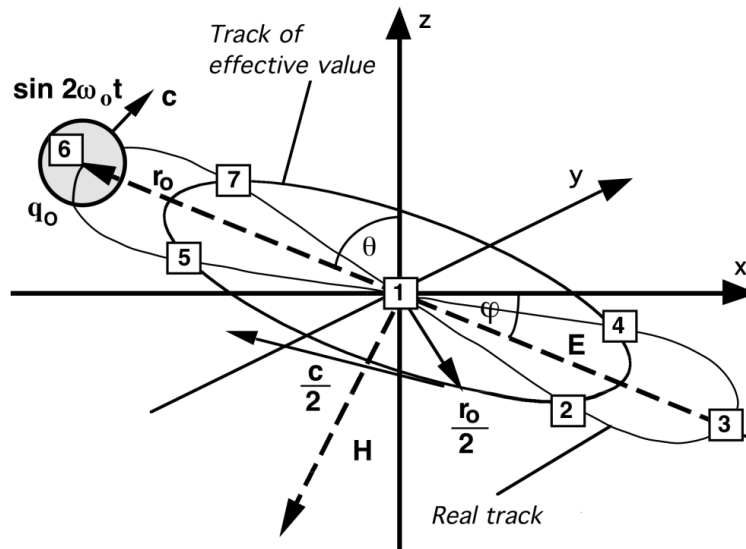


Figure 8:
Idealized and Actual Trajectory
of the MLE in Three-Dimensional Representation

2.4. Disadvantages of the static model

With the described static model, we have realized case (13[1]) $\sigma_i = \lambda$ and »the direction of the main-axes remains uncertain. The smallest interference here can have the consequence of an at will strong rotation of the main-axes.« The cause is following: With L_0 and C_0 , it is a matter of ideal components. That means, the Q-factor Q_0 of such an oscillatory circuit would be infinite with it, the bandwidth zero. The resonance-super-elevation is also infinitely with an infinite Q-factor however (voltage u_0 and current i_0). Therefore it has no exact phase and amplitude declared. This is just identical to the uncertainty of the main-axe's position however.

Another disadvantage is that the model doesn't change time wise. That means, all median values including r_0 remain constant forever. Now it is a known fact however, that the cosmos is expanding and the same should happen with the metrics too. Maybe, this is even the cause of expansion? We use this supposition as base and formulate our second hypothesis with it.

II. The expansion of the cosmos is evoked by the expansion of the metric lattice/radiation-field.

Furthermore, the question of origin and isotropy of the cosmologic background radiation remains unanswered. In order to avoid these disadvantages, we want to make dynamic the model.

2.5. Dynamic model

If we want to achieve an expansion of the metrics, so we must see to take away energy from the MLE. Now one assumes yet the vacuum as loss-free, since the propagation-velocity of electromagnetic radiation is independent from the frequency. Let's introduce the conductivity $\kappa_0 = 1/\rho_0$, so for the complex wave-propagation-impedance (j is the imaginary unit, as used in the electrotechnics) applies

$$\underline{Z} = \sqrt{\frac{j\omega\mu_0}{\kappa_0 + j\omega\varepsilon_0}} \quad (29)$$

and on reason of (8) for \underline{c}

$$\underline{c} = \sqrt{\frac{j\omega}{\mu_0(\kappa_0 + j\omega\varepsilon_0)}} \quad (30)$$

Two extreme-cases result. While (30) passes into equation (7) for a non-conductor, we get for an ideal conductor:

$$\underline{c} = \sqrt{\frac{j\omega}{\mu_0\kappa_0}} \quad (31)$$

Therefore generally applies: in a loss-affected medium, the wave-propagation-impedance becomes complex and with it \underline{c} too. Since \underline{c} determines the propagation rate $\underline{\gamma} = \alpha + j\beta = j\omega/\underline{c}$, the attenuation rate α would become unequal to zero and even moreover frequency-dependent with the appearance of an imaginary part of \underline{c} . It applies

$$\alpha = \frac{\omega}{c} \sqrt{\frac{1}{2} \left(\sqrt{1 + \left(\frac{\kappa_0}{\omega \varepsilon_0} \right)^2} - 1 \right)} = \frac{\omega}{c} \sinh \left(\frac{1}{2} \operatorname{arsinh} \frac{\kappa_0}{\omega \varepsilon_0} \right) \quad (32)$$

That means, additionally to the geometrically caused damping an additional damping $e^{-\alpha x}$ would appear and one could define a lower cut-off frequency for the space ($-3\text{dB}/\lambda$). Only if the conductivity is zero, that wouldn't be the situation. All this does neither has been observed in the vacuum and the wave-propagation occurs with light speed for all frequencies. The vacuum just acts like an ideal non-conductor [20].

Nevertheless, we want to try to find a solution, taking all these facts into account. At first we extend our equivalent circuit by the loss-resistor R_{0R} (Figure 9), index R stands here for a series connection of circuits, as well as by the shunt-resistor R_0 .

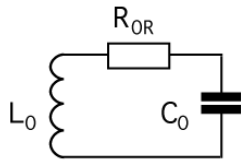


Figure 9:
Equivalent Circuit with
Series-Resistor

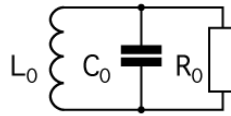


Figure 10:
Equivalent Circuit with
Shunt-Resistor

With our further contemplations, now we have to decide in favour of one of both equivalent circuits. For the conversion of both impedances applies

$$R_0 = \frac{Z_0^2}{R_{0R}} \quad (33)$$

We decide in favour of the second model, since a very large loss-impedance is the best approach to a non-conductor. Starting with Figure 9 we first define the loss-impedance R_{0R} which must be obviously very small in this case, in reference to a cube with the edge length of r_0 to

$$R_{0R} = \frac{1}{\kappa_0} \frac{r}{A} \quad A = r^2 \quad R_{0R} = \frac{1}{\kappa_0 r} \quad (34)$$

From it we obtain for R_0

$$R_0 = \kappa_0 r_0 Z_0^2 \quad (35)$$

Evidently, our MLE is a system of second order. By introduction of R_0 , we can now define even two time constants, namely

$$\tau_0 = \sqrt{L_0 C_0} \quad \text{and} \quad \tau_1 = R_0 C_0 \quad (36)$$

With τ_0 , a time-constant of second order, it is with largest probability a matter of the reciprocal of the angular frequency of our MLE. Which value in the nature then now that τ_1 can be assigned to? An additional temporal damping of electromagnetic waves doesn't appear as you know. Since R_0 has to be very large, then the same is applied to τ_1 . We now assume that τ_1 can be identified with the reciprocal of the HUBBLE-parameter H . This hypothesis is substantiated by the fact that H is a time-constant of first order, whatever is valid for τ_1 too. We can write then

$$H = \frac{\dot{r}_0}{r_0} = \frac{1}{R_0 C_0} = \frac{1}{\kappa_0 \mu_0 r_0^2} = \frac{\varepsilon_0}{\kappa_0} \frac{1}{L_0 C_0} = \frac{\varepsilon_0 \omega_0^2}{\kappa_0} \quad (37)$$

Furthermore generally applies $H = n/t$; n is a constant factor which depends on the used model (radiation-/dust-cosmos), t is the time and equates with the age here. Next we want to define the Q-factor of the oscillatory circuit according to [5]

$$Q_0 = \frac{W_0 \omega_0}{P_0} = \frac{\hbar \omega_0^2 R_0}{u_0^2} \quad (38)$$

and because of $u_0 = -\omega_0 \phi_0$ as well as ([29] 36)

$$Q_0 = \frac{\hbar R_0}{\varphi_0^2} = \kappa_0 r_0 Z_0 = \frac{R_0}{Z_0} = \sqrt{\frac{2\kappa_0}{\varepsilon_0}} \quad (39)$$

The numerical value according to [29] is about $8.3404711 \cdot 10^{60}$. If we go out from the last expression of (37), we can even write for H

$$H = \frac{\varepsilon_0 \omega_0^2}{\kappa_0} = \frac{\varepsilon_0 c \omega_0}{\kappa_0 r_0} = \frac{\omega_0}{\kappa_0 r_0 Z_0} = \frac{\omega_0}{Q_0} \quad (40)$$

Now we could think, up to the determination of H it's far no more. Unfortunately, the value of κ_0 is unknown however. It can be received e.g. from the astronomically determined value of H. But we use the current values from [29].

$$\kappa_0 = \frac{c^3}{\mu_0 G \hbar H} \quad (41)$$

with $1.36977766 \cdot 10^{93} \text{ AV}^{-1} \text{ m}^{-1}$. In this connection a value of $68.6241 \text{ kms}^{-1} \text{ Mpc}^{-1}$, has been set up for H, that is $2.223925 \cdot 10^{-18} \text{ s}^{-1}$. This is the latest value found in [29]. Furthermore applies $G\hbar H = \text{const}$. But now let's continue with our model. Using the relation $H = n/t$ and the third expression of (37) we are now in a position to determine the time-function of r_0

$$r_0 = \sqrt{\frac{t}{n\kappa_0\mu_0}} \quad \text{and} \quad (42)$$

$$\dot{r}_0 = \frac{1}{2} \sqrt{\frac{1}{n\kappa_0\mu_0 t}} \quad (43)$$

with it we get for the HUBBLE-parameter H

$$H = \frac{\dot{r}_0}{r_0} = \frac{1}{2t} \quad \text{and} \quad q = -\frac{r_0 \ddot{r}_0}{\dot{r}_0^2} = 1 \quad (44)$$

just the relationship for a radiation-cosmos. This neither is nor further remarkable, since we have assumed the MAXWELL equations however. q is the dilatory-parameter (do not confuse with the charge). It follows $n=1/2$ and we can write

$$r_0 = \sqrt{\frac{2t}{\kappa_0\mu_0}} \quad \text{and} \quad \dot{r}_0 = \frac{1}{\sqrt{2\kappa_0\mu_0 t}} \quad (45)$$

$$t = \frac{R_0 C_0}{2} = \frac{\kappa_0 \mu_0 r_0^2}{2} \quad (46)$$

3. Further contemplations

3.1. Definition of further base items

At first the base items of the theoretical electro-technics. They apply independently from the model (47). Beneath (48) the most important PLANCK-units are shown. The introduction of the specific conductivity of the vacuum turns out to be the *missing link* among each other and even to other values.

$$c = \frac{1}{\sqrt{\mu_0 \varepsilon_0}} \quad \left| \quad Z_0 = \sqrt{\frac{\mu_0}{\varepsilon_0}} = \sqrt{\frac{L_0}{C_0}} = \frac{\varphi_0}{q_0} = \frac{\mathbf{E}}{\mathbf{H}} \quad \left| \quad \begin{array}{l} L_0 = \mu_0 r_0 \quad C_0 = \varepsilon_0 r_0 \\ R_{0R} = 1/(\kappa_0 r_0) \text{ Series resistor} \end{array} \right. \quad (47)$$

$$r_0 = \sqrt{\frac{G\hbar}{c^3}} = \sqrt{\frac{2t}{\mu_0 \kappa_0}} \quad \left| \quad m_0 = \sqrt{\frac{\hbar c}{G}} = \frac{\mu_0 \kappa_0 \varphi_0^2}{Z_0} \quad \left| \quad \varphi_0 = \sqrt{\hbar Z_0} \quad q_0 = \sqrt{\hbar/Z_0} \quad (48)$$

One single line-element can be specified by the model of a lossy oscillating circuit with shunt resistor (Figure 10). One special property of that model only is, that the Q-factor of the circuit equals the phase angle $2\omega_0 t$ of the Bessel function. It applies $Q_0 = 2\omega_0 t$. The value ω_0 corresponds to the PLANCK-frequency in this connection.

$$\omega_0 = \sqrt{\frac{c^5}{G\hbar}} = \sqrt{\frac{\kappa_0}{2\varepsilon_0 t}} = \frac{1}{\sqrt{L_0 C_0}} = \frac{c}{r_0} \quad \left| \quad t_0 = \frac{1}{2} \sqrt{\frac{G\hbar}{c^5}} = \sqrt{\frac{\varepsilon_0 t}{2\kappa_0}} \quad (49)$$

$$Q_0 = 2\omega_0 t = \kappa_0 r_0 Z_0 = \frac{\hbar R_0}{\varphi_0^2} = \frac{R_0}{Z_0} = \frac{c^2}{v^2} = \sqrt{\frac{2\kappa_0 t}{\varepsilon_0}} \quad (50)$$

$$H_0 = \frac{\dot{r}_0}{r_0} = \frac{1}{R_0 C_0} = \frac{\varepsilon_0}{\kappa_0 L_0 C_0} = \frac{1}{\kappa_0 \mu_0 r_0^2} = \frac{\varepsilon_0 \omega_0^2}{\kappa_0} = \frac{1}{2T} = \frac{\omega_0}{Q_0} \quad (51)$$

Except for the quantities of subspace μ_0 , ε_0 , κ_0 and c all other ones are functions of space, time and even of the velocity v with respect to the metric wave field. The reason is, that the spatiotemporal function of the metric wave field should emulate the relativistic effects and it really does. The GR-dependencies aren't considered here furthermore.

That makes the PLANCK units depend on the frame of reference, which is even defined by them. And all of them are bound by the phase angle Q_0 . But the variations mostly cancel each other creating the impression, the values are constant. Reference-frame-dependent values are marked with a swung dash e.g. \tilde{Q}_0 being constants by character.

Still important are the values with a phase angle $Q_1=1$. They describe the conditions directly at the particle horizon. They are constants too, because they are defined only by quantities of subspace. Thus, they are mostly qualified for reference-frame-independent conversions of certain values, so-called couplings. One example is the conversion of the magnetic flux φ_1 to the magnetic field strength $H_1 = \varphi_1 / (\mu_0 r_1^2)$ as basis of a temporal function containing reference-frame-dependent elements (r_0). r_1 would be the so-called coupling-length then. Expression (54) shows the relations to the PLANCK-units and to the values of the universe as a whole.

$$r_1 = \frac{1}{\kappa_0 Z_0} \quad \left| \quad M_1 = \mu_0 \kappa_0 \hbar \quad \right| \quad t_1 = \frac{1}{2} \frac{\varepsilon_0}{\kappa_0} \quad \left| \quad \omega_1 = \frac{\kappa_0}{\varepsilon_0} = \frac{1}{2t_1} \quad \right. \quad (52)$$

$$R = Q_0 r_0 = Q_0^2 r_1 \quad \left| \quad M_1 = Q_0 m_0 \quad \right| \quad T = Q_0 t_0 = Q_0^2 t_1 \quad \left| \quad \omega_1 = Q_0 \omega_0 = Q_0^2 H_0 \quad \right. \quad (53)$$

$$\varphi_1 = \sqrt{\hbar_1 Z_0} \quad \left| \quad q_1 = \sqrt{\hbar_1 / Z_0} \quad \right| \quad \hbar_1 = \hbar Q_0 \quad \left| \quad \kappa_0 = \frac{c^3}{\mu_0 G \hbar H_0} \quad \right. \quad (54)$$

The action quantum \hbar_1 and $\tilde{\hbar}_1$ is not a quantity of subspace, but the initial action, our universe »got« in the early beginning. That value is the only one »set-screw«, with which »one« could exert influence on the future appearance of the universe. All other values are »hard-wired« with Q_0 depending on space and time. There is no »fine-tuning« either. With expression (48) right-hand and (54) it's about an effective value, i.e. $\tilde{\hbar}$, φ_0 and q_0 are temporal functions too. At least still the definition of NEWTON's gravitational constant:

$$G = \frac{c^3}{\mu_0 \kappa_0 \hbar H} = \frac{2c^3 t}{\mu_0 \kappa_0 \hbar} = c^2 \frac{R}{M_1} = c^2 \frac{r_0}{m_0} \quad (868 [74])$$

With these relationships we are now able to set up a differential equation for the oscillating circuit. Let's have a look at Figure 11.

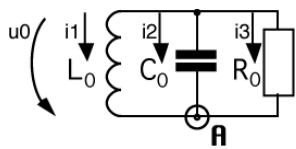


Figure 11:
Voltages and Currents
at the Oscillatory Circuit

3.2. Differential equation and solutions

3.2.1. Specification of the differential equation

We have a parallel-oscillatory circuit with the inductivity L_0 , the capacity C_0 and the loss-resistor R_0 on hand. Furthermore, the voltage u_0 is connected to all components simultaneously. In the node **A** the three currents i_1 , i_2 and i_3 unify. The KIRCHHOFF's first law applies:

$$i_1 + i_2 + i_3 = 0 \quad (55)$$

Furthermore applies because of $u_0 = d\varphi_0/dt$ and $\varphi_0 = i_1 L_0$

$$u_0 = \frac{d(i_1 L_0)}{dt} \quad (I)$$

$$u_0 = \frac{1}{C_0} \int i_2 dt \quad (II)$$

$$u_0 = i_3 R_0 \quad (III)$$

Now equation (I) can be resolved as follows

$$u_0 = \frac{d(i_1 L_0)}{dt} = L_0 \frac{di_1}{dt} + i_1 \frac{dL_0}{dt} \quad (56)$$

and we get the following differential equation

$$\dot{i}_1 + \frac{\dot{L}_0}{L_0} i_1 = \frac{u_0}{L_0} \quad \text{or} \quad (57)$$

$$y' + f(t)y = g(t) \quad (58)$$

$$M(t) = e^{\int f(t)dt} = e^{\int \frac{dL_0}{L_0} dt} = e^{\int \frac{dL_0}{L_0}} = L_0. \quad (59)$$

Now, we are able to resolve for i_1 [21]

$$i_1 = \frac{1}{M(t)} \left[\int g(t)M(t)dt + C \right] \quad (60)$$

With $C=0$ we get then

$$i_1 = \frac{1}{L_0} \int \frac{u_0}{L_0} L_0 dt = \frac{1}{L_0} \int u_0 dt \quad (61)$$

Now, we rearrange equation (II) for i_2 :

$$i_2 = \frac{d(u_0 C_0)}{dt} = C_0 \frac{du_0}{dt} + u_0 \frac{dC_0}{dt} \quad (62)$$

We receive the value of i_3 directly by rearrangement of (III) so that we can write

$$i_1 = \frac{1}{L_0} \int u_0 dt \quad (I)$$

$$i_2 = C_0 \frac{du_0}{dt} + u_0 \frac{dC_0}{dt} \quad (II)$$

$$i_3 = \frac{u_0}{R_0} \quad (III)$$

Put into (55) we obtain

$$\frac{1}{L_0} \int u_0 dt + C_0 \frac{du_0}{dt} + u_0 \left(\frac{dC_0}{dt} + \frac{1}{R_0} \right) = 0 \quad (63)$$

Since $u_0 = \dot{\phi}_0$ equation (63) turns into

$$C_0 \ddot{\phi}_0 + \left(\dot{C}_0 + \frac{1}{R_0} \right) \dot{\phi}_0 + \frac{1}{L_0} \phi_0 = 0 \quad (64)$$

and after division by C_0

$$\ddot{\phi}_0 + \left(\frac{\dot{C}_0}{C_0} + \frac{1}{R_0 C_0} \right) \dot{\phi}_0 + \frac{1}{L_0 C_0} \phi_0 = 0 \quad . \quad (65)$$

This is the differential equation of a parametric amplifier. But on reason of the definition of $C_0 = \varepsilon_0 r_0$ we also can write

$$\ddot{\phi}_0 + \left(\frac{\dot{r}_0}{r_0} + \frac{1}{R_0 C_0} \right) \dot{\phi}_0 + \frac{1}{L_0 C_0} \phi_0 = 0 \quad . \quad (66)$$

Of course it is somewhat difficult to imagine, that the capacitor quasi shall grow with the metrics. But considering C_0 as a basic quality of space, whereat its size depend on the dimensions of the MLE, it should be somewhat less difficult however. If we now assume, that no expansion would take place at all, equation (66) would change into the normal differential equation for a loss-affected oscillatory circuit with shunt-resistor with the well-known solution:

$$\omega_0 = \sqrt{\frac{1}{L_0 C_0} - \left(\frac{1}{2R_0 C_0} \right)^2} \quad . \quad (67)$$

Then however, we would get for the speed of light:

$$c = \sqrt{\frac{1}{\mu_0 \varepsilon_0} - \left(\frac{1}{2\mu_0 \kappa_0 r_0^2} \right)^2} \quad , \quad (68)$$

That would even mean that the (maximum-)speed of light is not constant. The constancy of the light speed however is a basic statement, that we may not negate. To the luck our metrics is expanding and the first partial factor of ϕ_0 in equation (66), namely H is $\neq 0$. According to (37) furthermore both augments are identically and we can write

$$\ddot{\phi}_0 + \frac{2}{R_0 C_0} \dot{\phi}_0 + \frac{1}{L_0 C_0} \phi_0 = 0 \quad \text{or} \quad (69)$$

$$\ddot{\phi}_0 + 2H_0 \dot{\phi}_0 + \omega_0^2 \phi_0 = 0 \quad . \quad (70)$$

Equation (70) is very interesting. If we want to determine the time-function of ϕ_0 however, we now have to insert (39) and (40):

$$\ddot{\phi}_0 + \frac{1}{t} \dot{\phi}_0 + \frac{\kappa_0}{2\varepsilon_0 t} \phi_0 = 0 \quad \text{or} \quad (71)$$

$$\ddot{\phi}_0 t + \dot{\phi}_0 + \frac{1}{2} \frac{\kappa_0}{\varepsilon_0 t} \phi_0 = 0 \quad . \quad (72)$$

With it we have laid down the differential equation for our model. When studying the literature, this type of differential equation has not been found and POOLE's equation [17] did not achieve the goal either. For the first time solution in [29], only an integration with the power series approach [21] comes into consideration. Since I will have found a better solution way later on (same result) and we will need the image function anyway, I would like to present the alternative here.

3.2.2. Solution by LAPLACE-transformation

LAPLACE-transformation: Also suitable for solving the differential equation, provided that the inverse transformation is possible. So we start from (72) and determine the image function:

$$y''x + y' + ay = 0 \quad (73)$$

According to the differentiation-rule [22] applies:

$$\mathcal{L}\{y'\} = p y(p) - f_0^{(0)} \quad \text{with} \quad f_0^{(v)} = \lim_{t \rightarrow +0} \frac{d^v f(t)}{dt^v} \quad (74)$$

Fortunately we have already solved the differential equation in [29] and know the initial values for $t=0$. Therefore applies:

$$\mathcal{L}\{y'\} = p y(p) - 1 \quad . \quad (75)$$

We get for the second derivative:

$$\mathcal{L}\{y''\} = p^2 y(p) - p f_0^{(0)} - f_0^{(1)} \quad \text{with the initial values 1 and 0} \quad (76)$$

$$\mathcal{L}\{y''\} = p^2 y(p) - p \quad (77)$$

We require the LAPLACE transform for the product of y'' and t however. According to the multiplication-rule and (75) applies:

$$\mathcal{L}\{t^n f(t)\} = (-1)^n F^{(n)}(p) \quad (78)$$

$$\frac{dy''(p)}{dp} = 2p y(p) + p^2 y'(p) - 2p y(p) \quad (79)$$

$$\mathcal{L}\{y''t\} = 1 - p^2 y'(p) - 2p y(p) \quad (80)$$

Substitution in (73) results in:

$$y'(p) - \frac{a-p}{p^2} y(p) = 0 \quad \text{with the solution} \quad (81)$$

$$y(p) = e^{\int \frac{a-p}{p^2} dp} = \frac{C_1}{p} e^{-\frac{a}{p}} = \frac{a}{p} e^{-\frac{a}{p}+C} = \frac{1}{2pt_1} e^{-\frac{1}{2pt_1}+C} \quad (82)$$

The function $\text{InverseLaplaceTransform}[\phi_1 E^{-(a/p)}/p,p,t]$ really turns out expression (87) now. That equals the general solution with the hypergeometric function ${}_0F_1$.

$$y = a_0 {}_0F_1(;1;-Bx) \quad (83)$$

$${}_0F_1(;b;x) = \Gamma(b)(jx)^{b-1} J_{b-1}(j2x^{\frac{1}{2}}) \quad \text{Hypergeometric function } {}_0F_1 \text{ as per [17]} \quad (84)$$

J_n is the Bessel function of n -th order, just

$${}_0F_1(;1;-Bx) = \Gamma(1)(jBx)^0 J_0(\sqrt{4Bx}) \quad (85)$$

$$y = a_0 J_0(\sqrt{4Bx}) \quad \text{with} \quad a_0 = \hat{\phi}_i/2 \quad B = \frac{1}{2} \frac{\kappa_0}{\varepsilon_0} \quad x = t \quad (86)$$

$$\phi_0 = a_0 J_0 \sqrt{\frac{2\kappa_0 t}{\varepsilon_0}} = a_0 J_0(Q_0) \quad (87)$$

$$\phi_0 = a_0 J_0 \left(2 \sqrt{\frac{\kappa_0}{2\varepsilon_0 t}} t \right) \quad \text{with} \quad \omega_0 = \sqrt{\frac{\kappa_0}{2\varepsilon_0 t}} \quad (88)$$

If we take a closer look at the root expression of equation (88), it should be equal to the angular frequency ω_0 and depend on time. The bracketed expression is the same as the term $2\omega_0 t = Q_0$ then. Since it's about a differential equation of second order and the degree of the Bessel function is integer, the universal solution is:

$$\phi_0 = \hat{\phi}_i (c_1 J_0(2\omega_0 t) + c_2 Y_0(2\omega_0 t)) \quad (89)$$

Even in this case c_1 and c_2 can be imaginary or complex. According to [22] it's often opportune to consider the two functions (Hankel functions)

$$H_0^{(1)}(x) = J_0(x) + Y_0(x) \quad \text{and} \quad (90)$$

$$H_0^{(2)}(x) = J_0(x) - Y_0(x) \quad (91)$$

as linearly independent solutions forming the universal solution

$$y(x) = c_1 H_0^{(1)}(x) + c_2 H_0^{(2)}(x) \quad (92)$$

With it, the general solution (89) reads then:

$$\phi_0 = \hat{\phi}_i (H_0^{(1)}(2\omega_0 t) + H_0^{(2)}(2\omega_0 t)) \quad (93)$$

For our further examinations, we set c_1 and c_2 in (92) equal to 1. Then we get as specific solution (94) and for the approximation, envelope curve and effective value:

$$\phi_0 = \hat{\phi}_i J_0(2\omega_0 t) = \hat{\phi}_i \text{Re}(H_0^{(1)}(2\omega_0 t)) \quad \phi_0 = \hat{\phi}_i J_0 \left(\sqrt{\frac{2\kappa_0 t}{\varepsilon_0}} \right) \quad (94)$$

$$\varphi_0 = \sqrt{\frac{2}{\pi}} \frac{1}{\sqrt{2\omega_0 t}} \cos\left(2\omega_0 t - \frac{\pi}{4}\right) \quad \text{Approximation} \quad (95)$$

$$\hat{\varphi}_0 = \sqrt{\frac{2}{\pi}} \frac{\hat{\varphi}_i}{\sqrt{2\omega_0 t}} \quad \text{Envelope} \quad (96)$$

$$\varphi_0 = \frac{\varphi_1}{\sqrt{2\omega_0 t}} \quad \varphi_0 \sim q_0 \sim Q_0^{-\frac{1}{2}} \mid \hbar = \varphi_0 q_0 \sim Q_0^{-1} \quad \text{Effective value} \quad (97)$$

The exact course of φ_0 (94), the approximate function (95), as well as of the approximate function of the envelope curve (96) and of the effective value (97) is shown in Figure 12. Also depicted are the original Bessel functions, which you can't see however, because they are completely covered by the approximation.

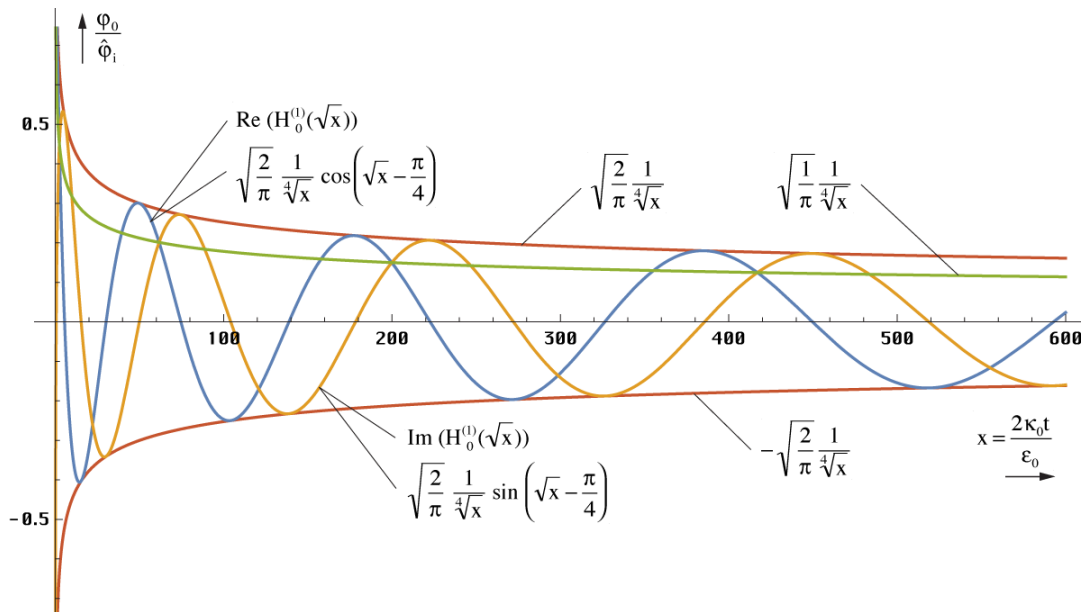


Figure 12: Course of magnetic flux as well as of approximation- and envelope-functions across a greater time period

Thus, with greater arguments, no differences are statable, neither in the amplitude, nor in the phase. Most important for the quality of the approximation is the course in the striking distance of $t=0$. The exact course of φ_0 as well as of the envelope functions (96) and (97) for small and very small values of t is shown in Figure 13. The course of the 1st derivative $q_0 = \hbar/\varphi_0 J_1(2\omega t)$ ([29] 123), has been omitted.

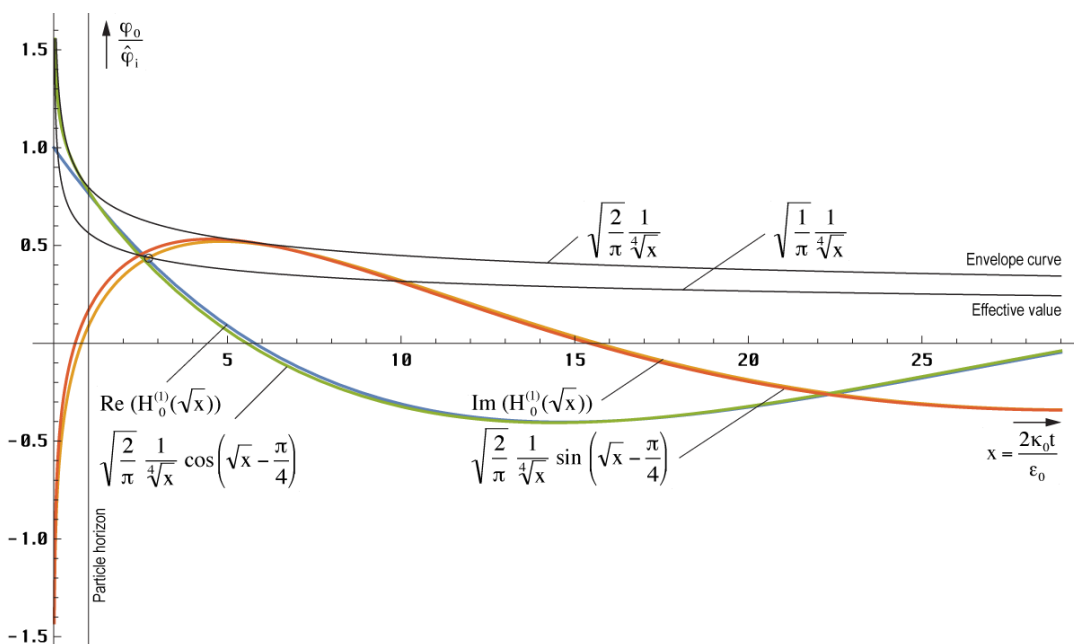


Figure 13: Course of flux as well as of the approximate- and envelope-functions nearby the singularity

All data up to this point is a summary. Please see [29] for the exact derivation. From this section we take over the time function (93), the PLANCK frequency ω_0 and, because of $c = \omega_0 r_0$, the definition of the PLANCK length r_0 .

3.3. LAPLACE-transform

3.3.1. Time domain

The time function (93) describes the course of φ_0 in the particular MLE. This is very important, but we are much more interested in the transfer function for EM waves. The idea behind this model is that these waves propagate as interference of the time functions of the individual MLEs connected in series. To do this, we first need to determine the frequency and phase response of a single MLE. The LAPLACE transformation is advantageous for this purpose.

$$\varphi_0 = \hat{\varphi}_i (H_0^{(1)}(2\omega_0 t) + H_0^{(2)}(2\omega_0 t)) \quad \text{Time function} \quad (93)$$

3.3.2. Figure domain

Alternative names: complex variable domain, s-domain, we use p instead. Evaluating, we get the figure function. We have already calculated this in the previous section. Starting from (72), we can therefore write

$$\ddot{\varphi}_0 t + \dot{\varphi}_0 + \frac{1}{2} \frac{\kappa_0}{\varepsilon_0 t} \varphi_0 = 0 \quad \text{Differential equation} \quad (72)$$

$$y(p) = e^{\int \frac{a-p}{p^2} dp} = \frac{C_1}{p} e^{-\frac{a}{p}} = \frac{a}{p} e^{-\frac{a}{p}+C} = \frac{1}{2pt_1} e^{-\frac{1}{2pt_1}+C} \quad \text{Figure function} \quad (82)$$

C_1 has the form of a time constant. With the primary function it's about a differential equation of 2nd order with only one time constant $\tau_1 = 1/(2a) = \varepsilon_0/\kappa_0 = 1/\omega_1 = 2t_1$ which occurs twice. So we do not have the problem of deciding which time constant belongs where. The value resulting from H_0 [49] has a magnitude of $6.46396 \cdot 10^{-105}$ s. In the figure domain with $C = -1$ then applies to the magnetic flux:

$$\varphi_0(p) = \frac{\hat{\varphi}_i}{pt_1} e^{-\frac{1}{pt_1}+C} \quad (98)$$

For signals with a duration of $t \gg \tau_1$ it's about an ideal I-gate (Integrating circuit) with a kind of inverse T-gate (Dead time circuit). It would be interesting too in that sense, to find the type of function, the model was activated with at the point of time $t=0$. Comparative contemplations lead to the conclusion that it could have been a DIRAC-impulse $\sigma(t)$ with the LAPLACE transform $\mathcal{L}\{\sigma(t)\} = 1$, which even agrees with the model of big bang in the best manner. The multiplication in the figure domain, corresponds to the convolution in the time domain:

$$\varphi_0 = \hat{\varphi}_i \sigma(t) * J_0 \left(\sqrt{\frac{2\kappa_0 t}{\varepsilon_0}} \right) \quad (99)$$

At the beginning, there was the »NOTHING« with the physical qualities μ_0 , ε_0 and κ_0 . Then, something was there suddenly (magnetic DIRAC-impulse). The DIRAC-impulse is an impulse with infinite amplitude and a duration of $t \rightarrow 0$. The integral below this impulse is equal to 1. This would speak in behalf of a finite initial value (Bessel-J). The response of the model (overshoot with a mean value of 0) can also be observed on electronic systems of second order using a DIRAC-like agitation (needle-impulse) but not using a jump- or ramp-function. The DIRAC-impulse is already known for a long time. Using technical methods however it won't be to realize whether at present nor in future. So far, there were even no parallels in nature, only in form of an approximation as needle-impulse. This way, another mathematical function would have found its exact correspondence in reality.

In any case, it's about a forced process. On the assumption, that it was actually a DIRAC-impulse, we get promptly for the transfer-function $G(p)$:

$$G(p) = \frac{1}{pt_1} e^{-\frac{1}{pt_1}+C} \quad (100)$$

Btw. the figure function of the simplest I-gate, the generic RC-low-pass-filter, reads $G(p) = K/(1+pt_1)$. The course of the transfer-function for the magnetic flux and of the charge q_0 (first derivative) is depicted in Figure 15, at first by setting $C=0$, since it has only an influence on the scale of the y-axis. Both functions point out a null at $p=+0$, a pole at $p=-0$ and a maximum at the point of time τ_1 resp. $\tau_1/2$. For longer impulses, the function changes into the one of an ideal I-gate. The contradiction in the earlier editions (D-gate, high pass) rather should have pointed out the error in (82) to me.

The PN-diagram doesn't need to be figured separately, null at $p=+0$, pole at $p=-0$. The number of poles is equal to the number of the nulls (realizability-condition). There are no pole in the left half-plane $p<0$ (stability-condition). Since the pole is located at the point 0, the system is loss-free anyway but still a passive component. That state is also named marginally stable.

With pole in the left half-plane, the system could come into an oscillation by itself. With pole in the right half-plane at $p>0$, losses appear, so that the oscillation grinds to a halt after a certain time, in contrast to the reality, in which the oscillation has neither faded away nor it will do so in the future. The null in the origin ($+0$) points to a blocking of higher frequencies.

Physically speaking it's about a low pass. Since the null is in the right half-plane ($p\geq 0$), it's just about a minimum-phase-system. Systems of this category have, according to [26], the quality of attenuation and phase being associated by the HILBERT-transformation. Since there are no conjugate complex pole available, even no resonance-effects appear.

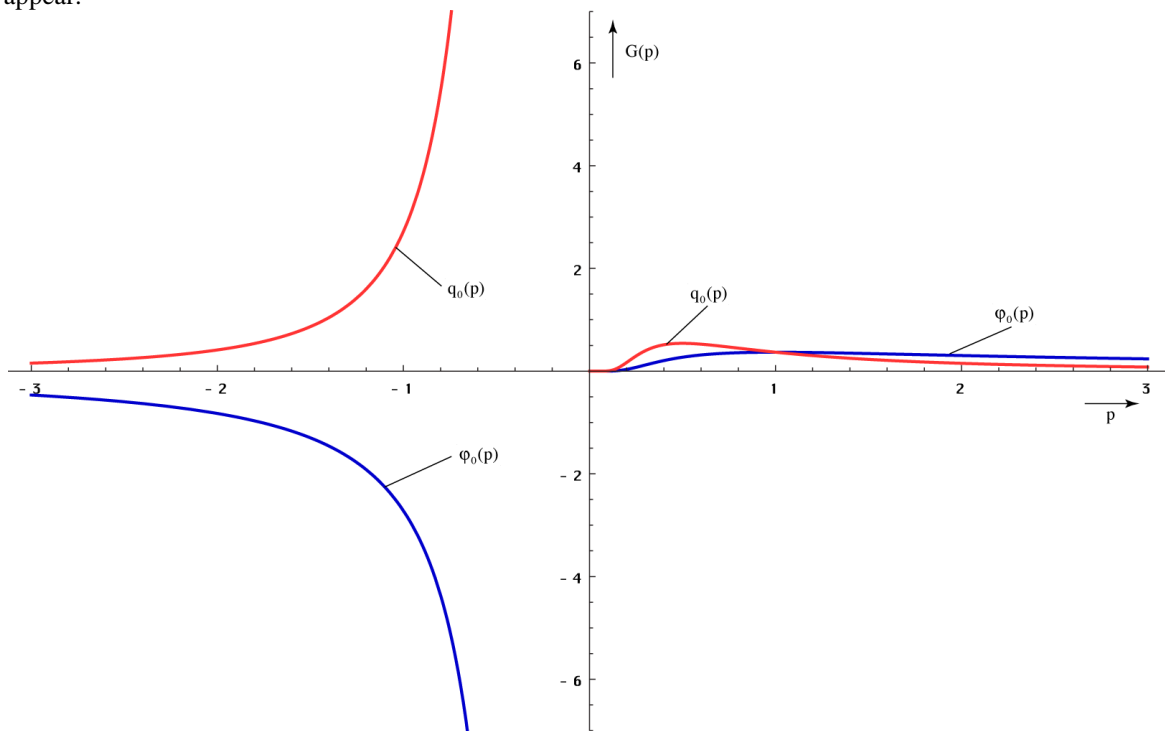


Figure 14:
Transfer-Functions (Figure Domain)
for Magnetic Flux and Charge ($C=0$)

From the figure-function we have read that it deals with a low pass of 2nd order. In general, such a system has a frequency-dependent attenuation. However, this stands in contradiction to the observations, resulting in a constant frequency response across all (technically observable) frequencies.

3.3.3. Frequency domain

To the calculation of the complex frequency response of our model we start with equation (100), in that we replace: $p = \sigma + j\omega$. A substitution $p = j\omega$ doesn't emerge any useful result, since the system is still oscillating so that the associated Fourier integral doesn't converge at all. The convergence is forced by the term σ . The frequency response of the magnetic flux gives also information about the vacuum wave propagation, since the separate dipoles (MLE) are interconnected via the magnetic field (resonant coupling). The value of σ arises from the half inverse of the right-hand time constant of (71). The free parameter can be determined to $C = 1$ with the help of the initial condition $G(j0)=1$.

With $\sigma = \frac{1}{\tau_1} = \frac{1}{2\tau_1} = \frac{\kappa_0}{\epsilon_0} = \omega_1$ as well as $\Omega = \frac{\omega}{\omega_1}$ and $\theta = \frac{\Omega}{1+\Omega^2}$ applies:

$$G(\sigma + j\omega) = \frac{1}{(\sigma + j\omega)\tau_1} e^{1 - \frac{1}{(\sigma + j\omega)\tau_1}} \quad (101)$$

$$G(j\omega) = \frac{\omega_1}{\omega_1 + j\omega} e^{1 - \frac{\omega_1}{\omega_1 + j\omega}} = \frac{1}{1 + j\Omega} e^{\frac{j\Omega}{1 + j\Omega}} = \frac{1 - j\Omega}{1 + \Omega^2} e^{\frac{j\Omega(1 - j\Omega)}{1 + \Omega^2}} \quad (102)$$

That yields the following expression (complex frequency response):

$$G(j\omega) = \left[\cos\theta + \Omega \sin\theta + j \sin\theta - \Omega \cos\theta \right] \frac{e^{\frac{\Omega^2}{1+\Omega^2}}}{1+\Omega^2} \quad (103)$$

The locus curve of frequency response in comparison with the one of a generic low pass is shown in Figure 15. Since both curves don't cut the y-axis, there is no aperiodic borderline case in this system.

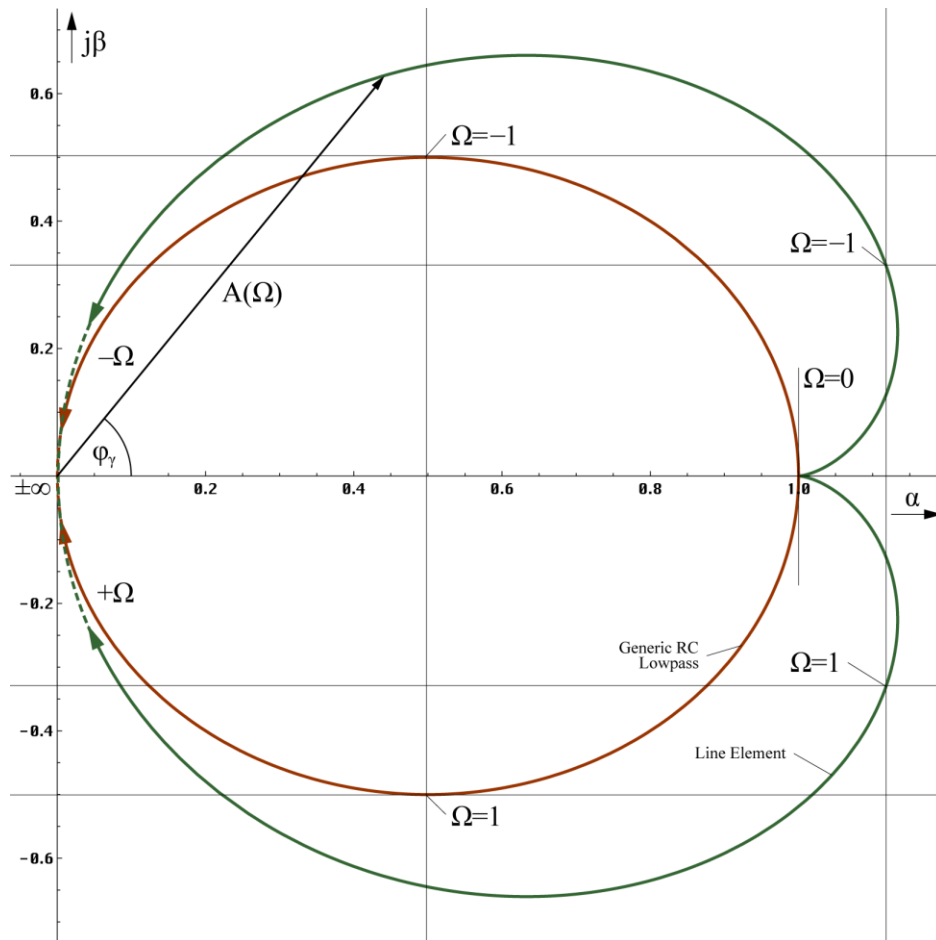


Figure 15:
Frequency Response Locus Curve

For frequency and phase response we get further

$$A(\omega) = \frac{1}{\sqrt{1+\Omega^2}} e^{\frac{\Omega^2}{1+\Omega^2}} \quad (104)$$

$$B(\omega) = \arctan \frac{\sin\theta - \Omega \cos\theta}{\cos\theta + \Omega \sin\theta} = -\arctan \Omega + \frac{\Omega}{1+\Omega^2} = \varphi_\gamma \quad (105)$$

We have got the right-hand expression of (105) by means of subtle application of the corresponding addition theorems and substitution. In this connection $-\arctan \Omega$ relates to the I-share, θ to the inverse T-share. Both functions (BODE-diagram) are depicted in Figure 16. The damping course (-6 dB/decade) points to a system of 2^{nd} order.

Interesting is the cosine of the phase response $\cos B(\omega) = \cos \varphi_\gamma$ as well. This value is used e.g. in the electrotechnics for the calculation of efficiency (power). It figures the size of the mutual coupling factor of the separate MLE's. Interestingly enough, because of $\cos \varphi = \cos(-\varphi)$, this value is not affected by the above mentioned error in (82).

$$\cos \varphi_\gamma = \cos \left(-\arctan \Omega + \frac{\Omega}{1+\Omega^2} \right) = \cos \left(\arctan \Omega - \frac{\Omega}{1+\Omega^2} \right) \quad (106)$$

Then equation (103) also can be written in the following manner:

$$G(j\omega) = (\cos \varphi_\gamma + j \sin \varphi_\gamma) \frac{1}{\sqrt{1+\Omega^2}} e^{\frac{\Omega^2}{1+\Omega^2}} = e^{\frac{\Omega^2}{1+\Omega^2} - \frac{1}{2} \ln(1+\Omega^2) + j\varphi_\gamma} \quad (107)$$

Figure 16, the BODE-diagram shows frequency- and phase-response up to $\omega_1/10$, after expansion until $\omega_0/10$, that's at least $1.855 \cdot 10^{42} \text{s}^{-1}$ resp. $2.952 \cdot 10^{41} \text{Hz}$, to be equal to 1 (0dB) constantly, exactly as observed. Technically speaking we are light-years away from the upper limit. There is also a lower cut-off frequency given by the requirement, that the wave length $\lambda_{\min} = 2cT$ must fit the universe's extension. The value ω_{\min} is equal to the HUBBLE-parameter H_0 , as can easily be proved.

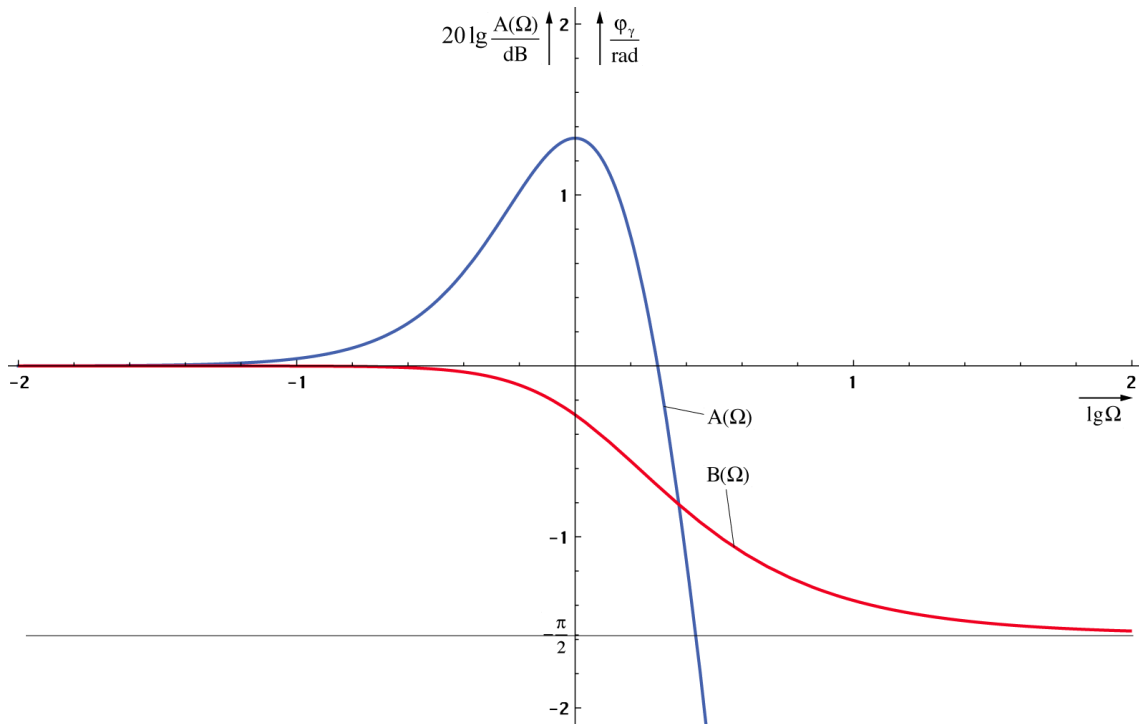


Figure 16:
Bode-Diagram: Frequency Response $A(\omega)$
and Phase Response $B(\omega)$ of the System

The course of $\cos \varphi_\gamma$ is shown in Figure 17. Furthermore the course of the second term in φ_γ is depicted. You can see that it only takes effect from frequencies near ω_1 onwards.

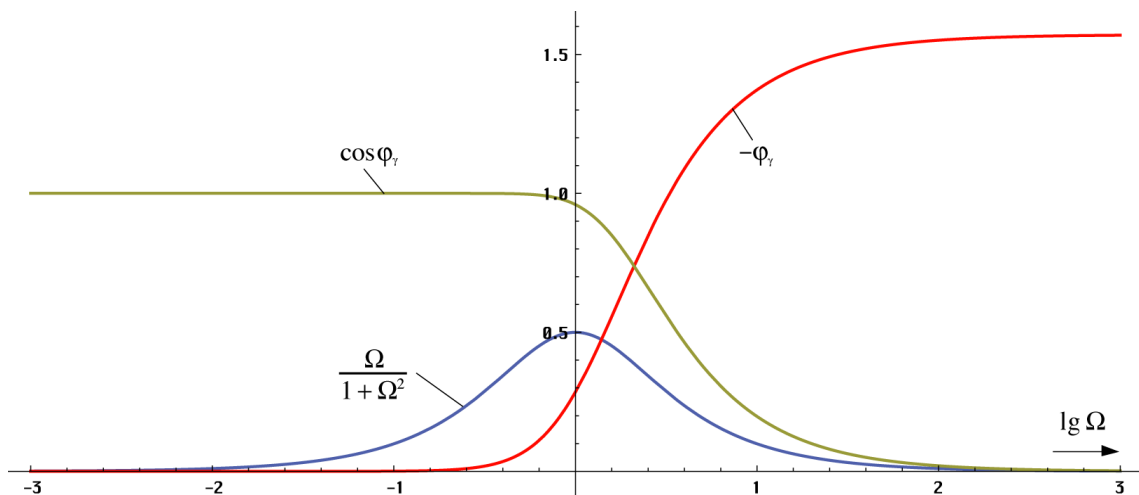


Figure 17:
Course of Phase Angle,
 $\cos \varphi$ and of the Expression θ

Finally, the phase- and group delay in dependence on the frequency should be examined. Both functions are depicted in Figure 18. They are defined in the following manner:

$$T_{\text{Ph}} = \frac{B(\omega)}{\omega} = -\frac{1}{\omega} \left(\arctan \Omega - \frac{\Omega}{1+\Omega^2} \right) \quad \text{Phase delay} \quad (108)$$

$$T_{\text{Gr}} = \frac{d}{d\omega} B(\omega) = -\frac{2}{\omega_1} \left(\frac{\Omega}{1+\Omega^2} \right)^2 = -2 \frac{\theta^2}{\omega_1} \quad \text{Group delay} \quad (109)$$

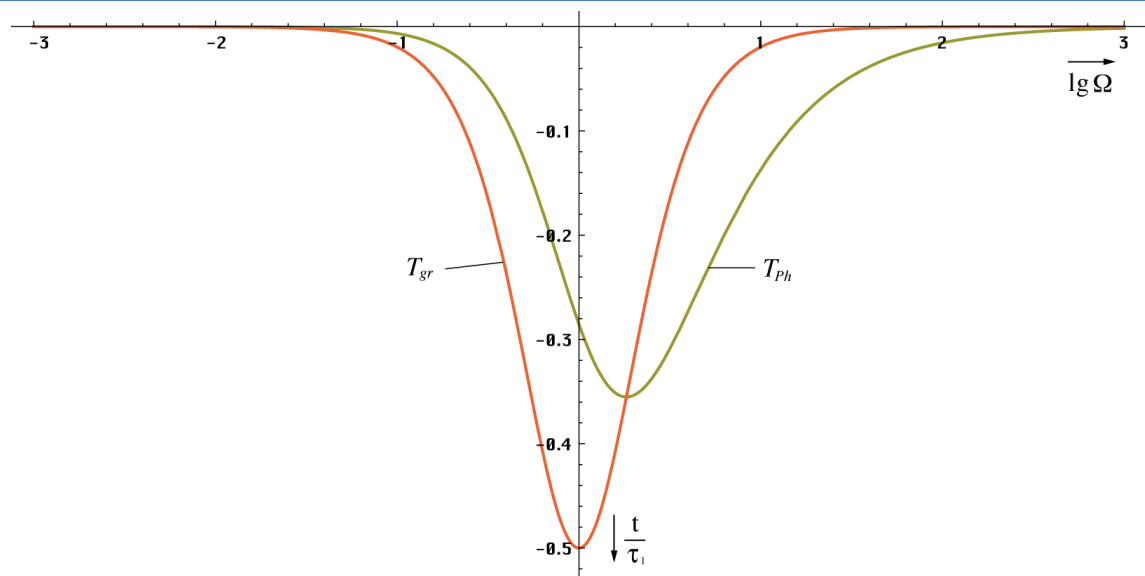


Figure 18:
Group- and Phase Delay

It are the same functions as with the wrong solution, but just negative. Are negative delay times physically possible? The answer is – Yes. That comes about very frequently in techno-logy and is not a breach of causality. See [50] for details.

3.3.4. Properties of the model

The following statements are applied to one single MLE only. More exact statements for wave-propagation as such are worked out later. You can see here quite clearly that frequency- and phase-response proceed approximately exact straight-line (0 dB) until one third of the frequency ω_1 and that phase-true. A noticeable attenuation and phase-shift does not occur until approximate one tenth of ω_1 . Since the amount of ω_1 is so extremely high (the supreme measured frequency, cosmic radiation is about 10^{42} Hz), this effect does not have been observed so far however.

The amplitude ascends around ω_1 , only to descend again irrevocably (Figure 16). There actually turns out a slight high-pass-behaviour within a low-pass. However, since the value $\cos \phi_\gamma$ strongly declines above $\omega_1/2$ (Figure 17), and with it the mutual coupling coefficient of the MLEs, both influences cancel each other, a mere hillock remains (Figure 19).

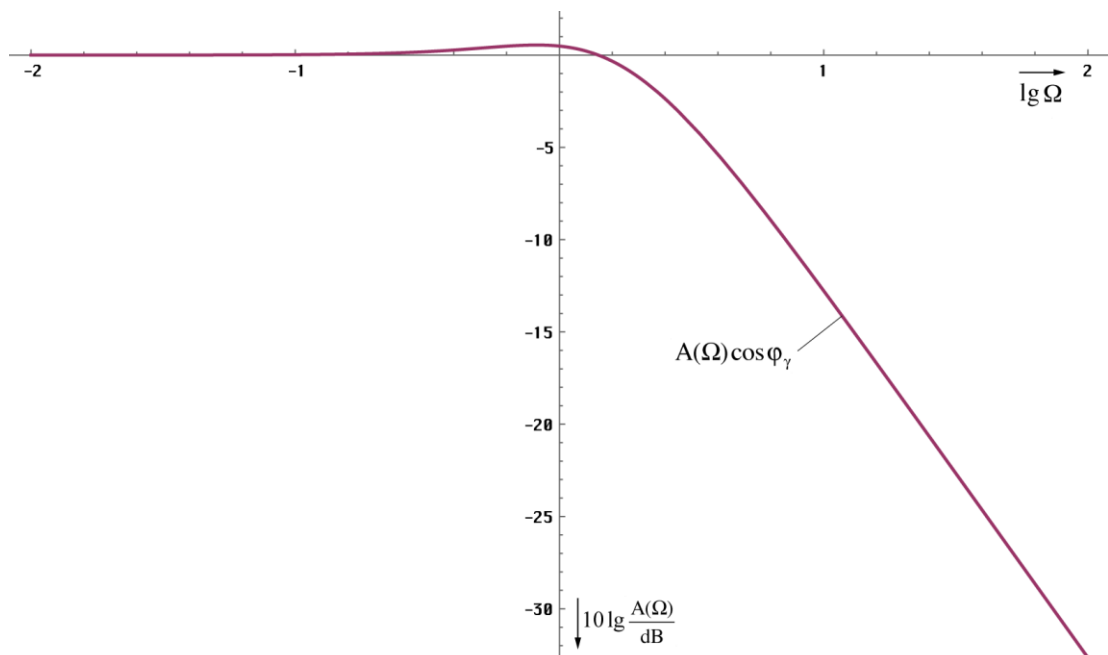


Figure 19:
Frequency Response for the Transfer
to the Adjacent MLE

The frequency response across two MLE's with the coupling coefficient $k = \cos\phi_\gamma$ is shown in Figure 19. The damping course (-12dB/decade) points to the fact, that it's about a group-delay-corrected low pass of 2nd order. The expression $1 + \Omega^2$ even occurs in the filter-theory and corresponds to the form-factor of a calibrated equally-tuned dual-circuit filter with identical attenuation-course [26].

With respect to the sampling-theorem we expect, that only frequencies below $\omega_0/2$ are transferred. Strictly speaking, the previous statements apply to the universal wave-field only in accordance with [1]. The propagation of radio waves or photons, as we understand, in reality takes place as propagation of interferences of this wave-field. Since the MLE's figure non-linear systems, several side frequencies occur. But only the sum- and difference-frequency $\omega_0 \pm \omega$ are important. With the other frequencies, no power-conversion is achieved (property of a non-linear circuit). But for the cut-off frequency of overlaid signals only the sum frequency is relevant. Since overlaid signals are being more red-shifted than the universal wave-field, the »relative cut-off frequency«, i.e. the spacing between the overlaid frequency ω and the cut-off frequency $\omega_0/2$, ascends continuously with rising age.

The course of group delay shows that the »processing« of changes in the magnetic induction of lower frequencies actually takes place »instantaneously«. The transfer to the adjacent MLE takes place on the basis of a resonance-coupling with a phase-shift of $\pi/2 = \omega_0 t_v$. For the delay time t_v we get the following expression then: $t_v = \pi / (2\omega_0) = \pi r_0 / (2c)$. For the transfer rate of \underline{c} (the half circumference of the field-line of the vector \mathbf{H}_0 proceeding through the centre of the track graphs of both MLE's is equal to $\pi r_0/2$), we receive an amount of:

$$c = \frac{\pi r_0}{2 t_v} = \frac{1}{\sqrt{\mu_0 \epsilon_0}} = c \quad (110)$$

With it, the vacuum-wave-propagation-velocity directly arises from the phase-shift $\pi/2$, which comes about with magnetic resonance-coupling of two oscillatory circuits. This effect even can be observed in technology with discrete components, which is figured in [26] extensively. With frequencies near ω_1 , the phase delay T_{Ph} , multiplied with 2π , has to be added to t_v . However, an accurate formula for \underline{c} for this case (critical photons) cannot be stated at this point, because we consider the single MLE only. We will work out an exact expression for the wave-propagation-velocity in Section 4.3.2.5. being valid near $t=0$ as well.

Further, we can say, that the propagation-velocity c decreases the more approaching to ω_1 . However, this value exactly corresponds to that value, at which the track-curve (Figure 7) is no longer defined. A phase-transition occurs, the rotation ends. There is only the straight-line-expansion then.

With it the phase-shift to the adjacent MLE also adds up and achieves a value of π , a destructive interference appears, a wave-propagation isn't possible at all (coupling-factor $k = \cos(\pi/2) = 0$). Furthermore, c and also the wave impedance \underline{Z} become complex, with the effect, that real and imaginary part take on the same value. That's the case of an electrically conductive medium.

All that arises from the going smaller and smaller value of R_0 , resulting from descending r_0 , and the Q-factor. That means, the impedance achieves the magnitude of the complex impedances X_C and X_L short-circuiting them more and more. Above ω_0 , R_0 only determines the behaviour of the system then (electric conductor). However this is not applied to the wave-field as such. Reverse behaviour appears here. Near $t=0$ as well as $\omega = \omega_0$, the field-wave impedance behaves like a non-conductor. First at larger distance, the behaviour approaches the one of an ideal conductor, as we will still see later. Decisive for it is the mutual coupling-factor of the MLE's however.

Now a wave-propagation-velocity different from c does not contradict our primary assumption $c = \text{const}$ and nor the SRT for so long, while its value is smaller or equal to c . This is always guaranteed even with frequencies near ω_1 respectively in the time just after the big bang. The previous results don't just stand in contradiction to prevailing discoveries.

4. Propagation function

First, we will briefly review the classical theory of MAXWELL's equations in order to work out -using analogies - an alternative solution that meets the requirements of our model. The equation-system (111) is under-determined, so that there is more than one solution fulfilling these equations.

4.1. Classic solution for a loss-free medium

In accordance with the previous discoveries, the cosmic vacuum seems to be a loss-free medium. It applies $\rho = 0$ (space-charge-density) as well as $\kappa = 0$. To the reminiscence here the MAXWELL equations once again:

$\text{div } \mathbf{B} = 0$	$\text{div } \mathbf{D} = \rho$	$\nabla \cdot \mathbf{F} = \text{div } \mathbf{F}$	(111)
$\text{curl } \mathbf{E} = -\dot{\mathbf{B}}$	$\text{curl } \mathbf{H} = \mathbf{i} + \dot{\mathbf{D}}$	$\nabla \times \mathbf{F} = \text{rot } \mathbf{F} = \text{curl } \mathbf{F}$	
		$\nabla = (\partial/\partial x, \partial/\partial y, \partial/\partial z)$	
		$\Delta = (\partial^2/\partial x^2, \partial^2/\partial y^2, \partial^2/\partial z^2)$	
		Laplace	

Furthermore applies:

$$\begin{aligned}
\mathbf{D} &= \varepsilon \mathbf{E} & \mathbf{B} &= \mu \mathbf{H} & \mathbf{i} &= \kappa \mathbf{E} \\
\text{curl } \mathbf{E} &= -\mu \dot{\mathbf{H}} & \text{curl } \mathbf{H} &= \varepsilon \dot{\mathbf{E}} & & \\
\text{curl } \mathbf{E} &= -\mu \frac{\partial \mathbf{H}}{\partial t} & \text{curl } \mathbf{H} &= \varepsilon \frac{\partial \mathbf{E}}{\partial t} & &
\end{aligned} \tag{112}$$

The solution will be skipped here because I presume that it is known to the reader, if not, see [29]. Finally, we receive for $\mu_r = \varepsilon_r = 1$

$$\Box \mathbf{E} = \frac{1}{c^2} \frac{\partial^2 \mathbf{E}}{\partial t^2} - \Delta \mathbf{E} = 0 \qquad \Box \mathbf{H} = \frac{1}{c^2} \frac{\partial^2 \mathbf{H}}{\partial t^2} - \Delta \mathbf{H} = 0 \tag{113}$$

\Box is the D'ALEMBERT-operator. Simplified with propagation in x-direction only:

$$\frac{d^2 \mathbf{E}}{dx^2} = \mu_0 \varepsilon_0 \frac{d^2 \mathbf{E}}{dt^2} \qquad \frac{d^2 \mathbf{H}}{dx^2} = \mu_0 \varepsilon_0 \frac{d^2 \mathbf{H}}{dt^2} \tag{114}$$

After division by $d^2 \mathbf{E}$ resp. $d^2 \mathbf{H}$, multiplication with dx^2 , division by $\mu_0 \varepsilon_0$ and subsequent extraction of the square-root, we will receive the known expressions for the wave-propagation-velocity \underline{c} (phase- and group velocity) as well as the field-wave-impedance $\underline{Z}_F = \mu_0 \underline{c}$:

$$\underline{c} = \frac{dx}{dt} = \frac{1}{\sqrt{\mu_0 \varepsilon_0}} = c \qquad \underline{Z}_F = \sqrt{\frac{\mu_0}{\varepsilon_0}} = Z_0 \tag{115}$$

The underlinings stand for complex values. Since the product $\mu_r \varepsilon_r$ is always larger than 1, the maximum wave-propagation-velocity is equal to c . It has an all-pass-behaviour on hand, no lower cut-off frequency exists and the wave-propagation-velocity is independent from the frequency. For the propagation rate $\underline{\gamma}$ applies:

$$\underline{\gamma} = \alpha + j\beta = \pm j\omega / \underline{c} = \pm j\omega \sqrt{\mu_0 \varepsilon_0} \tag{116}$$

In this connection is α the attenuation rate ($\alpha=0$) and β the phase-rate. Except for the geometrical attenuation ($\mathbf{S} \sim r^{-2}$) in this case just no additional attenuation appears. Then, for the propagation-function (into x-direction) we get (analogously for \mathbf{H}):

$$\underline{\mathbf{E}} = \mathbf{E} e^{j\omega(t-x/c)} = \mathbf{E} e^{j\omega t - \underline{\gamma} x} \tag{117}$$

This solution is good for normal extents, which normally occur in nature, but fails with the Supernova Ia cosmology project at $x \geq 260669 \text{ Mpc}$ ($z \geq 0.1$). The reason is that this model does not take into account, imply, or condition either expansion or cosmological redshift in any way.

4.2. Classic solution for a loss-affected medium

At a loss-affected medium (e.g. water) $\rho=0$ applies as well as $\kappa > 0$. $\underline{\mathbf{E}}$ and $\underline{\mathbf{H}}$ are understood as complex time-functions. Equation (112) is then:

$$\text{curl } \underline{\mathbf{E}} = -\mu \frac{\partial \underline{\mathbf{H}}}{\partial t} \qquad \text{curl } \underline{\mathbf{H}} = \left(\kappa + \varepsilon \frac{\partial}{\partial t} \right) \frac{\partial \underline{\mathbf{E}}}{\partial t} \tag{118}$$

When propagating in x direction only, it leads to the following solution:

$$\frac{d^2 \underline{\mathbf{E}}}{dx^2} = \left(\mu \left(\frac{\omega \varepsilon - j\kappa}{\omega} \right) \right) \frac{d^2 \underline{\mathbf{E}}}{dt^2} \qquad \frac{d^2 \underline{\mathbf{H}}}{dx^2} = \left(\mu \left(\frac{\omega \varepsilon - j\kappa}{\omega} \right) \right) \frac{d^2 \underline{\mathbf{H}}}{dt^2} \tag{119}$$

That would be a case with $\Box \mathbf{E} \neq 0$ and $\Box \mathbf{H} \neq 0$ then. For $\mu_r = \varepsilon_r = 1$, we get after division by $d^2 \underline{\mathbf{E}}$ as well as $d^2 \underline{\mathbf{H}}$, multiplication with dx^2 , division by the double bracketed expression, deparenthesizing of $-j$ and extraction of the root the known expressions for the propagation-velocity $\underline{c} = dx/dt$ and for the field-wave impedance \underline{Z}_F :

$$\underline{c} = \sqrt{\frac{j\omega}{\mu_0(\kappa + j\omega\varepsilon_0)}} \qquad \underline{Z}_F = \sqrt{\frac{j\omega\mu_0}{\kappa + j\omega\varepsilon_0}} \tag{120}$$

The propagation-function is the same like (117) however with the variant values for α and β (121). For $\kappa=0$ this solution passes into case 4.1. The propagation-velocity is dependent on κ and ω and amounts to c at most. There is a lower cut-off frequency. Since $\alpha \neq 0$, an additional attenuation of the electromagnetic field-strength (POYNTING-vector) appears to the geometrical one. With extreme values of κ , nonlinear distortions occur because of different group- and phase velocity.

$$\alpha = \frac{\omega}{c} \sinh\left(\frac{1}{2} \operatorname{arsinh} \frac{\kappa}{\omega \varepsilon_0}\right) \quad \beta = \frac{\omega}{c} \cosh\left(\frac{1}{2} \operatorname{arsinh} \frac{\kappa}{\omega \varepsilon_0}\right) \quad (121)$$

This solution describes wave-propagation in a medium of whatever qualities and zero space-charge-density. In no way, it describes the type of wave propagation that we observe in a vacuum. One application would be the propagation in water or in a plasma. But then $\mu_r \neq \varepsilon_r \neq 1$ applies and we have to leave out the zeros in (120).

If we apply the value κ_0 for κ , then there is no wave propagation at all, since we are at the transition to the aperiodic borderline case then. This is examined in more detail in [29] Section 4.6.5.2. A hypothetical EM wave already extinguishes after about 3 periods. This means, EM waves cannot propagate independently, but only with the help of a specific medium, for example the metric wave field. This solution also explains neither the expansion nor the cosmological redshift.

4.3. Solution for a medium with expansion and overlaid EM-wave

In order to be able to specify the propagation function of an overlaid EM wave, we must first determine the propagation function of the subjacent metric wave as transport layer, since both are wave functions, competing with respect to subspace. Now to the solution.

4.3.1. Propagation function of the metric wave field

In contrast to MAXWELL, which used the first term of the harmonic solution $e^{j\omega t}$ as ansatz, we choose the first term of expression (93), obtained as an independent solution of the differential equation (72). It's about the temporal function of the magnetic flux φ_0 there, relating to one single MLE, from which the charge q_0 can be derived. For the propagation function however we need the magnetic and electric field strength \mathbf{H} and \mathbf{E} . The relation:

$$\varphi = \int_A \mathbf{B} dA \quad \text{with } \mathbf{B} = \mu_0 \mathbf{H} \quad \text{leads to} \quad |\mathbf{H}| = \frac{\hat{\varphi}_0}{\mu_0 r_0^2} \quad (122)$$

Because of r_0 indeed the right-hand expression depends on the frame of reference. Moreover we are rather looking for the starting value at $T=0$. The temporal function is just known. Hence, we must carry out a reference-frame-independent coupling only. The coupling-length r_k is not arbitrary in this case. Because the imaginary part of the Hankel function is coming from infinity, the starting value φ_0 is defined at the point $2\omega_0 t = Q_0 = 1$. The coupling-length at this point is r_1 as already predicted more above. This value is denominated as \mathbf{H}_1 and \mathbf{E}_1 . With respect to the fact, that (97) is an effective value, we obtain the following relations:

$$\mathbf{E}_1 = \frac{q_1}{\varepsilon_0 r_1^2} \sqrt{2} = \frac{1}{Z_0} \frac{\varphi_0}{\varepsilon_0 r_0^2} \sqrt{2} \quad \mathbf{H}_1 = \frac{\varphi_0}{\mu_0 r_0^2} \sqrt{2} \quad (123)$$

$$\underline{\mathbf{E}} = \mathbf{E}_1 H_0^{(1)}(2\omega_0 t) \quad \underline{\mathbf{H}} = \mathbf{H}_1 H_0^{(1)}(2\omega_0 t) \quad (124)$$

Here again, the real part of the vector corresponds to an orientation in y-, the imaginary one in z-direction, x is the propagation direction. As already stated, there is an analogy between the exponential function $e^{j2\omega t}$ and the Hankel function. Both are transcendent complex functions and periodic respectively almost periodic. $\underline{\mathbf{E}}$ and $\underline{\mathbf{H}}$ are understood as complex time-functions again. We start with the same values as in the previous case: $\rho=0$ as well as $\kappa_0 > 0$. Since in the time just after big bang there is a pure radiation-cosmos and because we are considering the MLE, just the empty space, here the vacuum solution only can be of interest anyway. Equation (112) reads then:

$$\operatorname{rot} \underline{\mathbf{E}} = -\mu_0 \frac{\partial \underline{\mathbf{H}}}{\partial t} \quad \operatorname{rot} \underline{\mathbf{H}} = \left(\kappa_0 + \varepsilon_0 \frac{\partial}{\partial t} \right) \underline{\mathbf{E}} \quad (125)$$

We continue in that we substitute with the first term of equation (93). The coupling-length of r_k cannot be chosen freely. Because the imaginary part of the Hankel function comes from in-finity the initial value of φ is defined at the point $2\omega_0 t = Q_0 = 1$. The coupling-length there is r_1 .

$$\underline{\mathbf{E}} = \mathbf{E} H_0^{(1)}(2\omega_0 t) \quad \underline{\mathbf{H}} = \mathbf{H} H_0^{(1)}(2\omega_0 t) \quad (126)$$

In this connection again, the real-part corresponds to the vector's orientation in y, the imaginary-part to the one in z-direction, while x is the propagation direction. As already noticed, an analogy exists among the exponential-function $e^{j2\omega_0 t}$ and the Hankel function. Both are transcendent complex functions being periodic respectively nearly periodic. In the following, we want to find out, whether this base leads to a solution of the MAXWELL equations too. It is however to mark that ω_0 is time-dependent in this case. Therefore we will first work with the correct time-functions:

$$\underline{\mathbf{E}} = \mathbf{E} H_0^{(1)} \sqrt{\frac{2\kappa_0 t}{\varepsilon_0}} \quad \underline{\mathbf{H}} = \mathbf{H} H_0^{(1)} \sqrt{\frac{2\kappa_0 t}{\varepsilon_0}} \quad (127)$$

Let's proceed now like in 5.2. (analogously for $\underline{\mathbf{H}}$):

$$\frac{\partial \underline{\mathbf{E}}}{\partial t} = -\frac{2\kappa_0}{2\varepsilon_0} \sqrt{\frac{\varepsilon_0}{2\kappa_0 t}} \mathbf{E} H_1^{(1)} \sqrt{\frac{2\kappa_0 t}{\varepsilon_0}} = -\sqrt{\frac{\kappa_0}{2\varepsilon_0 t}} \mathbf{E} H_1^{(1)} \sqrt{\frac{2\kappa_0 t}{\varepsilon_0}} \quad (128)$$

The minus sign is caused by the derivative of the Hankel-function. Furthermore applies, according to the calculating rules for cylinder-functions [22]:

$$\frac{\partial \underline{\mathbf{E}}}{\partial t} = -\omega_0 \mathbf{E} H_1^{(1)}(2\omega_0 t) = -\omega_0^2 t \mathbf{E} (H_0^{(1)}(2\omega_0 t) + H_2^{(1)}(2\omega_0 t)) \quad (129)$$

$$\frac{\partial \underline{\mathbf{H}}}{\partial t} = -\omega_0 \mathbf{H} H_1^{(1)}(2\omega_0 t) = -\omega_0^2 t \mathbf{H} (H_0^{(1)}(2\omega_0 t) + H_2^{(1)}(2\omega_0 t)) \quad (130)$$

As next, we de-parenthesize the expression for the Hankel-function of 0th order so, because of (126), we can write for the first derivative as expression of the original-function:

$$\frac{\partial \underline{\mathbf{E}}}{\partial t} = -\omega_0^2 t \left(1 + \frac{H_2^{(1)}(2\omega_0 t)}{H_0^{(1)}(2\omega_0 t)} \right) \underline{\mathbf{E}} \quad \frac{\partial \underline{\mathbf{H}}}{\partial t} = -\omega_0^2 t \left(1 + \frac{H_2^{(1)}(2\omega_0 t)}{H_0^{(1)}(2\omega_0 t)} \right) \underline{\mathbf{H}} \quad (131)$$

We require the second derivatives as well. These we determine to the best, in that we differentiate the right expression of (128) once again (analogously for $\underline{\mathbf{H}}$):

$$\frac{\partial^2 \underline{\mathbf{E}}}{\partial t^2} = -\frac{\partial}{\partial t} \left(\sqrt{\frac{\kappa_0}{2\varepsilon_0 t}} H_1^{(1)} \sqrt{\frac{2\kappa_0 t}{\varepsilon_0}} \right) \mathbf{E} = -(\dot{u}v + u\dot{v}) \mathbf{E} \quad (132)$$

For u and v , we get the following expressions:

$$u = \omega_0 \quad \dot{u} = -\frac{\omega_0}{2t} \quad (133)$$

$$v = H_1^{(1)}(2\omega_0 t) = \omega_0 t H_0^{(1)}(2\omega_0 t) + H_2^{(1)}(2\omega_0 t) \quad (134)$$

$$\dot{v} = \omega_0 H_2^{(1)}(2\omega_0 t) - \frac{1}{2t} H_1^{(1)}(2\omega_0 t) = -\frac{\omega_0}{2} H_0^{(1)}(2\omega_0 t) - H_2^{(1)}(2\omega_0 t) \quad (135)$$

Replacement of the second expression of (132) results in:

$$\frac{\partial^2 \underline{\mathbf{E}}}{\partial t^2} = \omega_0^2 H_0^{(1)}(2\omega_0 t) \underline{\mathbf{E}} = \omega_0^2 \underline{\mathbf{E}} \quad (136)$$

$$\frac{\partial^2 \underline{\mathbf{H}}}{\partial t^2} = \omega_0^2 H_0^{(1)}(2\omega_0 t) \underline{\mathbf{H}} = \omega_0^2 \underline{\mathbf{H}} \quad (137)$$

Now, we put (131) into (125) obtaining:

$$\text{curl } \underline{\mathbf{H}} = \left(\kappa_0 + \varepsilon_0 \frac{\partial}{\partial t} \right) \underline{\mathbf{E}} = \left(\kappa_0 - \varepsilon_0 \omega_0^2 t \left(1 + \frac{H_2^{(1)}(2\omega_0 t)}{H_0^{(1)}(2\omega_0 t)} \right) \right) \underline{\mathbf{E}} \quad (138)$$

Expression (138) even can be written more simple:

$$\text{curl } \underline{\mathbf{H}} = \varepsilon_0 \omega_0^2 t \left(\frac{\kappa_0}{\varepsilon_0 \omega_0^2 t} - \left(1 + \frac{H_2^{(1)}(2\omega_0 t)}{H_0^{(1)}(2\omega_0 t)} \right) \right) \underline{\mathbf{E}} \quad (139)$$

$$\text{curl } \underline{\mathbf{H}} = \varepsilon_0 \omega_0^2 t \left(2 - \left(1 + \frac{H_2^{(1)}(2\omega_0 t)}{H_0^{(1)}(2\omega_0 t)} \right) \right) \underline{\mathbf{E}} \quad (140)$$

$$\text{curl } \underline{\mathbf{H}} = \varepsilon_0 \omega_0^2 t \left(1 - \frac{H_2^{(1)}(2\omega_0 t)}{H_0^{(1)}(2\omega_0 t)} \right) \underline{\mathbf{E}} \quad (141)$$

For $\text{curl } \underline{\mathbf{E}} = -\mu_0 \frac{\partial \underline{\mathbf{H}}}{\partial t}$ we obtain by substitution immediately:

$$\text{curl } \underline{\mathbf{E}} = \mu_0 \omega_0^2 t \left(1 + \frac{H_2^{(1)}(2\omega_0 t)}{H_0^{(1)}(2\omega_0 t)} \right) \underline{\mathbf{H}} \quad (142)$$

We apply the rotation-operation to both sides again:

$$\text{curl curl } \underline{\mathbf{H}} = \text{curl} \left(\varepsilon_0 \omega_0^2 t \left(1 - \frac{H_2^{(1)}(2\omega_0 t)}{H_0^{(1)}(2\omega_0 t)} \right) \underline{\mathbf{E}} \right) = \varepsilon_0 \omega_0^2 t \left(1 - \frac{H_2^{(1)}(2\omega_0 t)}{H_0^{(1)}(2\omega_0 t)} \right) \text{curl } \underline{\mathbf{E}} \quad (143)$$

$$\text{curl curl } \underline{\mathbf{H}} = \mu_0 \varepsilon_0 \omega_0^4 t^2 \left(1 - \frac{H_2^{(1)}(2\omega_0 t)}{H_0^{(1)}(2\omega_0 t)} \right) \left(1 + \frac{H_2^{(1)}(2\omega_0 t)}{H_0^{(1)}(2\omega_0 t)} \right) \underline{\mathbf{H}} = -\Delta \underline{\mathbf{H}} \quad (144)$$

$$\text{curl curl } \underline{\mathbf{H}} = \frac{\omega_0^2}{c^2} \omega_0^2 t^2 \left(1 - \left(\frac{H_2^{(1)}(2\omega_0 t)}{H_0^{(1)}(2\omega_0 t)} \right)^2 \right) \underline{\mathbf{H}} = -\Delta \underline{\mathbf{H}} \quad (145)$$

The result for $\underline{\mathbf{E}}$ is analogous. We continue like in Section 4.2.:

$$\Delta \underline{\mathbf{E}} = -\frac{\omega_0^2 t^2}{c^2} \left(1 - \left(\frac{H_2^{(1)}(2\omega_0 t)}{H_0^{(1)}(2\omega_0 t)} \right)^2 \right) (\omega_0^2 \underline{\mathbf{E}}) = -\frac{\omega_0^2 t^2}{c^2} \left(1 - \left(\frac{H_2^{(1)}(2\omega_0 t)}{H_0^{(1)}(2\omega_0 t)} \right)^2 \right) \frac{\partial^2 \underline{\mathbf{E}}}{\partial t^2} \quad (146)$$

$$\Delta \underline{\mathbf{H}} = -\frac{\omega_0^2 t^2}{c^2} \left(1 - \left(\frac{H_2^{(1)}(2\omega_0 t)}{H_0^{(1)}(2\omega_0 t)} \right)^2 \right) (\omega_0^2 \underline{\mathbf{H}}) = -\frac{\omega_0^2 t^2}{c^2} \left(1 - \left(\frac{H_2^{(1)}(2\omega_0 t)}{H_0^{(1)}(2\omega_0 t)} \right)^2 \right) \frac{\partial^2 \underline{\mathbf{H}}}{\partial t^2} \quad (147)$$

With propagation only into x-direction, the partial derivatives for y and z will be zero again and it applies $\Delta = d^2/dx^2$ (analogously for $\underline{\mathbf{H}}$):

$$\frac{\partial^2 \underline{\mathbf{E}}}{\partial x^2} = -\frac{\omega_0^2 t^2}{c^2} \left(1 - \left(\frac{H_2^{(1)}(2\omega_0 t)}{H_0^{(1)}(2\omega_0 t)} \right)^2 \right) \frac{\partial^2 \underline{\mathbf{E}}}{\partial t^2} \quad (148)$$

After rearrangement, we finally get for the wave-propagation-velocity \underline{c} and field-wave-impedance \underline{Z}_F :

$$\underline{c} = \frac{c}{j\omega_0 t} \frac{1}{\sqrt{1 - \left(\frac{H_2^{(1)}(2\omega_0 t)}{H_0^{(1)}(2\omega_0 t)} \right)^2}} \quad \text{with} \quad \Theta = \frac{H_2^{(1)}(Q_0)}{H_0^{(1)}(Q_0)} \quad Q_0 = 2\omega_0 t \quad (149)$$

$$\underline{c} = \frac{c}{j\omega_0 t} \frac{1}{\sqrt{1 - \Theta^2}} \quad \underline{Z}_F = \frac{Z_0}{j\omega_0 t} \frac{1}{\sqrt{1 - \Theta^2}} \quad (150)$$

We see that the propagation-velocity converges to zero for large t. The same is applied to the field-wave impedance too. We have to do it with a quasi-stationary wave-field (standing wave) filling very well the requests on a metrics. The propagation-velocity is complex again. A decomposition into real- and imaginary-part works out quite difficult, but it's mathematically possible however. The solution for \underline{c} reads:

$$A = \frac{J_0(Q_0)J_2(Q_0) + Y_0(Q_0)Y_2(Q_0)}{J_0^2(Q_0) + Y_0^2(Q_0)} \quad \rho_0 = \frac{1}{2} \sqrt{4(1-A^2+B^2)^2 + (2AB)^2} \quad \text{For programming reasons expression (152) turns out a slightly different result than expression (151) with AB. In order to maximize accuracy only the functions (152) are used.} \quad (151)$$

$$B = \frac{J_2(Q_0)Y_0(Q_0) - J_0(Q_0)Y_2(Q_0)}{J_0^2(Q_0) + Y_0^2(Q_0)} \quad \rho_0 = \frac{1}{2} \left| \sqrt{1 - \Theta^2} \right| \quad \theta = \frac{2AB}{1 - A^2 + B^2}$$

$$\frac{1}{\rho_0 Q_0} = \frac{c_M}{c} = \frac{1}{Q_0} \left| \frac{2}{\sqrt{1 - \Theta^2}} \right| \quad \text{RhoQ} = 2 / \# / \text{Abs}[\text{Sqrt}[1 - (\text{HankelH1}[2, \#] / \text{HankelH1}[\theta, \#])^2]] \& \quad (152)$$

$$\phi_0 = \frac{1}{2} \arctan \theta = \arg \left[\frac{1}{\sqrt{1 - \Theta^2}} \right] - \frac{\pi}{2} \quad \text{PhiQ} = \text{Arg}[1 / \text{Sqrt}[1 - (\text{HankelH1}[2, \#] / \text{HankelH1}[\theta, \#])^2]] - \pi / 2 \&$$

The factor 1/2 arises from the 4th root. Expression (149) may be split into a real- and an imaginary part (153). A starts at $+\infty$ converging to -1. The course resembles the function $1/A^2 - 1$ approximately, which cannot be used well as approximation however. B has a course like $1/B^2$ and is converging to zero. The same is applied to θ then. The bracketed expression converges to one with it. For $Q_0 \geq 5$ the approximation $\rho_0^2 Q_0^2 \approx Q_0$ applies with $\Delta \leq 1\%$.

$$\underline{c} = \frac{c}{\rho_0 Q_0} \left(\cos \frac{1}{2} \arctan \theta + j \sin \frac{1}{2} \arctan \theta \right) = \frac{c}{\rho_0 Q_0} e^{j \frac{1}{2} \arctan \theta} = \frac{c}{\rho_0 Q_0} e^{j \phi_0} \quad (153)$$

Unfortunately (153) cannot be transformed into an expression similar to (121) with area-functions, so that the ambiguity of the arctan-function leads to a partially wrong result. Thus we should better calculate with the following substitution:

$$\arctan \theta = \arg((1 - A^2 + B^2) + j2AB) \quad \arg \underline{c} = \frac{1}{2} \operatorname{arccot} \theta - \frac{\pi}{4} \quad (154)$$

While the real-part of \underline{c} is defined as the velocity in propagation direction, the imaginary-part can be interpreted as a velocity rectangular thereto. The appearance of an imaginary part in \underline{c} means also that there is an attenuation anywhere (refer to Figure 22). A numerical handling of (149) even can be processed with »Mathematica« resulting in the course figured in Figure 20. Since the Hankel functions, with larger arguments, can be expressed well by other analytic functions, we will try to declare approximate solutions later.

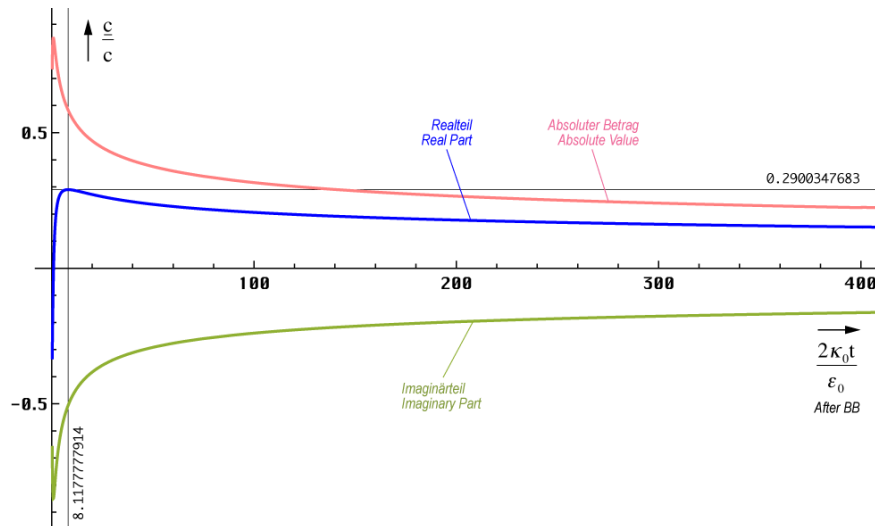


Figure 20: Propagation-Velocity in Dependence on Time (Linear Time-Scale)

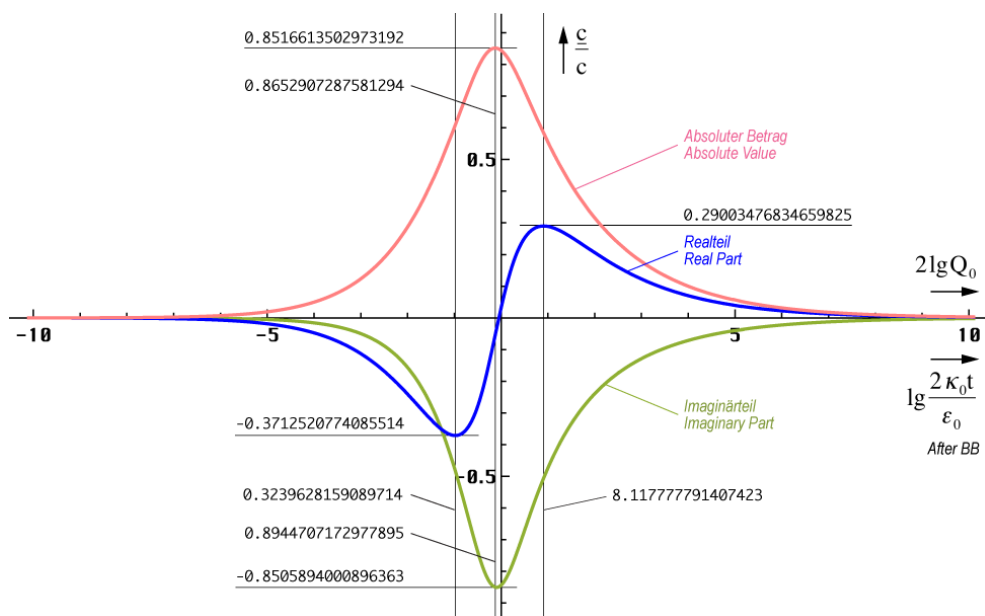


Figure 21: Propagation-Velocity in Dependence on Time (Logarithmic Time-Scale)

In the coarse, the propagation-velocity behaves proportionally to $t^{-1/4}$, as we will still see later. Overall, Figure 20 strongly reminds to the smooth curve of a discrete MLE (Figure 13). Near $t=0$ it looks somewhat differently however. A logarithmic scale helps on in this case (Figure 21). As exact examination emerged, have real- and imaginary-part of \underline{c} the same amount from $20\kappa_0 t/\epsilon_0$ on approximately. We must pay attention to this with the specification of an approximation function.

With it, the world-radius (wave-front) of this model doesn't expand with c but with $0.851661c$ only. That figures no violation of the SRT anyway. This means that wave sections that are emitted later virtually overtake the wave front. Since the ratio of real and imaginary part is different, it does not happen on the same path – rather, the wave fronts cross each other.

To specify the propagation-function, let's have a look at the classic solutions (117), (155) once again and at our primary function (126).

$$\underline{\mathbf{E}} = \mathbf{E} e^{j\omega(t-\frac{x}{c})} = \mathbf{E} e^{j\omega t - j\gamma x} = \mathbf{E} e^{j(\omega t + j\gamma x)} \quad (155)$$

In contrast to (117) the argument in the expansion case is real. Strictly speaking, it's not the Hankel function but the modified Hankel function $M_0^{(2)} = I_0(z) - jK_0(z)$ what's the equivalent to the exponential function. It applies $I_0(z) = J_0(jz)$ but only for purely imaginary arguments. With complex arguments, the real part cannot be placed as a factor in front of the Hankel function in the form of $e^a \times e^{jb}$, as usual with exponential functions, since the power laws don't apply to Hankel functions. This is only possible for larger arguments z . However, the modified Hankel function is generally not used. Therefore, we use for the base the »ordinary« Hankel function adapting the propagation-function accordingly. To avoid contradictions with the classic definition of propagation rate – real-part equals the attenuation rate, imaginary-part equals the phase-rate – the propagation-function should read as follows then (analogously for $\underline{\mathbf{H}}$):

$$\underline{\mathbf{E}} = \mathbf{E} H_0^{(1)}\left(2\omega_0\left(t - \frac{x}{c}\right)\right) = \mathbf{E} H_0^{(1)}(2\omega_0 t - j\gamma x) \quad (156)$$

This is not quite the classic expression for a propagation-function. Attention should be paid to the factor 2 which can be assigned both to the frequency, as well as the time-constant. With the definition of propagation rate $\gamma = \alpha + j\beta$ it obviously belongs to the frequency since γ depends on phase velocity dx/dt , but not on the half of $dx/(2dt)$. Equating both arguments of (156) we get then:

$$\underline{\gamma} = -\frac{2\omega_0}{c} = j\kappa_0 Z_0 \sqrt{1 - \Theta^2} \quad (157)$$

From (153) the reciprocal of c can be determined very easy. Due to (116) we get for γ :

$$\frac{1}{c} = -\frac{\omega_0 t \rho_0}{c} \left(\cos \frac{1}{2} \arctan \theta - j \sin \frac{1}{2} \arctan \theta \right) \quad (158)$$

$$\underline{\gamma} = \alpha + j\beta = -\frac{2\omega_0}{c} = \frac{2\omega_0^2 t \rho_0}{c} \left(\cos \frac{1}{2} \arctan \theta - j \sin \frac{1}{2} \arctan \theta \right) \quad (159)$$

$$\underline{\gamma} = \rho_0 \kappa_0 Z_0 \left(\cos \frac{1}{2} \arctan \theta - j \sin \frac{1}{2} \arctan \theta \right) \quad (160)$$

Upon closer inspection you can see that α and β are actually swapped with respect to their effect (α = phase rate, β = attenuation rate). This is caused by the fact that a rotation about 90° (j) occurs during propagation (Figure 26 of [29]). x turns into y and y into $-x$. The damping α decreases exponentially from infinity starting at time $t=0$. At this point in time, one can say that there is basically no more attenuation. However, this does not apply if we consider cosmological time periods.

At the point of time $0.897 t_1$ ($Q=0.947$), the function β has a zero-passage. This supplies the somewhat particular course in logarithmic presentation (Figure 23). It's about a phase-jump of 180° in this case. Possibly, this is even that point, in which the wave-front, sent at the point of time $t=0$, is passed by the faster, later transmitted. Furthermore, even the formation of the crystalline structure of space takes place approximately to this point of time (folding of parable into rotation). Up to this point of time, the space is closed, after it open. From the point of time $100 t_1$ on we are able to declare, referring to Figure 23, the following approximation:

$$\underline{\gamma} \approx (1+j)\kappa_0 Z_0 \sqrt{\frac{\epsilon_0}{2\kappa_0 t}} \quad \underline{\gamma} \approx (1+j) \frac{\kappa_0 Z_0}{\sqrt{2\omega_0 t}} = \frac{(1+j)}{r_1} Q^{-1/2} \quad (161)$$

These relationships can be derived as well graphically from Figure 23, as explicitly using (157) by application of (162). However, it's necessary to multiply (157) with j , in order to take account of the 90° turning (Figure 26 of [29]). Then, to the approximation $\gamma = 2\omega_0/c$ is applied. The factor $\kappa_0 Z_0$ is the reciprocal of our r_0 with a Q -factor of 1, marked with $1/r_1$. Phase rate and attenuation rate are the same from $100 t_1$ on approximately. This is the behaviour of an ideal conductor.

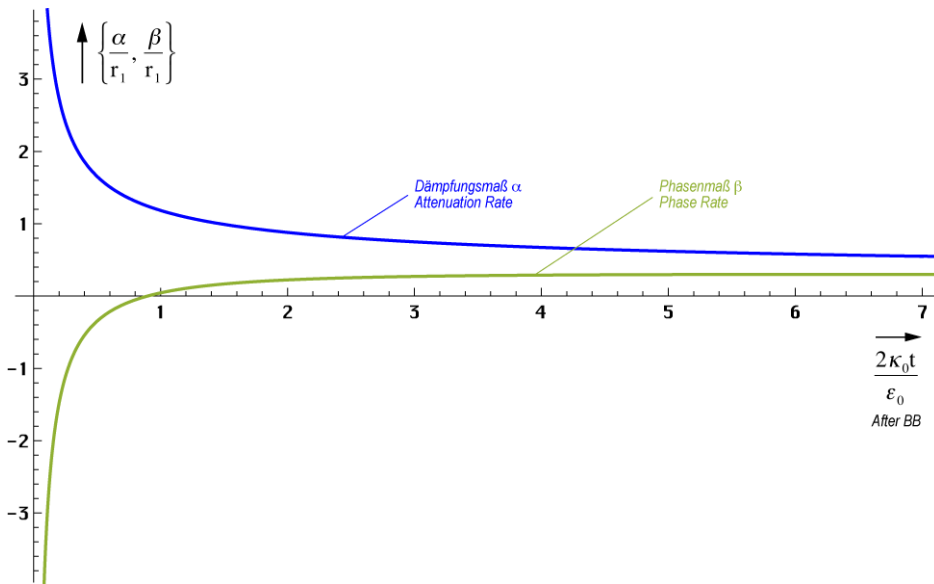


Figure 22:
Phase-Rate and Attenuation Rate
in Dependence on Time (Linear Scale)

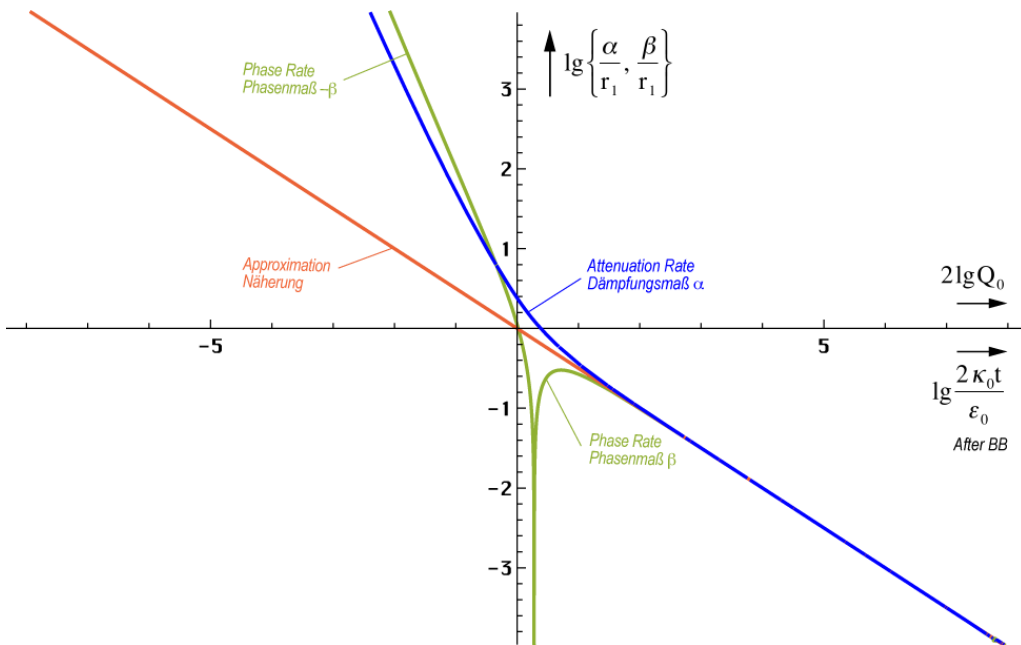


Figure 23:
Phase Rate and Attenuation Rate
in Dependence on Time (Logarithmic Scale)

Possibly a lot of known physical effects like e.g. superconductivity and electron conductivity of the vacuum are basing hereupon. For \underline{c} we have already found an approximation, still remain \underline{c} and \underline{Z}_F . In Figure 21 we have already figured the course of \underline{c} . To the graphic determination of an approximation, we require the logarithmic representation however (Figure 24). To be considered is the fact, that the imaginary part is actually negative.

$$\underline{c} = \frac{1-j}{\sqrt{2}} c \sqrt[4]{\frac{\varepsilon_0}{2\kappa_0 t}} \quad \underline{c} = \frac{1-j}{2} \frac{c}{\sqrt{\omega_0 t}} \quad (162)$$

$$|\underline{c}| = c \sqrt[4]{\frac{\varepsilon_0}{2\kappa_0 t}} \quad |\underline{c}| = \frac{c}{\sqrt{2\omega_0 t}} \quad (1.03807 \cdot 10^{-22} \text{ ms}^{-1}) \quad (163)$$

$$\underline{Z}_F = \frac{1-j}{\sqrt{2}} Z_0 \sqrt[4]{\frac{\varepsilon_0}{2\kappa_0 t}} \quad \underline{c} = \frac{1-j}{2} \frac{Z_0}{\sqrt{\omega_0 t}} \quad (164)$$

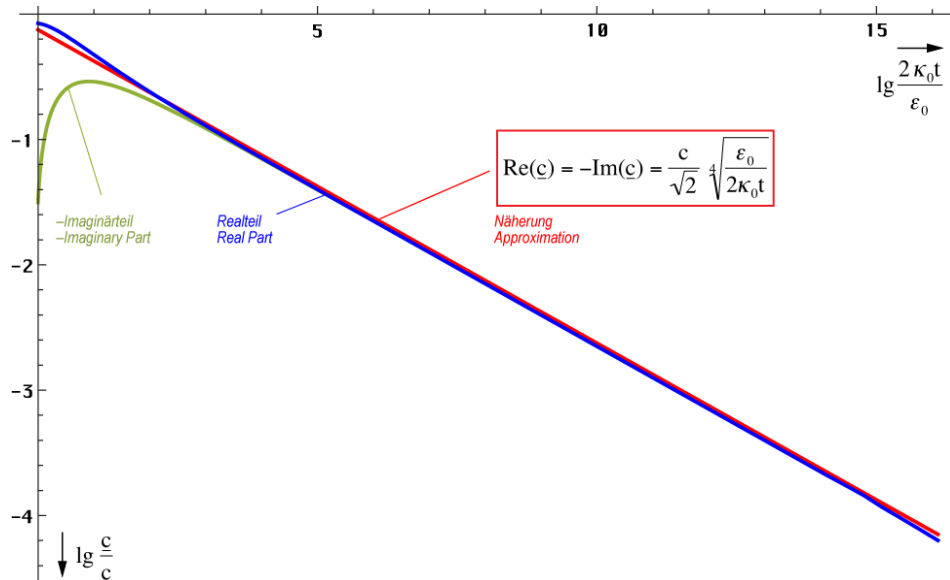


Figure 24:
Propagation-Velocity in Dependence
on Time (Double Logarithmic)

4.3.1.1. Propagation function

Now we want to set up a propagation function. The normal form is $\mathbf{E} = \hat{\mathbf{E}} e^{i\omega t - \gamma x}$ with $\gamma = \alpha + j\beta$. But with the exact solution (161) there is a case on hand, at which α and β contain both damping- and phase-information and the wave function isn't harmonic either. That way we aren't able to form a reasonable propagation function. Therefore, we try an approximate solution with variable coefficients.

4.3.1.2. Approximate solution

In the case $t \gg t_1$ phase- and attenuation rate are of the same size. Thus, the model behaves similar to a metal. There α does not stand for a damping, but for a rotation, namely as long as, with vertical incidence, a value of π is reached so that the wave exits the metal in the opposite direction after a minimal intrusion. The depth of penetration depends on the material properties, the wave length and the angle of incidence. In case of this model the material properties aren't constant either, γ decreases with t and x . Hence it suffices to a rotation of 90° only and the wave remains in the medium (vacuum). In any case, there is a rotation too.

To cope with it, we do a rotation of the coordinate system about $\pi/4$. That corresponds to a multiplication with \sqrt{j} and we get a purely imaginary solution. So becomes $\alpha=0$ and $\gamma=j\beta$ and the exponentially related attenuation vanishes. Indeed, we still have to multiply the result with $\sqrt{2}$ and to replace x by r .

Despite $\alpha=0$ the amplitude of \mathbf{E} and \mathbf{H} is decreasing continuously. That's caused by the Hankel function alone, resp. by the radical expression in (165). With it amplitude and phase are firmly interlinked (minimum phase system). Now the rotation angle in space is equal to $\theta + \pi/4$. But a separation of phase- and damping-information isn't possible yet. But we can work with very high precision using the approximation equations in this case. To the general Hankel function $H_0^{(1)}(\omega t - \beta x)$ the following approximation applies (analogously for \mathbf{H}):

$$\underline{\mathbf{E}} = \hat{\mathbf{E}} H_0^{(1)}(\omega t - \beta x) \approx \hat{\mathbf{E}} \sqrt{\frac{2}{\pi(\omega t - \beta x)}} e^{j(\omega t - \frac{\pi}{4} - \beta x)} \quad (165)$$

Instead of γx only the product βx with the phase rate appears in the exponent, since the amplitude rate is already emulated by the radical expression. With $t \gg 0$ the angle $\pi/4$ can be omitted. After rotation and transition $x \rightarrow r$ and $\omega \rightarrow 2\omega_0$ turns out:

$$\underline{\mathbf{E}} = \hat{\mathbf{E}} H_0^{(1)}(2\omega_0 t - 2\beta_0 r) \approx \frac{2\mathbf{E}_1}{\sqrt{2\omega_0 t - 2\beta_0 r}} e^{j(2\omega_0 t - \frac{\pi}{4} - 2\beta_0 r)} \quad \begin{aligned} H_1 &= \frac{\varphi_1}{\mu_0 r_1^2} \\ E_1 &= \frac{q_1}{\varepsilon_0 r_1^2} = \frac{1}{Z_0} \frac{\varphi_1}{\varepsilon_0 r_1^2} \end{aligned} \quad (166)$$

\mathbf{E}_1 is the peak value of \mathbf{E} with $Q_0=1$. Indeed are both $\omega = 2\omega_0$ and $\beta = 2\beta_0$ (with double frequency even the phase rate must be doubled) no constants at all. That means, they depend on t and r at the same time, limiting the manageability of the approximation very much. You can see that also with the phase velocity v_{ph} . It is defined in the following manner:

$$v_{ph} = \frac{2\omega_0}{\beta} = \frac{2c}{\sqrt{2\omega_0 t}} = 2|c| \quad \text{for } t \gg 0 \quad (167)$$

Thus, the phase velocity is equal to the double absolute value of propagation velocity. That's caused by the factor 2, since phasing with double frequency propagates with double velocity too. For interest, also the group velocity should be stated here:

$$v_{gr} = \frac{1}{d\beta/d\omega_0} = -2|c| \quad \text{for } t \gg 0 \quad (168)$$

Except for the algebraic sign both results are equal. That means, the propagation takes place free from any bias. Further to the approximation. With (96) in Section 3.2.2. we had already found a very good approximation, almost exact, for the same temporal function.

$$\underline{\mathbf{E}} \approx \hat{\mathbf{E}} \sqrt{\frac{2}{\pi}} \frac{e^{j(2\omega_0 t + 2\beta_0 x)}}{\sqrt{2\omega_0 t + 2\beta_0 x}} = 2\mathbf{E}_1 \frac{e^{j2(\omega_0 t + \beta_0 r)}}{\sqrt{2\omega_0 t + 2\beta_0 r}} \quad \text{with} \quad \beta_0 = \frac{\kappa_0 Z_0}{\sqrt{2\omega_0 t}} \quad (169)$$

Now, expression (169) enables to define an equivalent- $\alpha = \alpha_0$ and, with it, even an equivalent- $\gamma_0 = \alpha_0 + j2\beta_0$, in order to get it up to the normal form for propagation functions.

$$\underline{\mathbf{E}} \approx 2\mathbf{E}_1 e^{j2\omega_0 t - \gamma_0 r} \quad \text{with} \quad \gamma_0 = \frac{1}{2r} \ln \left(2\omega_0 t + \frac{2\kappa_0 Z_0}{\sqrt{2\omega_0 t}} r \right) + j \frac{2\kappa_0 Z_0}{\sqrt{2\omega_0 t}} \quad (170)$$

That's already a big step forward. Unfortunately, both ω_0 and γ_0 depend on time. It's not critical for $2\omega_0 t$, because it's multiplied by t anyway. Else with γ_0 , it should depend on r only. To the substitution of t in (229 et seq.) we firstly put (163) left-hand into $t=r/|c|$. The real propagation velocity becomes effective here and not v_{ph} or v_{gr} . Then we rearrange after t . Putting into (169) right-hand we get:

$$t = \frac{r}{c} \sqrt[4]{\frac{2\kappa_0 t}{\epsilon_0}} \quad t^{4/3} = \frac{r^4}{c^4} \frac{2\kappa_0 t}{\epsilon_0} = 2r^4 \mu_0^2 \epsilon_0 \kappa_0 \quad (171)$$

$$\beta_0^{12} = \frac{1}{8} \kappa_0^{12} Z_0^{12} \frac{\epsilon_0^8}{\kappa_0^8} \cdot \frac{1}{2r^4 \mu_0^2 \epsilon_0 \kappa_0} = \frac{\kappa_0^8 Z_0^8}{2^4 r^4} \quad \left| \quad \beta_0 = \sqrt[3]{\frac{1}{2r r_1^2}} \quad (176)$$

With it, we obtain for γ_0 and the product $\gamma_0 r$ the following expressions:

$$\gamma_0 = \frac{1}{2r} \ln \left(2\omega_0 t + \left(\frac{2r}{r_1} \right)^{\frac{2}{3}} \right) + j \left(\frac{2}{r r_1^2} \right)^{\frac{1}{3}} \quad \text{for } t \gg 0 \quad (177)$$

$$\gamma_0 r = \frac{1}{2} \ln \left(2\omega_0 t + \left(\frac{2r}{r_1} \right)^{\frac{2}{3}} \right) + j \left(\frac{2r}{r_1} \right)^{\frac{2}{3}} \quad \text{for } t \gg 0 \quad (178)$$

Last but not least the time t can be completely eliminated. The value γ_0 is proportional to $r^{-1/3}$ and, even more important, the product $\gamma_0 r$ is proportional to $r^{2/3}$. Unfortunately, as already said, we can explicitly state $\gamma_0(r)$ by approximation only. With the exact function (160) a separation, especially from t is impossible. But generally speaking, an exact solution is not required at all, since the approximation yields very good results until a striking distance to the particle horizon at $Q_0=1$, see Figure 13. Therefore, we won't follow up that matter at this point.

All hitherto stated approximations are based on the 4D-expansion-centre $\{r_1, r_1, r_1, t_1\}$. But it's more practicable to find a function, related to another centre. Most suitable seems to be the point, where we are, the point being. At first we substitute the time according to $t \rightarrow \tilde{T} + t$. The swung dash stands for the initial value at the point $t=0$ (nowadays) describing an inertial system. Hence it's about a constant. Because of $\tilde{T} = t_1 \tilde{Q}_0^2$ we are able to factor out \tilde{Q}_0 . The direction of time doesn't change. To the temporal part applies:

$$2\omega_0 t = \tilde{Q}_0 \left(1 + \frac{t}{\tilde{T}} \right)^{\frac{1}{2}} \quad (179)$$

For the spatial part β_0 we build up the inertial system once again using the substitution $r_1 \rightarrow \tilde{R}$. Because of $\tilde{R} = r_1 \tilde{Q}_0^2$, as well as $\tilde{r} \tilde{Q}_0 = -r$, now we are measuring from the other end, we can write for $2\beta_0$:

$$2\beta_0 = \tilde{Q}_0 \left| \frac{2}{\tilde{r}\tilde{Q}_0\tilde{r}_1^2\tilde{Q}_0^2} \right|^{\frac{1}{3}} = -\tilde{Q}_0 \left| \frac{2}{r\tilde{R}^2} \right|^{\frac{1}{3}} \quad 2\beta_0 r = -\tilde{Q}_0 \left| \frac{2r-\tilde{r}_0}{\tilde{R}} \right|^{\frac{2}{3}} = -\tilde{Q}_0 \left| \frac{2r}{\tilde{R}} - \frac{1}{\tilde{Q}_0} \right|^{\frac{2}{3}} \quad (180)$$

Approximation

Exactly ($Q_0 \ll 10^3$)

Actually I should have to write \tilde{r} instead of r . But because it's the argument of the function the tilde has been omitted. The right-hand expression considers the fact, that r_0 as smallest increment never can be underrun. The value α_0 is definitely determined by the envelope curve of the Hankel function, else it would be equal to zero. With it, we obtain for $\underline{\gamma}_0$ and the product $\underline{\gamma}_0 r$:

$$\underline{\gamma}_0 = \frac{1}{2r} \ln \tilde{Q}_0 \left(\left(1 + \frac{t}{\tilde{T}} \right)^{\frac{1}{2}} - \left(\frac{2r}{\tilde{R}} \right)^{\frac{2}{3}} \right) + j \tilde{Q}_0 \left(\frac{2}{r\tilde{R}^2} \right)^{\frac{1}{3}} \quad (181)$$

$$\underline{\gamma}_0 r = \frac{1}{2} \ln \tilde{Q}_0 \left(\left(1 + \frac{t}{\tilde{T}} \right)^{\frac{1}{2}} - \left(\frac{2r}{\tilde{R}} \right)^{\frac{2}{3}} \right) + j \tilde{Q}_0 \left(\frac{2r}{\tilde{R}} \right)^{\frac{2}{3}} \quad (182)$$

With r_0 we have already found one elementary length. But LANCZOS speaks about another one [1]. That's the wave length of the metric wave field $\lambda_0 = 2\pi/\beta$. The approximation of λ_0 must be divided by 2 once again, due to the double phase velocity. Hence $\lambda_0 = 2\pi/\beta_0$ applies. To the comparison the expression for r_0 once again:

$$\lambda_0 = \frac{2\pi}{\rho_0(2\omega_0 t) \kappa_0 Z_0} \operatorname{cosec} \frac{1}{2} \arctan \theta(2\omega_0 t) \quad (183)$$

$$\lambda_0 = \frac{\pi}{\kappa_0 Z_0} \sqrt[4]{\frac{2\kappa_0 t}{\epsilon_0}} = \frac{\pi}{\kappa_0 Z_0} \sqrt{2\omega_0 t} \quad \text{for } \omega_0 t \gg 0 \quad (184)$$

$$r_0 = \frac{1}{\kappa_0 Z_0} \sqrt{\frac{2\kappa_0 t}{\epsilon_0}} = \frac{2\omega_0 t}{\kappa_0 Z_0} = \sqrt{\frac{2t}{\kappa_0 \mu_0}} \quad (185)$$

Though λ_0 is smaller than r_0 and not identical to HEISENBERG's elementary length with it. λ_0 now is in the range of $10^{-68}m$. Thus, LANCZOS was wrong in that point. But it only has been a guess on his part. In fact, it's about the wave length of the wave function forming the metric lattice itself. Expression (183) until (185) only represent the temporal functions. Then, the functions of time and space read as follows.

$$\lambda_0 = \frac{2\pi}{\rho_0(2\omega_0 t - \underline{\gamma}_0 r) \kappa_0 Z_0} \operatorname{cosec} \frac{1}{2} \arctan \theta(2\omega_0 t - \underline{\gamma}_0 r) \quad (186)$$

$$\lambda_0 = \pi r_0 \tilde{Q}_0^{-\frac{1}{2}} \left(\left(1 + \frac{t}{\tilde{T}} \right)^{\frac{1}{2}} - \left(\frac{2r}{\tilde{R}} \right)^{\frac{2}{3}} \right)^{\frac{1}{2}} = \frac{\pi}{\kappa_0 Z_0} \sqrt{2\omega_0 t - 2\beta_0 r} \quad (187)$$

$$r_0 = dr = \tilde{r}_0 \left(\left(1 + \frac{t}{\tilde{T}} \right)^{\frac{1}{2}} - \left(\frac{2r}{\tilde{R}} \right)^{\frac{2}{3}} \right) = \frac{2\omega_0 t - 2\beta_0 r}{\kappa_0 Z_0} \quad (188)$$

The temporal course of $\lambda_0(r=0)$, and of $r_0(r=0)$ is shown in Figure 25 and 26. Figure 26 is a little bit deceptive. It looks like r_0 is smaller than λ_0 . In fact, the curve of r_0 cuts the one of λ_0 with an argument of $100t_1$ at $10r_1$. The phase jump, not visible in Figure 26, occurs with an argument of 0.0525.

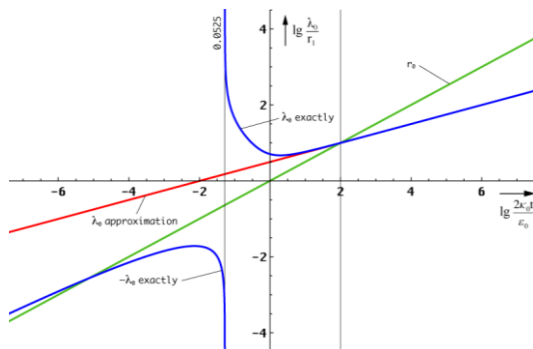


Figure 25:
Course of λ_0 Exact Logarithmic Scale

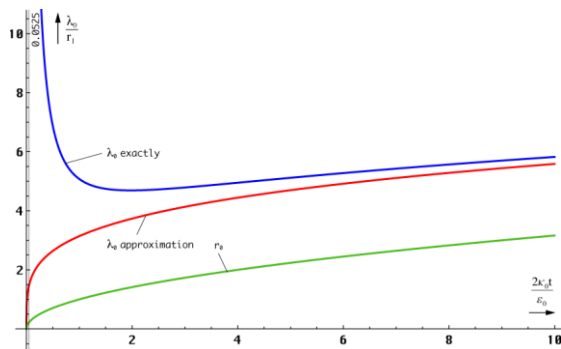


Figure 26:
Course of λ_0 Exact and Approximation as well as r_0 Linear Scale

We only know the local age T , which results from the local HUBBLE-parameter (189). It quasi represents the temporal distance to the expansion centre. But we are able to determine the spatial distance to the world radius R . This forms a spatial singularity (event horizon) with it. The value arises from the ansatz (190):

$$2\omega_0 t - \beta_0 r = \frac{\omega_0(H)}{H} \quad \text{with } r = 0 \quad T = \frac{1}{2H} \quad (189)$$

$$R = -\frac{\omega_0(H)}{\beta_0 H} = -\frac{\omega_0 r_0}{H} = -2ct \quad \text{with } 2\omega_0 t = 0 \quad (190)$$

$$\beta_0 = \kappa_0 Z_0^4 \sqrt{\frac{\epsilon_0 H}{\kappa_0}} = \sqrt{\frac{c^3}{G\hbar}} = \frac{1}{r_0} \quad \text{Phase rate of the metric wave field} \quad (191)$$

Hence, the value of $\beta_0=1/r_0$ even can be obtained from (221), in that we replace time with the HUBBLE-parameter H_0 . To R applies:

$$R = -\frac{c}{H_0} = -1.22471 \cdot 10^{26} \text{ m} = -1.2946 \cdot 10^{10} \text{ Ly} = -3.96896 \text{ Gpc} \quad (192)$$

$$R = -\frac{c}{H_0} = -1.34803 \cdot 10^{26} \text{ m} = -1.4249 \cdot 10^{10} \text{ Ly} = -4.36862 \text{ Gpc} \quad (193)$$

That's about 13 billion light years for $H_0=71.9963 \text{ kms}^{-1} \text{ Mpc}^{-1}$. The result (193) for the alternative value of $H_0=68.6241 \text{ kms}^{-1} \text{ Mpc}^{-1}$ has been calculated with the help of (1049 [29]) and the CODATA₂₀₁₈-values. The local age has the character of a time-constant and amounts only to the half, namely 6.6/7.1 billion years. The world radius (great circle) is equal to cT . More extended time-like vectors up to $2cT$ are possible due to expansion and propagation of the metric wave field (cf. Figure 27). The particulars are described in sections 3.3.2. of [49], resp. 4.5. of [29] in detail.

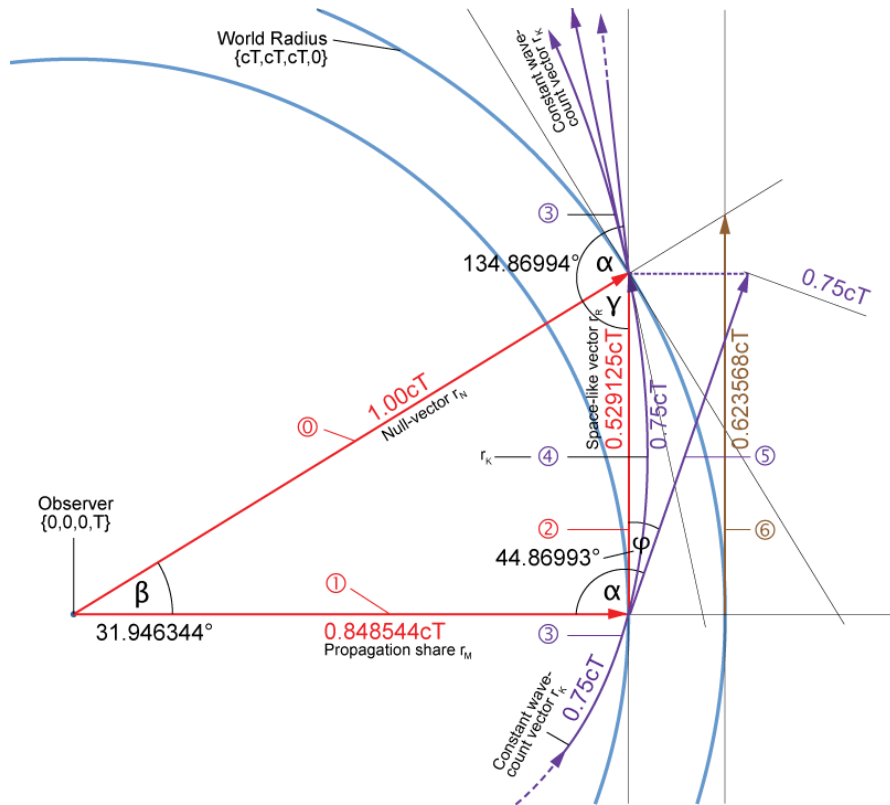


Figure 27:
Expansion Velocity and World
Radius Without a Correction Factor

4.3.2. Propagation function of the overlaid wave

4.3.2.1. The metric wave field as conduction

We assumed, that the vacuum is not loss-free by introduction of a specific conductance κ_0 . With it, we could find a maximally rational solution of the MAXWELL equations, which fills the requests to a metrics, being not in contradiction to SR. According to [1], the propagation of photons takes place as an interference of this wave-field. Furthermore we determined, that this happens exactly with the speed of light, at which point it should be added here that this is only the case with respect to subspace (zero vector).

With the wave propagation as an interference of the metric wave field, we want to consider now, different conditions occur. As generally known, solution 5.2 can also be determined in that we solve equation (66) without expansion, based on the equivalent circuit in Figure 11, if $R_0 \rightarrow \infty$. With a solution with expansion, R_0 depends on place and time and is also close to infinity. If we count back using the approach $\kappa = \kappa_0$, we get a value close to zero. In order to restore correspondence with reality, we are just forced to use another model.

In Section 4.3.2. we had determined that the MLE as per Figure 11 behaves like a low pass of 2nd order for overlaid signals. Therefore, we want to transform the equivalent circuit of the MLE into a low pass. The exact procedure is shown in Figure 28. First we disconnect the circuit at the marked position elevating the coil L_0 . Thus, the proper low pass (centre right) is just ready. Although, the therein contained loss-resistor R_0 only characterizes the losses within the MLE. If we now want to model wave-propagation, we must daisy-chain a lot of these elements (Figure 29).

We examine the coupling of two line elements in the interval r_0 . The coupling factor shall be equal to 1. The coupling itself takes place via the magnetic field (Figure 4). And exactly with this coupling there are further losses not characterised by the resistor R_0 . This can also be interpreted as the exclusive losses of the capacitance C_0 . For the coupling-losses, we introduce yet another impedance R_{0R} , already know from Figure 10, assigning it to the inductivity L_0 , after all, it's a matter of losses during the inductive transmission. The value of R_{0R} is generally calculated according to (34).

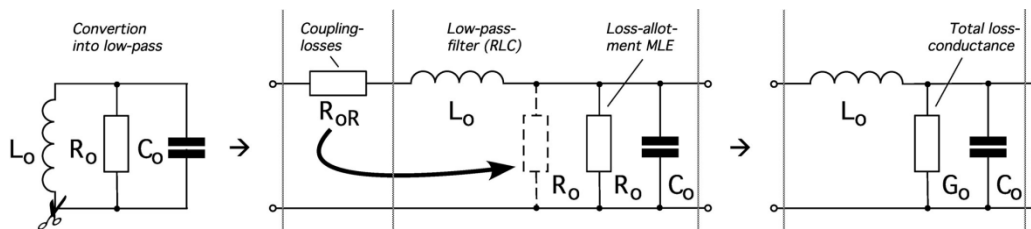


Figure 28:
Conversion of the Equivalent-Circuit of the MLE into a Low-Pass Under Consideration of the Additional Coupling Losses

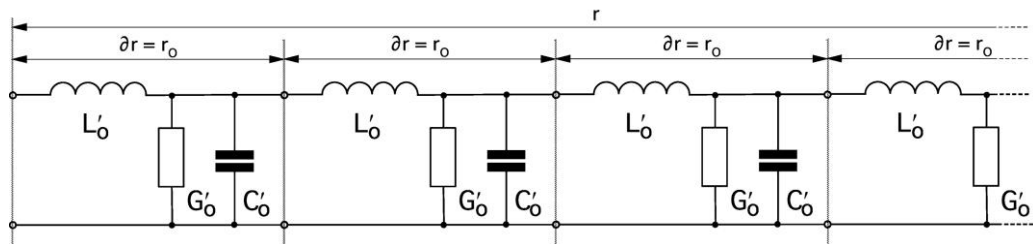


Figure 29:
Line-Equivalent-Circuit with Shunt-Resistor

The interesting thing is that all these values R_0 , R_{0R} , L_0 , C_0 and G_0 change over time, but only very slowly, so that we speak of a quasi-static process. However, quasi-static changes can be generally neglected when solving differential equations. Nevertheless, they do have an effect in the end, as we will see.

So we use the model of a conduction to describe wave propagation in the vacuum. As a result, we hope to find a propagation function similar to that, we found by application of the classic solution for a loss-free medium ($\square \mathbf{E} = 0$ and $\square \mathbf{H} = 0$), which is not in contradiction to the observations.

At least, we already transform the impedance R_{0R} into a second parallel loss-resistor R_0 , with the help of (33), bunching both together to the total-loss-conductance G_0 with which $G_0 = 2/R_0$ applies. Figure 28 centre and right are equivalent.

4.3.2.2. Approximate solution

First we want to check, if we cannot use solution 5.2. applying a substitution to κ_0 ($\mu_r = \epsilon_r = 1$). Yes indeed. But we don't get a constant in this case, since R_0 isn't static. We introduce a substitute value κ_{0R} for that purpose. With the help of (39), (45), (161) and (190) we obtain:

$$R_{0R} = \frac{1}{\kappa_0 r_0} \quad r_1 = \frac{1}{\kappa_0 Z_0} \quad r_0 = r_1 Q_0 = \sqrt{\frac{2t}{\kappa_0 \mu_0}} \quad R_{0R} = \sqrt{\frac{\mu_0}{2\kappa_0 t}} \quad (194)$$

$$R_0 = \frac{Z_0^2}{R_{0R}} = Z_0 Q_0 \quad G_0 = \frac{2}{R_0} = \frac{2}{Z_0 Q_0} = \kappa_{0R} \frac{r_0^2}{r_0} = \kappa_{0R} r_0 \quad (195)$$

$$\kappa_{0R} = \frac{2}{Z_0 Q_0 r_0} = \frac{2}{Z_0 R} = \frac{2}{Z_0 2ct} = \frac{\varepsilon_0}{t} \quad \kappa_{0R} = 2\varepsilon_0 H = \frac{2\kappa_0}{Q_0^2} \quad (196)$$

R is the world-radius $2ct$. Then, inserting (196) into (120) we obtain for the complex propagation-velocity \underline{c} and the field-wave-impedance \underline{Z}_F :

$$\underline{c} = c \sqrt{\frac{j\omega t}{1+j\omega t}} \quad \underline{Z}_F = Z_0 \sqrt{\frac{j\omega t}{1+j\omega t}} \quad (197)$$

Now light speed will only be reached in infinite time. Nevertheless, the propagation speed is *close* to c . The remainder is filled up by the propagation velocity \underline{c}_M of the metrics, so that the total velocity is equal to c in turn, which was a basic assumption of this work. The same result is also obtained from the solution of the telegraph equation [5] (198) for the transient state ($c_1=0$) by inserting the values for C_0, L_0, G_0 as well as $R_0=0$.

Figure 29 shows the associated equivalent circuit. Furthermore, we yet derive with respect to ∂r , that is each low-pass gate now represents the properties of a conductive section of the length ∂r . The discrete components turn into the capacity, inductivity and conductance covering C'_0, L'_0 and G'_0 . Since the vacuum in this model has a finite structure with the smallest increment $r_0, \partial r \rightarrow r_0$ applies. Fortunately r_0 is sufficiently small, so that we can work with the difference-quotient. For the coverings we get $C'_0 = C_0/r_0 = \varepsilon_0, L'_0 = L_0/r_0 = \mu_0$ and $G'_0 = \varepsilon_0/t = \kappa_{0R}$ then. With it, the fundamental physical constants ε_0, μ_0 and the substitutive value κ_{0R} are identical to the capacity, inductivity and conductance covering of our »conduction«, the metric wave field.

$$\frac{\partial^2 u}{\partial t^2} = c^2 \frac{\partial^2 u}{\partial r^2} + c_1 \frac{\partial u}{\partial r} + c_2 \frac{\partial u}{\partial t} + c_3 u \quad \text{with} \quad (198)$$

$$c = \frac{1}{\sqrt{L'_0 C'_0}} \quad c_1 = 0 \quad c_2 = -\frac{R'_0}{L'_0} - \frac{G'_0}{C'_0} \quad c_3 = -\frac{G'_0 R'_0}{L'_0 C'_0} \quad R'_0 = 0$$

$$\frac{\partial^2 u}{\partial r^2} - L'_0 C'_0 \frac{\partial^2 u}{\partial t^2} - (C'_0 R'_0 + G'_0 L'_0) \frac{\partial u}{\partial t} - G'_0 R'_0 u = 0 \quad \text{analogously for } i \quad (199)$$

$$-\frac{\partial u}{\partial r} = R'_0 i + L'_0 \frac{\partial i}{\partial t} \quad -\frac{\partial i}{\partial r} = G'_0 u + C'_0 \frac{\partial u}{\partial t} \quad (200)$$

$$-\frac{\partial u}{\partial r} = \mu_0 \frac{\partial i}{\partial t} \quad -\frac{\partial i}{\partial r} = \frac{\varepsilon_0}{t} u + \varepsilon_0 \frac{\partial u}{\partial t} \quad (201)$$

This corresponds to a loss-affected line in general. Because of $\mathbf{E} = -\mathbf{u}/r_0$ as well as $\mathbf{H} = -\mathbf{i}/r_0$ we obtain after division by r_0 :

$$\frac{\partial \mathbf{E}}{\partial r} = \mu_0 \frac{\partial \mathbf{H}}{\partial t} \quad \hat{=} \quad \text{curl } \mathbf{E} \quad \frac{\partial \mathbf{H}}{\partial r} = \left(\kappa_{0R} + \varepsilon_0 \frac{\partial}{\partial t} \right) \mathbf{E} \quad \hat{=} \quad \text{curl } \mathbf{H} \quad (202)$$

This way, the MAXWELL equations can be derived directly. Unlike 4.2. however, the parameter κ_{0R} decreases steadily in this case. The solution itself is not loss-free. A damping-factor different from zero occurs, which can be attributed to the variable parameter κ_{0R} . Therefore, it is also named parametric attenuation. Starting with (199), we get for the line-/field-wave-impedance ($\underline{Z}_L = \underline{Z}_F$):

$$\underline{Z}_L = \sqrt{\frac{R'_0 + j\omega L'_0}{G'_0 + j\omega C'_0}} = \sqrt{\frac{j\omega \mu_0}{\varepsilon_0/t + j\omega \varepsilon_0}} = Z_0 \sqrt{\frac{j\omega t}{1+j\omega t}} \quad (203)$$

That's the same solution as (197). Because of $Z_0 = \mu_0 c$, even the expression for \underline{c} applies. Altogether it's about an autonomous solution with different properties as the hitherto introduced ones. Since no discrete components are involved, the attenuation takes place completely free of noise. The solution is distortion-free. Even no scatter occurs.

Because of the currently low value of κ_{0R} ($3.93821 \cdot 10^{-29} \text{ Sm}^{-1}$), the attenuation is not detectable nowadays. Thus, it seems, that wave-propagation would proceed according to the classic loss-less solution. But strictly speaking, it applies only in a universe without expansion ($\kappa_0 = \kappa_{0R} = 0$) and figures a special-case of the solution introduced here. Now, let's have a look at the propagation-velocity \underline{c} in detail.

III. *The metric wave-field behaves for overlaid electromagnetic radiation-fields like a conduction with variable coefficients. It behaves in the first approximation like the classic loss-less vacuum solution of Maxwell's equations, at which point the speed with respect to the subspace is $c = \text{const}$.*

$$\underline{c} = \underline{c}_M + \underline{c}_\lambda \qquad \underline{c} = c \left(\sqrt{\frac{1}{j2\omega_0 t}} + \sqrt{\frac{j\omega t}{1+j\omega t}} \right) \quad (204)$$

Thus, we have formulated an important condition. With the metric wave function and the superimposed EM-wave we are dealing with two competing wave functions. The value of c is defined by the properties of the subspace μ_0 and ε_0 (7). Therefore, both wave functions must share c . Since one function represents an interference of the other, only the sum of the complex amounts comes into question here. That corresponds to a geometric addition:

$$c^2 = c_M^2 + c_\lambda^2 \qquad c^2 = c^2 \left(\frac{1}{2\omega_0 t} + \frac{1}{\sqrt{1 + \frac{1}{\omega^2 t^2}}} \right) \quad (205)$$

This expression is even achieved from the line element (262[29]) after division by dt^2 with $c^2 = ds^2/dt^2$. c_M is the propagation-speed of the metrics. With it, the overlaid wave moves always rectangularly to the metrics with exact c (Figure 32). After rearrangement of (204) we obtain:

$$\omega t = \frac{1}{\sqrt{\left(1 - \frac{1}{2\omega_0 t}\right)^{-2} - 1}} \qquad \omega = \frac{2H}{\sqrt{\left(1 - \frac{1}{2\omega_0 t}\right)^{-2} - 1}} \quad (206)$$

Since it's about an approximate solution with expression (276), we want to try, whether it already can be simplified. With $y = 1/(2\omega_0 t)$ we get for $2\omega_0 t \gg 1$:

$$\omega = \frac{2H}{\sqrt{\frac{2y - y^2}{1 - 2y + y^2}}} \approx 2H \sqrt{\frac{1 - 2y}{2y}} = 2H \sqrt{\frac{1}{2y} - 1} \quad (207)$$

We finally receive after substitution:

$$\omega = 2H \sqrt{\omega_0 t - 1} \approx \sqrt{2} H \sqrt{2\omega_0 t} \quad (208)$$

Because of $H = 1/(2t)$ (radiation cosmos) the frequency decreases according to $\omega \sim t^{-3/4}$. But we are particularly interested in the wavelength $\lambda = \sqrt{2}\pi/\beta = \sqrt{2}\pi c/\omega$. The sign of (193) has been neglected. The factor $\sqrt{2}$ stands here instead of 2, as even already with λ_0 , to cancel rotation around $\pi/4$ of the coordinate-system applied with the definition of the approximate formula of $\chi(r)$. Then we get the following result:

$$\lambda = \pi \frac{c}{H_0} \frac{1}{\sqrt{2\omega_0 t}} = \frac{\pi R}{\sqrt{2\omega_0 t}} \qquad \lambda \sim t^{3/4} \sim Q_0^{3/2} \quad (209)$$

To this we must remark that we have assumed, for the previous contemplation, the expansion-centre as basis of the coordinate-system, at which no length is actually defined. More essential qualities result for the two singular points.

For the spatial singularity (expansion-centre) applies: Each length, measured from this point, always has the quantity $R/2$. Each period, measured at this point, always has the amount T , each frequency $2H$. It's about an event-horizon. It's a drain of the electromagnetic field. To the approximation applies $r = \infty$, $t = \infty$.

For the temporal singularity (wave-front) applies: Each length, measured from this point, always has the quantity $r/2$. Each period, measured at this point, always has the amount $t/1$, each frequency $2\omega/1$. It's about a particle-horizon. It's a source of the electromagnetic field. To the approximation applies $r = 0$, $t = 0$.

A particle horizon on the inside is an event horizon on the outside and vice versa. It looks similar to the magnetic and electric fields. No matter at which pole you are located, you always believe that you are at the centre, since all field lines always converge rectangularly to the observer from all directions (Figure 31 [76]). Except that he is unable to really reach the particle horizon. I can't say whether the two poles are connected in the background like with the horseshoe magnet. In any case, there is more than only one event horizon, once for the universe as a whole, as well as a huge number what with black holes.

The spatial singularity is only suitable as basis of a space-independent temporal, the temporal singularity only as basis of a time-independent spatial coordinate-system. As basis of a four-dimensional space-temporal coordinate-system, both singularities are equally inappropriate. Seen from the spatial singularity, all time-like vectors have an

equal frequency and wave-length. We must pay attention to this on a coordinate-transformation to our local coordinates. It applies $t = \tilde{T} + t'$ and for the wavelength λ :

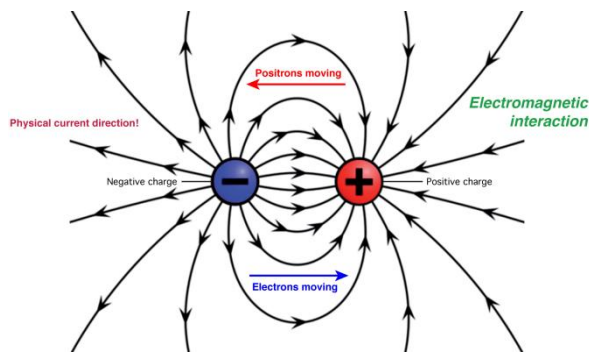


Figure 30:
Poles and Field Lines in the Electric Field

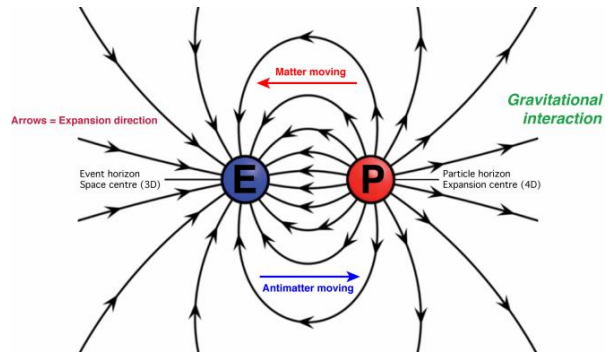


Figure 31:
Horizons and Field Lines in the Gravitational Field

$$\lambda = 2\pi c(\tilde{T} + t')(1 + t'/\tilde{T})^{-1/4} C\tilde{Q}_0^{-1/2} = \pi\tilde{R}(1 + t'/\tilde{T})^{3/4} C\tilde{Q}_0^{-1/2} \quad (210)$$

$$\lambda = \tilde{\lambda} \left(1 + \frac{t'}{\tilde{T}}\right)^{3/4} = \tilde{\lambda} \left(\sqrt{1 + \frac{t'}{\tilde{T}}}\right)^{3/2} \quad (211)$$

C is an arbitrary constant, it disappears on a retransformation. Expression (211) represents the temporal dependence. To the determination of spatial dependence, we must visualize that this case differs from the preceding λ_0 and r_0 .

Having to do until now with a wave-field which shows different conditions at different places (quantity of r_0 , propagation-velocity etc. – therefore different dependences of space and time), the circumstances are deviating in this case. It is about a purely time-like vector, which propagates everywhere with the same velocity, namely c . The dependence on space and time is identical to it, following the same function. Even $R/2$ expands time-like with a constant velocity of c . Just only, we have to replace t by r . Therefore we expand the fraction in (211) with $2c$ obtaining:

$$\lambda = \tilde{\lambda} \left(1 + \frac{2ct'}{2c\tilde{T}}\right)^{3/4} = \tilde{\lambda} \left(1 + \frac{2r}{\tilde{R}}\right)^{3/4} \quad (212)$$

With it, the overlaid wave doesn't behave like the metrics r_0 as well as λ_0 concerning wavelength and frequency. But differences exist also between r_0 and λ_0 . There are even more differences then again. So, the distance, the light covers from the source to the observer, is different from the distance, a material body must cover. Latter one amounts to $R/2$ maximally, while theoretically whatever large distances are possible in the first case. This is clearly the behaviour of a particle-horizon. We denote the first as time-like (incoming vector), the second as space-like distance (outgoing vector). See Section 7.5.2. of [29] for details.

With the help of (212) we can also find a substitution for the expression β being applied to signals overlaid to the metrics. In contrast to (179), which applies to the metrics itself, because of $\lambda = 2\pi c/\omega = 2\pi/\beta$, we get for the phase rate β of the overlaid wave (not the β_0 of the metrics):

$$\beta = \frac{\tilde{\omega}}{c} \left(1 + \frac{2r}{\tilde{R}}\right)^{-3/4} = \frac{\tilde{\omega}}{c} \Xi(r) \quad \text{with} \quad \Xi(r) = \left(1 + \frac{2r}{\tilde{R}}\right)^{-3/4} \quad \Xi(t) = \left(1 + \frac{t}{\tilde{T}}\right)^{-3/4} \quad (213)$$

We introduce the two right-hand functions to the better presentation. Such, we can incorporate the cosmological redshift into the propagation function now. With the propagation of overlaid waves, β is not identical to α obviously. We obtain α and β from (121) if we replace κ_0 with κ_{0R}

$$\alpha = \frac{\omega}{c} \sinh\left(\frac{1}{2} \operatorname{arsinh} \frac{1}{\omega t}\right) \quad \beta = \frac{\omega}{c} \cosh\left(\frac{1}{2} \operatorname{arsinh} \frac{1}{\omega t}\right) \quad (214)$$

For $\omega t \gg 1$ outside the near field of a beaming dipole (inside other relationships apply any-way), with help of the approximations $\operatorname{arsinh} \varepsilon \approx \varepsilon$, $\sinh \varepsilon \approx \varepsilon$, $\cosh \varepsilon \approx 1 + \varepsilon^2/2$ follows:

$$\alpha = \frac{1}{R} \quad \beta = \frac{\omega}{c} = \pm \omega \sqrt{\mu_0 \varepsilon_0} \quad (215)$$

With it, we get for the phase rate β the same result, as with the classic solution for a loss-free medium. It fits the observations. Deviating from this, an attenuation rate $\alpha \neq 0$ applies. That also causes an attenuation of the amplitude,

which could actually be the cause of the darkening of the SN-Ia. But it's so small that it can only be detected on cosmological scales with $z \geq 0.1$.

For the amplitude response A of the electric and magnetic field-strength applies the following:

$$A = 20 \lg e^{-\frac{r}{R}} = -8.686 \frac{r}{R} \text{ dB}^1 \quad (216)$$

$$A = 20 \lg e^{-\frac{t}{2T}} = -4.343 \frac{t}{T} \text{ dB} \quad (217)$$

Also $A' = -1 \text{ Np/R}$ [Neper]. Both expressions are equivalent. With it, the half-life period (-6 dB) is about $1.382T$, the half-life width about $0.691R$.

¹ We use the standard unit of measurement in electrical engineering, dB [decibels]. The 20 applies to the electric [V/m] and magnetic [A/m] field strengths. For the Poynting vector [W/m²] the 10 is used.

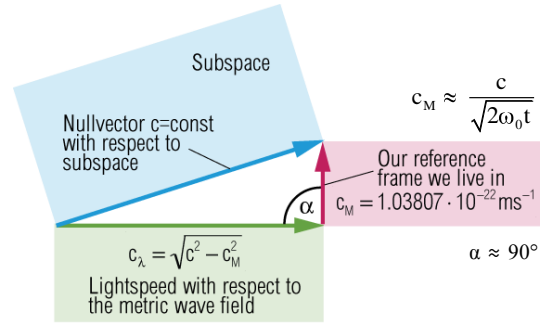


Figure 32: Propagation Velocity of the Metrics and of an Overlaid Electromagnetic Wave

The parametric attenuation is so low that it can be largely neglected, as it is far below the geometric one. It obviously also occurs with the metrics included. However, it is independent of this, as can be easily be seen from (203). The influence of the metrics is given by r_0 and, as you can see, all r_0 cancel each other. With it, our solution (215) completely emulates wave-propagation and $-$ attenuation admittedly, but not the cosmologic red-shift.

Since it is not caused by the electrical properties of the conduction or space, but rather by the conduction itself, it belongs in the propagation function as factor $\Xi(r)$. Just once imagine the following: A line is flowed through by an alternating current. A certain wavelength appears. If this line is manufactured from an ideally elastic material now and one pulls at an end, so the line is stretched. Simultaneously, also an enlargement of the wavelength occurs with simultaneous diminution of the conducting-velocity (c in sum).

In order to incorporate red-shift, we divide the part β (the attenuation rate α is not affected) by the bracketed expression of (212) obtaining our substitute- $\underline{\gamma}$, \underline{c} and \underline{Z}_L , it applies $R=r_0Q_0$:

$$\underline{\gamma} = \frac{\tilde{H}}{c} + j \frac{\tilde{\omega}}{c} \Xi(r) \quad \underline{c} = c \quad \underline{Z}_L = Z_0 \quad (218)$$

Expression (218) is the propagation rate for signals, which are overlaid the metrics ($\underline{\gamma} = \alpha + j\beta$). The non-zero attenuation rate α describes the so-called parametric damping, caused by changing parameters of the conduction during expansion. In addition, of course, geometric damping occurs too. However, latter one is generally not represented in the propagation function, as there are special cases without it, e.g. lasers.

The solution is applied to the entire domain $r \gg r_0$, however not shortly after BB, in the proximity of the (of a) temporal singularity and with very strong gravitational fields (black holes). Thereto, the complete solution 4.3.8. is required. The expressions (215) and (218) are sufficient for solving the SN-Ia problem. Thus, we are now able to set up a propagation function.

4.3.2.3. Propagation function with red-shift and parametric attenuation

We assume the solution of the telegraph equation for the transient state [5]. The equation-system is also known as conducting-equations.

$$\begin{aligned} \underline{u}_2 \cosh \underline{\gamma} r + \underline{i}_2 \underline{Z}_L \sinh \underline{\gamma} r &= \underline{u}_1 \\ \frac{\underline{u}_2}{\underline{Z}_L} \sinh \underline{\gamma} r + \underline{i}_2 \cosh \underline{\gamma} r &= \underline{i}_1 \end{aligned} \quad (219)$$

In this connection, the index 1 means the input-signal, the index 2 the output-signal. We now replace in the following manner:

$$\underline{E}_1 = -\frac{\hat{u}_1}{r_0} \mathbf{e}_r e^{j\omega t} = \underline{E}_1 e^{j\omega t} \quad \underline{H}_1 = -\frac{\hat{i}_1}{r_0} \mathbf{e}_r e^{j\omega t} = \underline{H}_1 e^{j\omega t} \quad (220)$$

\mathbf{e}_r is the unit-vector. Furthermore, $\underline{Z}_L \approx Z_0$ applies (transient state) and $\underline{u} = j Z_0$. Then we get as solution of (219):

$$\underline{E}_2 = \underline{E}_1 e^{j\omega t - \underline{\gamma} r} \quad \underline{H}_2 = \underline{H}_1 e^{j\omega t - \underline{\gamma} r} \quad \omega = \tilde{\omega} \Xi(t) \quad (221)$$

This solution is identical to (117) but it considers the cosmologic red-shift only for $\underline{\gamma}$ (218). We also must notice the temporal dependence of the expression $j\omega t$, i.e. at the source of the signal. The right expression of (221) is used for

it. With it, we have found a solution explaining as well the propagation as the cosmologic red-shift of electromagnetic waves.

4.3.2.4. Complete solution with frequency and phase response

If we want to find a solution, being valid even in the proximity of very strong gravitational fields and/or of the temporal singularity, we are forced to calculate with the complete formula. In Section 3.3.3. we had noticed that the space owns also an upper cut-off frequency. Solution (221) shows all-pass behaviour and doesn't reflect the real circumstances anyway, but it's adequate for more than 99% of all cases. A solution with const-deration of the cut-off frequency (downward the frequency is really restricted by the age only) must be a complete solution. Therefore, let's try to find first an approach for a comp-late solution with and without consideration of the cut-off frequency. We go out from (204), however using the correct expression for the propagation-velocity \underline{c}_M of the metrics (153):

$$\underline{c} = \underline{c}_M + \underline{c}_\lambda = c \qquad \underline{c} = c \left(\frac{e^{j\frac{1}{2}\arctan\theta}}{j\rho_0\omega_0 t} + \sqrt{1+j\omega t} \right) \quad (222)$$

We reconsider the absolute value function, although it should be noted that the angle α , which also depends on θ , even may be unequal to $\pi/2$ (Figure 94). Therefore, the cosine-rule applies:

$$c^2 = c_M^2 + c_\lambda^2 - 2c_M c_\lambda \cos\alpha \qquad \frac{1}{2\rho_0\omega_0 t} = \frac{c_M}{c} \quad (223)$$

$$\frac{1}{\sqrt{1+\frac{1}{\omega^2 t^2}}} - \frac{\cos\alpha}{\rho_0\omega_0 t \sqrt{1+\frac{1}{\omega^2 t^2}}} + \left(\frac{1}{4\rho_0^2\omega_0^2 t^2} - 1 \right) = 0 \quad (224)$$

analogously for $Z_0 = \mu_0 c$. After reiterated substitution, we get the following solutions:

$$\omega = 2H \sqrt{\frac{y^4}{1-y^4}} \qquad \text{with}^1 \qquad y = \beta_x^{-1} = \frac{c_M}{c} \cos\alpha \pm \sqrt{1 - \frac{c_M^2}{c^2} \sin^2\alpha} \quad (225)$$

¹ See (621[75]) relativistic dilatation factor β with $v=c_M$, see also section 4.3.

The second solution is applied to space-like photons. Obviously, similarities exist with the reciprocal of (207). The value of y tends to 1 for $Q_0 \gg 1$. Since the real transfer-function is independent from the metrics, (215) is also applied to the complete solution in the far field $\omega t \gg 1$. We continue as in 4.3.2.2. To that purpose we first transform:

$$\omega = \frac{2H}{\sqrt{\frac{1}{y^4} - 1}} = \frac{2H}{\sqrt{\left(\frac{c_M}{c} \cos\alpha \pm \sqrt{1 - \frac{c_M^2}{c^2} \sin^2\alpha} \right)^{-4} - 1}} \quad (226)$$

The transition from the exact solution to the approximation will be described more exactly in Section 4.3.1. The factor 2 turns out by itself with it, that means, with the exact solution the rotation of the coordinate-system is automatically done by the function. We are interested in the wavelength $\lambda = 2\pi/\beta = 2\pi c/\omega$ once again:

$$\lambda = \pi R \sqrt{\left(\frac{c_M}{c} \cos\alpha \pm \sqrt{1 - \frac{c_M^2}{c^2} \sin^2\alpha} \right)^{-4} - 1} \quad (227)$$

$$\lambda = CR(Q) \sqrt{\beta_x^4 - 1} \qquad Q = \tilde{Q}_0 \left(1 + \frac{r}{c\tilde{T}} \right)^{\frac{1}{2}} = \tilde{Q}_0 \left(1 + \frac{t}{\tilde{T}} \right)^{\frac{1}{2}} \quad (228)$$

$$r_k = \frac{3}{2} r_1 Q^{1/2} \int_0^Q \frac{1}{\rho_0} dQ \approx \frac{3}{2} r_1 Q^{1/2} \int_0^Q Q^{1/2} dQ = r_1 Q^2 \quad \text{for } Q \gg 1 \quad (782[29])$$

C is that arbitrary constant to the conversion upon the R^4 -coordinate system once more. The function r_k (782[29]) i.e. $R(Q)$ describes the *exact* dependence of R concerning the phase-angle/Q-factor Q. The definition of A and B can be taken from (151). We were already able to set $R(t) = 1 + t/\tilde{T}$ in the approximation. With the complete solution it is unfortunately impossible, because R is propagating and expanding at the same time (see Section 6.2.3.1. of [29]). The relation $R = r_1 Q_0^2$ exactly applies only for $Q_0 \gg 1$. The spatial and temporary dependence of R for zero-vectors is given by the right expression of (228). Furthermore $\tilde{Q} = \tilde{Q}_0$ and $R(\tilde{Q}) = \tilde{R}$ applies. Finally, we get for the wavelength and frequency:

$$\lambda = \tilde{\lambda} \frac{R(Q)}{R(\tilde{Q})} \sqrt{\frac{\beta_x^4 - 1}{\tilde{\beta}_x^4 - 1}} \quad \omega = \tilde{\omega} \frac{R(\tilde{Q})}{R(Q)} \sqrt{\frac{\tilde{\beta}_x^4 - 1}{\beta_x^4 - 1}} \quad (229)$$

All values except c and ω are a function of the phase-angle/Q-factor $Q_0 = 2\omega_0 t$. For just two kinds of photons and neutrinos we define the eight functions $\Xi_x(r)$ and $\Xi_x(t)$:

$$\begin{aligned} \Xi_\gamma(r) = \Xi_\gamma(t) &= \frac{R(\tilde{Q})}{R(Q)} \sqrt{\frac{\tilde{\beta}_\gamma^4 - 1}{\beta_\gamma^4 - 1}} & \Xi_{\tilde{\gamma}}(r) = \Xi_{\tilde{\gamma}}(t) &= \frac{R(\tilde{Q})}{R(Q)} \sqrt{\frac{\tilde{\beta}_\gamma^4 - 1}{\beta_\gamma^4 - 1}} \\ \Xi_\nu(r) = \Xi_\nu(t) &= \frac{R(\tilde{Q})}{R(Q)} \sqrt{\frac{\tilde{\beta}_\nu^4 - 1}{\beta_\nu^4 - 1}} & \Xi_{\tilde{\nu}}(r) = \Xi_{\tilde{\nu}}(t) &= \frac{R(\tilde{Q})}{R(Q)} \sqrt{\frac{\tilde{\beta}_\nu^4 - 1}{\beta_\nu^4 - 1}} \end{aligned} \quad (230)$$

See also (621[75]) relativistic dilatation factor β with $v=c_M$, see also section 4.3. Responsible for the insertion of the right relationships (substitution $r=ct$) is the reader himself. But the function is explicitly calculable yet. (218) and (221) are applied. This is the complete transfer-function without consideration of the cut-off frequency. It is valid even in strong gravitational fields and at the »edge« of the universe.

4.3.2.5. Frequency- and phase response

In Section 3.3.2. we have worked out the transfer-function of a single MLE of the size r_0 . The solution is applicable for the metric wave field itself, but it can also be used for superimposed waves if we understand the superimposed wave as an interference of the differential equation (70). In this case, we have to apply ω_0 for σ in (101) instead of ω_1 , it applies $\Omega = \omega/\omega_0$. First, let's have a look at the share of the total attenuation factor α , caused by ω_g , which can be calculated from the amplitude response $A(\omega)$. Only the real part is being transferred. In connection with the phase-angle φ_γ in reference to the length $r_0 = c/\omega_0$ applies:

$$\Psi(\omega) = \ln|A(j\omega)| = \ln(A(\omega) \cos \varphi_\gamma) \quad (231)$$

$$\Psi(\omega) = \ln\left(\frac{1}{\sqrt{1+\Omega^2}} e^{\frac{\Omega^2}{1+\Omega^2}} \cos\left(\arctan \Omega - \frac{\Omega}{1+\Omega^2}\right)\right) \quad \text{with} \quad \Omega = \frac{1}{2} \frac{\tilde{\omega}}{\tilde{\omega}_0} \left(1 + \frac{2r}{R}\right)^{\frac{1}{2}} \Xi(r) \quad (232)$$

$$\Psi(\omega) = -\frac{1}{2} \ln(1 + \Omega^2) + \frac{\Omega^2}{1 + \Omega^2} + \ln \cos\left(\arctan \Omega - \frac{\Omega}{1 + \Omega^2}\right) \quad (233)$$

$$\alpha = \frac{\tilde{H}}{c} - \frac{\tilde{\omega}_0}{c} \Psi(\omega) \quad \Psi(\omega) = 0 \quad \text{for} \quad \omega \ll \omega_0 \quad (234)$$

The share $\Psi(\omega)$ depends on space and time indeed, since it depends on Ω too, on the ratio of two frequencies, changing according to different functions ($\omega \sim t^{-3/4}$, $\omega_0 \sim t^{-1/2}$). The negative sign arises from the re-exchange of the integration limits. With it the change doesn't cancel out. In the approximation $\Omega \sim t^{-1/4}$ applies.

But the cut-off frequency affects the phase rate β . The more approaching the cut-off frequency, all the more the phase-shift φ_γ (106) is making noticeable, caused by the ascending phase delay T_{Ph} (108) during the transfer from one MLE to the other ($t_1 \rightarrow t_0$). Since the phase-defects add up, there's going to be a retardation of the overall phase-shift $\Phi(\omega)$. This causes a ramp down of the propagation-velocity onto values smaller than c (permitted), so that ω remains unchanged and λ declines on the other hand. The smaller value of $|\underline{c}|$ affects α and β in the same manner. With the nowadays manageable frequencies however, the phase-defect is practically equal to zero. Before we can calculate on, we already have to convert the phase-shift $\Phi(\omega)$ into units of wavelength however. It applies $\Phi(\omega) = 1 + T_{Ph}/T_\omega$, at which point T_ω is the period of ω :

$$\Phi(\omega) = \left(1 - \frac{1}{2\pi} \left(\arctan \Omega - \frac{\Omega}{1 + \Omega^2}\right)\right) \quad \Phi(\omega) = 1 \quad \text{for} \quad \omega \ll \omega_0 \quad (235)$$

With it, we can specify the following universal propagation-function for the vacuum:

$$\underline{\mathbf{E}}_2 = \underline{\mathbf{E}}_1 e^{j\omega t - \underline{\gamma} r} \quad \underline{\mathbf{H}}_2 = \underline{\mathbf{H}}_1 e^{j\omega t - \underline{\gamma} r} \quad \omega = \tilde{\omega} \Xi(t) \quad (236)$$

$$\underline{\gamma} = \left(\left(\frac{\tilde{H}}{c} + \frac{\tilde{\omega}_0}{c} \Psi(\omega) \right) + j \frac{\tilde{\omega}}{c} \Xi(r) \right) \Phi(\omega) \quad |\underline{c}| \leq c \quad |\underline{Z}_L| \leq Z_0 \quad (237)$$

The complete solution with frequency response is not required in most cases. One possible use case is the calculation of the spectrum of the CMBR in [46]. We will work with expression (237) there. In cases, where the cut-off frequency plays no role, applies $\Phi(\omega) = 1$.

4.3.3. Cosmologic red-shift and distance to the source

In order to clarify the discrepancies with the SN-Ia cosmology project, we also need a relation enabling us to calculate the distance r to the source using the redshift z . Depending on the world model used, there are many different variants. This point has already been discussed in detail in Section 2. and [71]. As already explained, it's space itself that expands.

While the SN-Ia cosmology project relies on the standard model (Λ CDM), we prefer the MLE model [29] already used with the determination of the propagation function in the previous section for reasons of consistency of the premises. Regarding the Λ CDM, there does not seem to be any major deviations with the function $r(z)$ if we abstain from such luxuries as the cosmological constant Λ and the parameters Ω_b and Ω_m . But then it's just a CDM (Cold Dark Matter) universe. And if that only means normal matter which has been cooled so much that it no longer radiates and which can't be recognized as a dark nebula in front of a radiation source, then it's no wonder either.

According to the MLE-model, directly from (212) an expression for the cosmologic red-shift can be derived:

$$\lambda = \tilde{\lambda} \left(1 + \frac{2r}{\tilde{R}} \right)^{\frac{3}{4}} \quad z = \frac{\lambda - \tilde{\lambda}}{\tilde{\lambda}} = \frac{\lambda}{\tilde{\lambda}} - 1 \quad (238)$$

$$\left(1 + \frac{2r}{\tilde{R}} \right)^{\frac{3}{4}} = z + 1 \quad \frac{2r}{\tilde{R}} = (z + 1)^{\frac{4}{3}} - 1 \quad (239)$$

$$r = \frac{\tilde{R}^\uparrow}{2} \left((z + 1)^{\frac{4}{3}} - 1 \right) \quad v^\uparrow = c \left((z + 1)^{\frac{4}{3}} - 1 \right) \quad (240)$$

v is the escape velocity. Now one often claims in the literature that this could be also larger than c . But this is not the case. Reason for the wrong claim is a cardinal-mistake that is liked to do even by experts again and again and, I don't want to exclude myself here, in the first edition also by myself. One simply substitutes \tilde{R} with the current value at the observer, obtaining escape-velocities larger c then.

A further erroneous conclusion is that signals with $z > 1.28$ should come from regions behind the event horizon $\tilde{R} = 2c\tilde{T}$, or better, they should have covered a distance greater than \tilde{R} . However, this contradicts the observations. It should be noted, that we assumed a radiation cosmos in which the world age is $2T$. The world radius (4D great circle) expands with c .

As long as the options of observation were restricted to smaller z -values, this was not noticeable at all. Meanwhile, already objects with a red-shift of $z = 6$ have been found and the red-shift of the cosmologic background-radiation has even a value of $z = (2Q_0)^{3/2} \approx 10^{90}$, as described in Section 4.6.4.2.3. of [29]. However, the reason for the high values of z is not that the universe is actually much larger than assumed. Even if this would be the case, no zero vectors with a length greater than $\tilde{R} = 2c\tilde{T}$ could exist, since they return to their starting point having covered this distance, i.e. they are a closed-loop.

The real mistake is the misinterpretation of (240). The expressions are based on the propagation function (221) and this is always related to the starting point of the wave, the signal source. So it applies to outgoing vectors only. Therefore, we must always substitute \tilde{R} with the value at the source to the point of time of emission, and all distances and the velocity v^\uparrow are always been referred to the source then. The expansion of the universe since that point of time namely, is already included in the exponent $4/3$, as one easily can recognize with the help of (210). By the way, this is also applied to calculations according to the classic model of cosmology, even if the exponent may differ from $4/3$ there. For this reason, I have marked both values with the upward-arrow \uparrow for outgoing vectors. It reminds something to the wiring sign of a transmitting aerial, which may serve as mnemonic device.

However, we don't know the exact value of \tilde{R}^\uparrow as it is linked to the distance of the source from the observer, which we actually want to determine. What we do know, however, is the value \tilde{R}^\downarrow . Since the distances r^\uparrow and r^\downarrow as well as the velocities c^\uparrow and c^\downarrow are equal, a simple relation, that works with the value \tilde{R}^\downarrow at the observer, can be found. We do the following approach:

$$r = \frac{\tilde{R}^\uparrow}{2} \left((z + 1)^{\frac{4}{3}} - 1 \right) = c (\tilde{T}^\downarrow - t) \left((z + 1)^{\frac{4}{3}} - 1 \right) = c \left(\tilde{T}^\downarrow - \frac{r}{c} \right) \left((z + 1)^{\frac{4}{3}} - 1 \right) \quad (241)$$

$$r = \left(\frac{\tilde{R}^\downarrow}{2} - r \right) \left((z + 1)^{\frac{4}{3}} - 1 \right) = \frac{\tilde{R}^\downarrow}{2} \left((z + 1)^{\frac{4}{3}} - 1 \right) - r \left((z + 1)^{\frac{4}{3}} - 1 \right) \quad (242)$$

After reducing to r , we get the following expressions for r and v :

$$r = \frac{\tilde{R}^\downarrow}{2} \left(1 - (z+1)^{-\frac{4}{3}}\right) \quad v^\downarrow = c \left(1 - (z+1)^{-\frac{4}{3}}\right) \quad (243)$$

The expressions (240) and (243) yield the same result when substituting the correct values. The contradiction has been solved with it. But it is not yet the whole thing. What applies to the value r applies to \tilde{R} , r_0 , \tilde{H} , $\tilde{\omega}_0$ and $\tilde{\omega}$ in the propagation function too, i.e. if you work with \tilde{R}^\downarrow , also these values must be corrected. You only ever work with either the values at the source or those at the observer. In more final case, the expressions γ and ω must be multiplied with a correction-factor. For the world-radius R applies:

$$\tilde{R}^\uparrow = 2c(\tilde{T}^\downarrow - t) = 2c\left(\tilde{T}^\downarrow - \frac{r}{c}\right) = \tilde{R}^\downarrow - 2r = \tilde{R}^\downarrow - \tilde{R}^\downarrow(1 - (z+1)^{-4/3}) \quad (244)$$

$$\tilde{R}^\uparrow = \tilde{R}^\downarrow \frac{1}{(z+1)^{4/3}} \quad \tilde{R}^\downarrow = \tilde{R}^\uparrow (z+1)^{4/3} \quad \tilde{H}^\uparrow = \tilde{H}^\downarrow (z+1)^{4/3} \quad \tilde{H}^\downarrow = \tilde{H}^\uparrow \frac{1}{(z+1)^{4/3}} \quad (245)$$

By using of (239) can be shown that the expression $(z+1)$ is corresponding to the relativistic dilatation factor β . Then further $(z+1)^{2/3} \sim \beta^{-2/3} \sim Q_0$ applies and:

$$\tilde{r}_0^\uparrow = \tilde{r}_0^\downarrow \frac{1}{(z+1)^{2/3}} \quad \tilde{r}_0^\downarrow = \tilde{r}_0^\uparrow (z+1)^{2/3} \quad \tilde{\omega}_0^\uparrow = \tilde{\omega}_0^\downarrow (z+1)^{2/3} \quad \tilde{\omega}_0^\downarrow = \tilde{\omega}_0^\uparrow \frac{1}{(z+1)^{2/3}} \quad (246)$$

$$\tilde{r}_1^\uparrow = \tilde{r}_1^\downarrow = \frac{1}{\kappa_0 Z_0} \sim (z+1)^{-0/3} = \text{const} \quad \tilde{\omega}_1^\uparrow = \tilde{\omega}_1^\downarrow = \frac{\kappa_0}{\varepsilon_0} \sim (z+1)^{0/3} = \text{const} \quad (247)$$

An exception forms the frequency ω . In contrast to $H \sim Q_0^{-2}$ resp. $\omega_0 \sim Q_0^{-1}$ applies $\omega \sim Q_0^{-3/2}$:

$$\tilde{\lambda}^\uparrow = \tilde{\lambda}^\downarrow \frac{1}{(z+1)} \quad \tilde{\lambda}^\downarrow = \tilde{\lambda}^\uparrow (z+1) \quad \tilde{\omega}^\uparrow = \tilde{\omega}^\downarrow (z+1) \quad \tilde{\omega}^\downarrow = \tilde{\omega}^\uparrow \frac{1}{(z+1)} \quad (248)$$

To the correction of γ and ω , we next consider the product αr :

$$\frac{\tilde{H}}{c} r = \frac{1}{\tilde{R}^\uparrow} \frac{\tilde{R}^\uparrow}{2} ((z+1)^{\frac{4}{3}} - 1) = \frac{1}{\tilde{R}^\downarrow} \frac{1}{(z+1)^{-\frac{4}{3}}} \frac{\tilde{R}^\downarrow}{2} (1 - (z+1)^{-\frac{4}{3}}) = \frac{1}{2} ((z+1)^{\frac{4}{3}} - 1) \quad (249)$$

$$\frac{\tilde{\omega}_0}{c} r = \frac{1}{\tilde{r}_0^\uparrow} \frac{\tilde{R}^\uparrow}{2} ((z+1)^{\frac{4}{3}} - 1) = \frac{1}{\tilde{r}_0^\downarrow} \frac{1}{(z+1)^{-\frac{2}{3}}} \frac{\tilde{r}_0^\downarrow \tilde{Q}_0^\uparrow (1 - (z+1)^{-\frac{4}{3}})}{2} = \frac{\tilde{Q}_0^\uparrow}{2} ((z+1)^{\frac{4}{3}} - 1) \quad (250)$$

With it, the parametric attenuation is really unattached from the frame of reference, exactly, as determined by the solution of the telegraph equation. The remaining quantities depend on the respective reference frame however. With it, we can define the universal propagation function using the values at the observer. At first however once again correctly with arrows for the values at the source:

$$\underline{\mathbf{E}}_2 = \mathbf{E}_1 e^{j\omega t - \gamma r} \quad \underline{\mathbf{H}}_2 = \mathbf{H}_1 e^{j\omega t - \gamma r} \quad \omega = \tilde{\omega}^\uparrow \Xi(t) \quad (251)$$

$$\underline{\gamma} = \left(\left(\frac{\tilde{H}^\uparrow}{c} + \frac{\tilde{\omega}_0^\uparrow}{c} \Psi(\omega) \right) + j \frac{\tilde{\omega}^\uparrow}{c} \Xi(r) \right) \Phi(\omega) \quad |c| \leq c \quad |Z_L| \leq Z_0 \quad (252)$$

These expressions may even be applied to pass-through signals, followed up into future. In this case, we must insert the values at the observer instead those at the source, doing just so, as if the observer would be the source. The distance r indeed is defined in reference to the observer then. The same applies even to z . At the place of the observer applies $z=0$, which is not favourable straightaway, since z is defined absolutely in general, namely on the basis of the red-shift of the absorption-lines of stars. Therefore however, a propagation function, using the values at the observer, with which r and z are defined in reference to the source, would be suitable better. This arises to:

$$\underline{\mathbf{E}}_2 = \mathbf{E}_1 e^{j\omega t - \gamma r} \quad \underline{\mathbf{H}}_2 = \mathbf{H}_1 e^{j\omega t - \gamma r} \quad \omega = \tilde{\omega}^\downarrow (z+1) \Xi(t) \quad (253)$$

$$\underline{\gamma} = \left(\left(\frac{\tilde{H}^\downarrow}{c} (z+1)^{\frac{4}{3}} + \frac{\tilde{\omega}_0^\downarrow}{c} (z+1)^{\frac{2}{3}} \Psi(\omega) \right) + j \frac{\tilde{\omega}^\downarrow}{c} (z+1) \Xi(r) \right) \Phi(\omega) \quad \dots \quad (254)$$

After having figured the real relations extensively once again, it was simply necessary, we now come to the real topic. In Table 1, which has been gathered from [27] in excerpts, some quasi-stellar radio-sources are figured with distance-information. The values marked with an * have been taken from the original, the rest has been calculated. H is always the local HUBBLE-parameter H_0 .

For the interpretation of the measuring results, the author used, willy-nilly, the classic model of cosmology with several parameters (parabolic and elliptical). Since the elliptical model with $q=1$ has the best fit with my model, the elliptical values have been taken over. Therefore, one must not expect an exact agreement with the values calculated

by me. In order to document the mistake in the first edition more exactly, in column 3 have been figured the escape-velocities $>c$ calculated with the wrong value of \dot{R} . Column 4 is containing the correct values.

Column 7 shows the incorrectly calculated distances according to (240) for a value of $H_0=55 \text{ kms}^{-1}\text{Mpc}^{-1}$. One can see, the values are too high, H_0 has been estimated too low. One furthermore sees, that the author of [27] committed the same cardinal-mistake obviously. Indeed, the values are only shifted in reference to the photometric distance in the logarithmic presentation (Figure 33), which corresponds to a multiplication. The corresponding factor has been determined with statistical methods. It amounts to 1.38 ± 0.08 . That results in a probable value of the HUBBLE-parameter of $75.89\pm 4.4 \text{ kms}^{-1}\text{Mpc}^{-1}$ (column 6). The correlation-coefficient to the photometric values is 0.792. The value of H_0 is within the limits determined with modern methods. Obviously, one can achieve right results even with wrong data comparing two wrong results...

* Source	* z	Escape velocity [v/c] [†]	Escape velocity [v/c] [‡]	* Distance photo-metric [Gpc] [†]	Distance [Gpc] Eq.(312) [H=76] [†]	Distance [Gpc] Eq.(312) [H=55] [†]	* Distance geometric [Gpc] [‡]	Distance [Gpc] Eq. (315) [H=76] [‡]
3C 273B	0.158	0.108	0.089	0.470	0.427	0.588	0.420	0.484
3C 48	0.367	0.259	0.170	1.100	1.023	1.408	0.800	0.928
3C 47	0.425	0.302	0.188	1.270	1.194	1.644	0.900	1.025
3C 279	0.536	0.386	0.218	1.610	1.528	2.103	1.070	1.187
3C 147	0.545	0.393	0.220	1.630	1.555	2.141	1.090	1.198
3C 254	0.734	0.542	0.260	2.200	2.143	2.950	1.310	1.416
3C 138	0.759	0.566	0.265	2.280	2.222	3.054	1.340	1.441
3C 196	0.871	0.643	0.283	2.610	2.583	3.544	1.450	1.542
3C 245	1.028	0.783	0.305	3.080	3.080	4.100	1.590	1.662
CTA 102	1.037	0.791	0.306	3.110	3.130	4.108	1.600	1.668
3C 287	1.055	0.806	0.309	3.160	3.190	4.191	1.620	1.681
3C 208	1.109	0.852	0.315	3.320	3.372	4.642	1.660	1.716
3C 446	1.404	1.110	0.345	4.200	4.392	6.046	1.870	1.877
3C 298	1.436	1.139	0.347	4.300	4.506	6.202	1.890	1.892
3C 270,1	1.519	1.214	0.354	4.550	4.802	6.610	1.940	1.929
3C 191	1.946	1.612	0.382	5.830	6.376	8.777	2.160	2.078
3C 9	2.012	1.675	0.385	6.030	6.627	9.122	2.190	2.097

Table 1: Some Quasi-Stellar Radio Sources

All results of Table 1 are visualized in Figure 33. One sees that the values, calculated correctly according to expression (243) with $75.89 \rightarrow 76$ also fit well the geometrical distance (light-way) calculated by the author of [27]. The correlation-coefficient between these two data-series amounts to 0.795. This corresponds to the one of the incorrectly calculated values approximately. We pursue the 76 as an astronomically determined value for later comparison, since the failed evaluation of the SN-Ia project data naturally only allows a standard H_0 besides the SM.

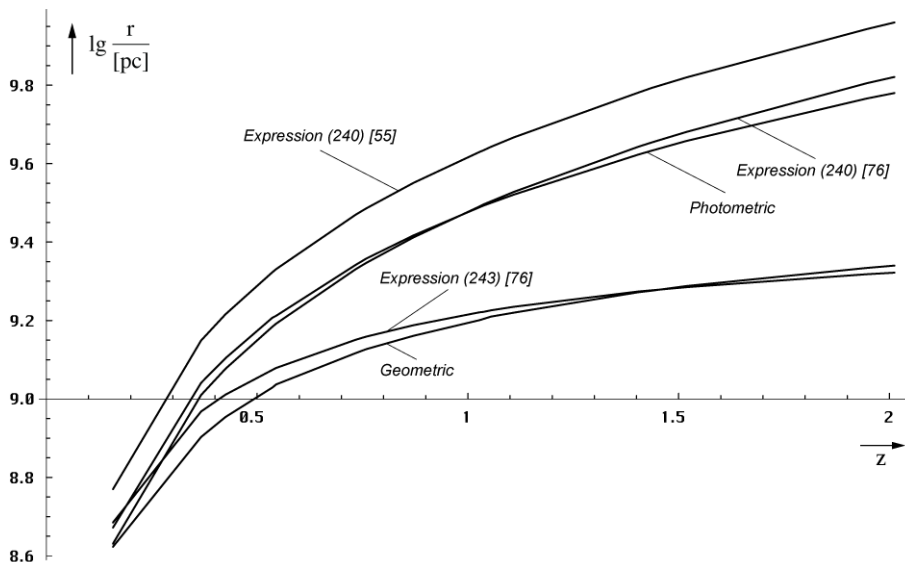


Figure 33: Distance in Dependence on the Red-Shift for Elliptical Models ($q=1$)

The difference in the ascend of both pairs of curves is to be attributed to the application of the classic model of cosmology and is also an indication of the discrepancy in the SN-Ia cosmology project.

4.3.4. The HUBBLE-parameter

In order to replace the world radius $R=c/H_0$ in the calculation, we need also the correct value of the HUBBLE parameter H_0 for a correct calculation. In addition to various astronomically determined values, two main values have been established in the meantime, with the so-called HUBBLE-tension in between. These can even be calculated precisely using the MLE model. The key is the exact value of the phase angle $Q_0=2\omega_0 t$ of the time function ϕ_0 (93). This can be easily calculated from the PLANCK-, electron and proton mass according to (255). With $H_0=\omega_0/Q_0$ we are able to determine H_0 then:

$$Q_0 = \left(\frac{1}{18\pi^2} \sqrt{2} \delta^{-1} \frac{m_0}{m_e} \right)^3 = 8.34047113224285 \cdot 10^{60} \quad \text{with} \quad \delta = \frac{4\pi m_e}{\alpha m_p} \quad (255)$$

$$Q_0 = \frac{3}{2} \left(\frac{r_e}{r_0} \right)^3 = \frac{3}{2} \left(\frac{1}{4\pi} \frac{e^2 Z_0}{m_e} \sqrt{\frac{c}{G\hbar}} \right)^3 = 7.94981 \cdot 10^{60} \quad [71.99] \quad (256)$$

An extremely precise solution is possible within the framework of the Concerted System of Units [49] and [29]. The program to the calculation of the values also can be found in the appendix. The alternative value of H_0 arises from the ratio of the classical electron radius r_e and the PLANCK-radius r_0 . In order to match both solutions, we also determine the so-called tension factor ζ . It corrects the curvature of the electron radius.

$$Q_0 = \frac{3}{2} \left(\frac{\zeta r_e}{r_0} \right)^3 = \left(9\pi^2 \sqrt{2} \delta \frac{m_e}{\mu_0 \kappa_0 \hbar_1} \right)^{-\frac{3}{7}} = 8.34047 \cdot 10^{60} \quad [68.62] \quad (257)$$

$$H_0 = \frac{\omega_0}{Q_0} = \frac{2}{3} \frac{64\pi^3 \epsilon_0 G \hbar m_e^3}{\zeta^3 \mu_0^2 e^6} = \begin{cases} 2.447866 \cdot 10^{-18} \text{s}^{-1} = 71.9963 \text{kms}^{-1} \text{Mpc}^{-1} \\ 2.223925 \cdot 10^{-18} \text{s}^{-1} = 68.6241 \text{kms}^{-1} \text{Mpc}^{-1} \text{ with } \zeta \end{cases} \quad (258)$$

$$\zeta = \frac{1}{9\pi^2} \frac{1}{\sqrt[3]{3\sqrt{2}\alpha\delta}} = \frac{1}{36\pi^3} \frac{1}{\sqrt[3]{3\sqrt{2}}} \frac{m_p}{m_e} = 1.016119033114739' = \text{const} \quad (259)$$

Which of both values is the correct one shall be determined during the evaluation of the SN-Ia project data. It is (255) and (257), I can tell you that much. It is also important to note that the constant wave count vector r_K expands with $v=3/4c$ at the world radius (Figure 27). So $H_1=3/2H_0$ applies for the universe as a whole. This follows from [29] Section 4.5.2.

Expression	Q_0	H_0	H_0	H_1	H_1	QED	
	[1]	[s ⁻¹]	[kms ⁻¹ Mpc ⁻¹]	[s ⁻¹]	[kms ⁻¹ Mpc ⁻¹]	Correction Factor	
(TAB1)	$7.5419 \cdot 10^{60}$	$2.460 \cdot 10^{-18}$	75.8903	$3.691 \cdot 10^{-18}$	113.836	–	–
(256)	$7.9498 \cdot 10^{60}$	$2.448 \cdot 10^{-18}$	71.9963	$3.500 \cdot 10^{-18}$	107.995	1.00000	δ^0
(257)	$8.3405 \cdot 10^{60}$	$2.224 \cdot 10^{-18}$	68.6241	$3.336 \cdot 10^{-18}$	102.936	1.01612	ζ
(255)	$8.3405 \cdot 10^{60}$	$2.224 \cdot 10^{-18}$	68.6241	$3.336 \cdot 10^{-18}$	102.936	–	–
(COBE)	$8.3397 \cdot 10^{60}$	$2.224 \cdot 10^{-18}$	68.6307	$3.336 \cdot 10^{-18}$	102.946	–	–

Table 2:
Hubble-Parameters as a Function
of Local Quantities (Overview)

The COBE-value is obtained from the measured CMBR temperature in that we rearrange (477 [29]) for Q_0 which corresponds to (255) in principle:

$$T_k = \frac{\hbar\omega_0}{18k} Q_0^{-\frac{1}{2}} = \frac{\hbar_1\omega_1}{18k} Q_0^{-\frac{5}{2}} = 2.725436049K \quad \Delta = -1.61258 \cdot 10^{-5} \quad (477 [29])$$

However, the table is not complete. Strictly speaking, the number of possible solutions is unlimited. But there is only one correct solution. So if you have chosen a value from the table at random and found that the real measured values do not match your model, simply try another one.

5. The Supernova-Ia cosmology project verification

At this point we have gathered all the information to verify the measurement data from the SN-Ia cosmology project by means of the MLE model. Since we only use this one model, the premises are consistent. Before we go on into detail, at first yet another section, which deals with the fundamental values of observation, being focused to physicists, astronomers and technicians, which as known, work with different units of measurement. So it's difficult to understand one another.

5.1. Measurands and conversions

Since we want to deal with one concrete project, only the quantities, which are specifically relevant for the supernova-cosmology-project, should be exemplified. In reality, in physics, astronomy and radio-astronomy there is yet a large number of further quantities. I recommend [44] to any interested person, which the information given here, is based on.

Initially with the project, astronomic objects, supernovae of the type Ia, which appear to the observer as punctual objects with a certain luminosity, have been observed. The measured luminosities were compared with the redshift z (238) and with the luminosities predicted by the various world models. What do we mean by luminosity however?

In astronomy there are four types thereof at all, once the apparent brightness, the bolometric brightness, the absolute and the absolute bolometric brightness. It is given in magnitudes $[m, m_b, M, M_b]$. It is about a logarithmic unit of measurement, which is defined historically. With the bolometric brightness, the entire frequency domain in accordance with the STEFAN-BOLTZMANN radiation-rule is considered, it's about the logarithm of the quotient of the two values power and surface $[Wm^{-2}]$, which the physicist marks as POYNTING-vector \mathbf{S} . In the astronomy, this value is called flux F , in the technical department field-strength \mathbf{S} .

With the non-bolometric values the unit of measurement $[Wm^{-2}Hz^{-1}]$ is used. The measurements are dependent on frequency and bandwidth then. But for us only the bolometric values are of note. Another important value is the (bolometric) luminosity L . In the physics and in the technical domain it is marked as power P as well as level p . Unit of measurement is the Watt $[W]$ as well as the decibel $[dB]$. Thus, we can define:

$$M_b = -2.5 \lg \frac{F}{F_0} = -2.5 \lg \frac{L/4\pi r^2}{L_0/4\pi r^2} = -2.5 \lg \frac{L}{L_0} \quad \text{Brightness} \quad (260)$$

As usual with logarithmic units of measurement, always a reference-quantity F_0 as well as L_0 is needed. The values has been taken from [42] and [44] and read as follows:

$$F_0 = 2.51 \cdot 10^{-8} Wm^{-2} \quad L_0 = 3.09 \cdot 10^{28} W \quad (261)$$

A star with the luminosity L_0 has exactly 0 magnitudes (written 0^M). The absolute brightness (flux) is defined in a distance of 10pc of the source, but it has no meaning for us. Even in the technical domain there is such a logarithmic dimension, the dB (decibel):

$$S = P = 10 \lg \frac{S}{S_0} \text{ dB} = 10 \lg \frac{P/4\pi r^2}{P_0/4\pi r^2} \text{ dB} = 10 \lg \frac{P}{P_0} \text{ dB} \quad \text{Field-strength/level} \quad (262)$$

Another, more rarely used logarithmic unit of measurement is the Neper $p[Np] = \ln(P/P_0)$. The original definition of P_0 comes from the telecommunication and is defined as a power $P = 1mW$ on 600Ω . But in the radio-technology and with it even in the radio-astronomy this value is not used, since we are concerned there with much smaller quantities in general. Therefore, the following relative values are used:

$$S_0 = 1 \text{ p}Wm^{-2} = 10^{-12} Wm^{-2} \quad P_0 = 1 \text{ p}W = 10^{-12} W \quad (263)$$

In order to avoid a confusion with the historical definition, instead of dB mostly the unit $dBpWm^{-2}$ or $dBpW$ as well as $dBpWm^{-2}Hz^{-1}$ or $dBpWHz^{-1}$, if there is not the entire spectrum included. The power P at the input of a receiver with adaptation simply results from the POYNTING-vector \mathbf{S} , the effective surface A of the antenna used and the gain G of the antenna:

$$P[dBpW] = S[dBpWm^{-2}] + 10 \lg A[m^2] + G[dB] \quad (264)$$

Since the decibel is also a logarithmic unit, a simple conversion is possible into the astronomic units. For $P[dBpW]$, $M_b[M]$, $S[dBpWm^{-2}]$, $m_b[m]$, $L[W]$, $F[Wm^{-2}]$ applies:

$$P = 404.9 - 4M_b \quad M_b = 101.225 - 0.25P \quad \text{Power Absolute bolom. Brightness} \quad (265)$$

$$S = 44 - 4m_b \quad m_b = 11 - 0.25S \quad \text{Poynting-vector Apparent bolom. Brightness} \quad (266)$$

$$P = 120 + 10 \lg L \quad L = 10^{0.1P-12} \quad \text{Power Luminosity} \quad (267)$$

$$S = 120 + 10 \lg F \quad F = 10^{0.1S-12} \quad \text{Poynting-vector Flux} \quad (268)$$

$$L = 10^{28.5-0.4M_b} \quad M_b = 71.225 - 2.5 \lg L \quad \text{Luminosity Absolute bolom. brightness} \quad (269)$$

$$F = 10^{-7.6-0.4m_b} \quad m_b = 19 - 2.5 \lg F \quad \text{Flux Apparent bolom. brightness} \quad (270)$$

All obscurities should be removed with it, so that we can turn to the results of the supernova-cosmology-project.

5.2. Measurement data from the Supernova Cosmology Project

The results of the project were published by PERLMUTTER in [45] in detail. Unfortunately, the website is meanwhile orphaned, i.e. it still exists, but the links to graphics and tables are dead. Fortunately, these are now available on the new, updated homepage.

For a better understanding of what a type Ia supernova actually is, I recommend the work of HERRMANN [42]. The most important thing is that an SN-Ia has a maximum absolute brightness resulting from its structure. If the star is larger, a supernova of a different type develops, which can be recognised by its characteristics. Thus, an SN-Ia can be used as a standard candle, although the brightness is slightly lower than the maximum, as not all SN-Ia reach the maximum brightness.

The apparent bolometric brightness at the observer has been compared by PERLMUTTER in a diagram with the associated red-shift z . Even HERRMANN [42] and HEBBEKER [43] are using the same diagram, at which point in [43] is deferred in detail to the common standard-big-bang-model once again, being based on the classical EINSTEIN evolution-equation with and without cosmologic constant.

The observations now submitted, that further (older) SN-Ia appear somewhat darker, as they actually should be according to the standard-model without cosmologic constant ($\Lambda=0$). The case $\Lambda=0$ just doesn't fit the observations. The possibility that SN-Ia could have had other properties earlier is ruled out by all the authors, including myself.

Rather, the deviation is interpreted in such a way that Λ should have a value other than zero, which means that the expansion rate of the universe, i.e. the HUBBLE-parameter, is not decreasing at the present time, as has always been assumed, but increasing on the contrary. Thus, the observed SNae would be farther away, than it would arise from the measured red-shift z . The lower brightness would be explained with it. However this leads to incongruities with other observations. In order to avoid them, a complicated construct is used, which demands extremely exact synchronizations to the point of time $T=0$ and even afterwards, which appears to be pretty implausible, because nobody can exactly say, on which physical phenomenon this effect should be based on.

While PERLMUTTER contents himself with the hint on the option $\Lambda \neq 0$, HERRMANN and HEBBEKER even demand the existence of »dark matter« with hitherto yet unknown qualities and of an effect with the name »quintessence« which should be the cause for the increasing expansion-rate, quasi a sort of anti-gravity. For my part, however, I consider this hypothesis to be erroneous, since the discrepancy can be explained even more simply, only with the help of known physical rules (Ockham's razor). Only then, one must have the courage to use an alternative model. The standard-big-bang-model has flopped for a long time, even in respect of other points. Unfortunately, the common view latterly seems to tend more and more into the direction »dark matter« and »quintessence«, which can be regarded as criterion, that the proponents of the standard-model are at their wit's end.

But if the HUBBLE-parameter continues to decrease and the observed objects are being located in the correct distance, the only possible explanation is, that the photons are subject to an additional attenuation during their propagation, not known until now. And exactly this is an essential quality of the model on hand. Of course, already previously models existed (e.g. tired light) which work with an additional attenuation. All they have failed however, since they wanted to attribute the attenuation to the particle properties of the photons only. But the wave properties are the cause in reality. Nevertheless, the tired-light-hypothesis appears essentially more plausible, than the assumption of the existence of dark matter and quintessence.

In Section 4.3.2. we had worked out the propagation-function for a loss-affected medium with expansion and overlaid wave. Different from the propagation-function for a loss-free medium the attenuation rate α is different from zero there. It has the value $1/R$. Therefore we want to forecast the observed brightnesses of SNae Ia with the help of this function. For the graphic representation, we need the function $m_b(z)$. Starting from (260) we obtain for the apparent magnitude m_b :

$$m_b = -2.5 \lg \frac{F}{F_0} = -2.5 \lg \left(\frac{1}{4\pi r^2} \frac{L_{Ia}}{F_0} \right) = -2.5 \lg \frac{L_{Ia}}{4\pi r^2 \cdot 2.51 \cdot 10^{-8} \text{ W m}^{-2}} \quad (271)$$

In doing so we notice, that the value L_{Ia} , the luminosity (power) of the standard-candle supernova Ia is missing. And indeed, neither in [42], [43], [44] nor in [45] such a one is specified. Fortunately, the colleague Wolfgang Hillebrandt from the Max-Planck-Institute for Astrophysics (MPA) Garching could help me with this problem. According to his information, the maximum luminosity of a SN-Ia has a value of 10^{36} W approximately. That's the upper limit. If we put it into (271) still the distance r is missing. Since we look at the matter starting from the source toward the observer, we obtain it with the help of (240) without correction-term. It applies:

$$m_b = -2.5 \lg \frac{10^{36} \text{ W}}{4\pi r^2 \cdot 2.51 \cdot 10^{-8} \text{ W m}^{-2}} = -2.5 \lg \left(\frac{1}{\tilde{R}^2} \frac{10^{44} \text{ m}^2}{2.51\pi} \frac{1}{((z+1)^{4/3} - 1)^2} \right) \quad (272)$$

$$m_b = -2.5 \lg \left(\frac{\tilde{H}_0^2 \cdot 10^{44} \text{ m}^2}{c^2 \cdot 2.51 \pi \cdot ((z+1)^{4/3} - 1)^2} \right) = -2.5 \lg \left(1.41103 \cdot 10^{26} \text{ s}^2 \frac{\tilde{H}_0^2}{((z+1)^{4/3} - 1)^2} \right) \quad (273)$$

This is the function $m_b(z)$ without consideration of the additional attenuation. Since also the z -axis needs to have a logarithmic scale, we apply the value 10^w with $-2 \leq w \leq 0$ instead of z . Now indeed, PERLMUTTER has published all measurements in [45], but since I do not dispose of any procedure, to present it so nice, including the tolerance-limits, I decided, to take up the comparison with (273) by overlay of both charts.

Figure 34 presents the relative brightnesses, calculated with the help of (273), in comparison with the observations of the supernova-cosmology-project. Also to be seen are the curves of the standard-big-bang-model for various adjustments calculated by PERLMUTTER. The overlay-markers (+) are located at all corners except for top left.

In the presentation meets the eye that the three brightness-functions (according to this model without consideration of the parametric attenuation) are below the observed values, just they have been computed too bright. This is even no miracle, since we used the maximum-value as standard-candle. Figure 34 also shows, that solution (256) with $71.996 \text{ km s}^{-1} \text{ Mpc}^{-1}$ for the HUBBLE-parameter (red) comes quite very close to reality, because it is located at the outer margin of the error tolerance corridor. Using the updated value (255) in the amount of $68.624 \text{ km s}^{-1} \text{ Mpc}^{-1}$ we are already within. The same applies to the value derived from the COBE-measurements, which would follow the same curve (blue) in the graphics. Now, in contrast to the previous editions we'll use value (477) for the following contemplations.

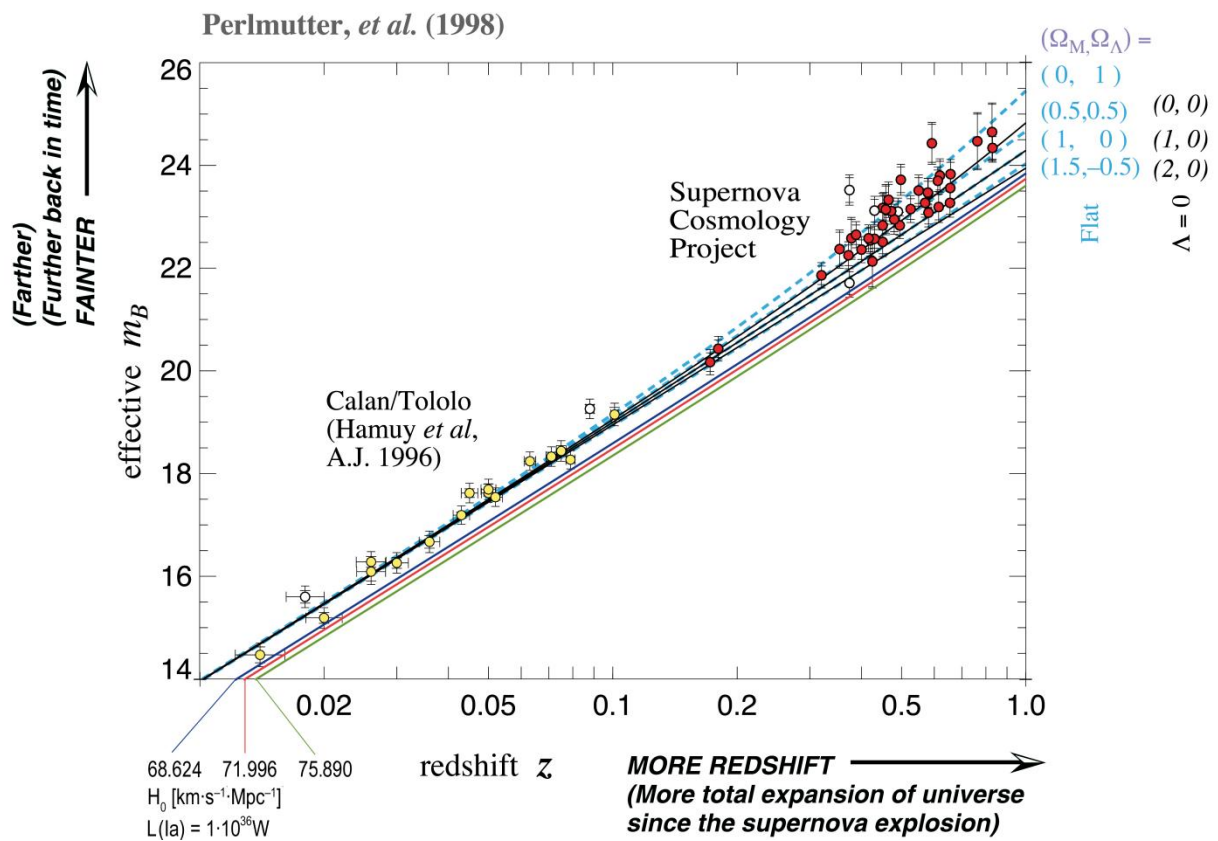


Figure 34: Calculated Apparent Bolometric Brightness for the Three Values of the Hubble-Parameter in Comparison with the Observations of the Supernova-Cosmology-Project (Standard-Candle = Maximum)

We determine the updated value of the standard-candle, which is the statistical average of all observed SNaIa, numerically with the help of (255) for a value at the lower end of the z -axis to $L_{Ia} = 6.40949 \cdot 10^{35} \text{ W}$. Applied to (271) using the example of $\tilde{H}_0(255)$ we obtain :

$$m_b = -2.5 \lg \left(\frac{\tilde{H}_0^2 \cdot 6.41 \cdot 10^{35} \text{ m}^2}{c^2 \cdot 2.51 \cdot 10^{-8} \pi \cdot ((z+1)^{4/3} - 1)^2} \right) = -2.5 \lg \frac{4.4734 \cdot 10^{-10}}{((z+1)^{4/3} - 1)^2} \quad (274)$$

$$m_b = -2.5 \lg 4.4734 \cdot 10^{-10} + 2 \cdot 2.5 \lg ((z+1)^{4/3} - 1) = 23.3734 + 5 \lg ((z+1)^{4/3} - 1) \quad (275)$$

We need the function $m_b(z)$ with parametric attenuation as well. On this occasion we have to consider the factor $e^{-\tau/R} = 10^{-\tau/R \cdot \lg e}$ from the propagation-function (236). It applies:

$$m_b = -2.5 \lg \left(\tilde{H}_0^2 9.0447 \cdot 10^{25} s^2 \frac{e^{-\tau/\bar{R}}}{((z+1)^{4/3}-1)^2} \right) = -2.5 \lg \frac{4.4734 \cdot 10^{-10}}{((z+1)^{4/3}-1)^2} e^{-\frac{1}{2}((z+1)^{4/3}-1)} \quad (276)$$

$$m_b = -2.5 \lg \frac{4.4734 \cdot 10^{-10}}{((z+1)^{4/3}-1)^2} 10^{-\frac{1}{2}((z+1)^{4/3}-1) \lg e} \quad (277)$$

$$m_b = 23.3734 + 5 \lg((z+1)^{4/3}-1) + 0.5429((z+1)^{4/3}-1) \quad \text{With parametric attenuation} \quad (278)$$

Figure 35 shows the graphs of expression (275) and (278) in comparison with the measurements of the supernova-cosmology-project for solution (477) of the HUBBLE-parameter. The thin black lines show the expectation-values of the standard-model for $\Lambda=0$ with a mass-energy-density $\Omega_M=0, 1$ and 2 . For one time, it is an empty universe (0),

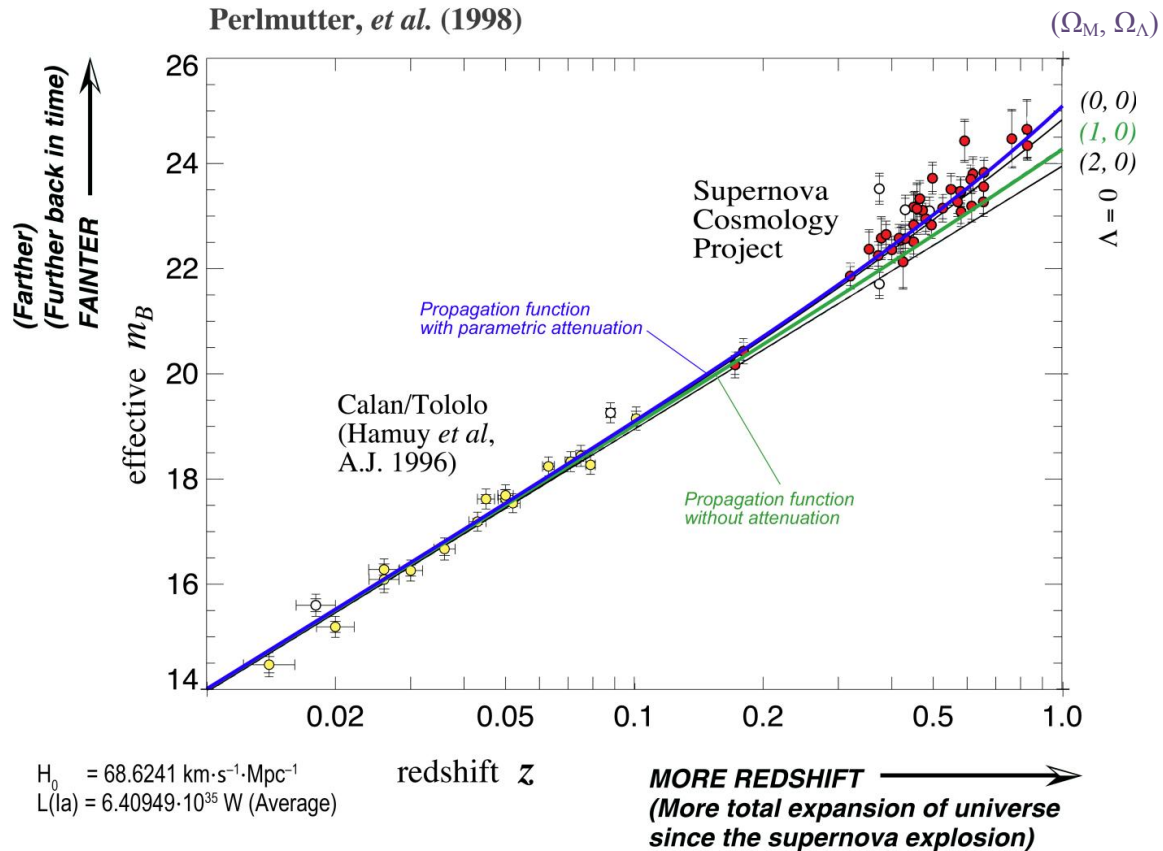


Figure 35: Calculated Apparent Bolometric Brightness for Solution (257) of the Hubble-Parameters in Comparison with the Observations of the Supernova-Cosmology-Project (Standard-Candle = Average)

for the time a universe with normal energy-density (1) and at last a universe with double energy-density (2). In this connection, the standard-BB-solution for the »normal« universe covers the propagation-function for a loss-free medium (275). That is also no miracle, because both have the same exponent 4/3 in (240). This case however is not confirmed by the observations, neither an empty universe. For $\Lambda=0$ even a universe with negative mass-energy-density (filled with antimatter) would be necessary. Then, according to [45] the best match is with $\Omega_M=0.28$ and $\Omega_\Lambda=0.72$. Thereat, all along, the sum of both values must always be equal to one. The value Ω_Λ is the so-called »dark energy-density« which indeed could be identical to our metric wave-field (OK = absolutely dark).

IV. *The observed values of the supernova-cosmology-project are exactly described by the propagation-function (236) under consideration of the geometric and parametric attenuation (215). The assumption of the existence of any new exotic kind of matter or unknown physical effects is not necessary. There is neither dark matter, quintessence nor increasing expansion!!*

As I said, the whole thing sounds rather improbable, especially as this optimal course is »coincidentally« described exactly by the function (278) (blue curve in Figure 35), and all this with the help of known physical objects and relationships. However, Figure 35 only shows the curve up to $z = 1$, whereby the two measured values with the highest z are even below 0.9. The whole thing looks good in the graphic, but in my opinion it is not meaningful enough. Also, the number of properties analysed in the first stage of the project leaves a lot to be desired. The more values, the more exact statistics.

Therefore, it would be nice, to be in the position to analyse and display SN α -Ia with $z > 0.9$. Blessedly the High- z -Supernova-Search-Team added further observational data [73] since 1994, so that the limit has been moved upwards to $z = 1.414$ now. There are in total 580 values in the range $0.015 \leq z \leq 1.414$ on hand, 48 thereof with $z > 0.9$. They are shown in Figure 36 to 38.

The data was taken from [45]. They are available there as the file SCPUnion2.1_mu_vs_z.txt. It can be imported as a .csv file into Excel, where further processing is possible. This is necessary because, in contrast to the first project section, the distance module $\mu = m_b - M_b$ (column 3) instead of the apparent bolometric magnitude m_b has been specified beside the z -values (column 2). To ensure comparability with the previous data, we need the exact value of M_b . In [77] the definition of μ is given, but without the extinction A_v . It are the losses caused by atmospheric and interstellar influences, as well as by the instruments used, e.g. bolometers. We obtain the complete definition with the help of [78]:

$$\mu = m_b - M_b = A_v - 5 + 5 \lg r \quad r[\text{pc}] \quad \text{Distance module} \quad (279)$$

The distance from the source r must be given in parsecs [pc] here due to the definition of absolute magnitudes at a distance of 10 pc. That makes it easier to understand. If A_v is neglected, the right-hand side turns into zero and $M_b = m_b$ applies. Thus, the absolute bolometric brightness M_b represents a sort of target value. It depends on the (average) luminosity L_{Ia} of the SN α -Ia only. If you know it, you can even calculate it. With the previously determined value for L_{Ia} for $r = 10$ pc we get:

$$M_b = m_b - A_v = -2.5 \lg \frac{F_{\text{Ia}}}{F_0} - A_v = -2.5 \lg \left(\frac{1}{4\pi r^2} \frac{L_{\text{Ia}}}{F_0} \right) - A_v \quad (280)$$

$$M_b = -2.5 \lg \frac{6.40949 \cdot 10^{35}}{4\pi \cdot 9.52167 \cdot 10^{32} \cdot 2.51 \cdot 10^{-8}} - A_v = -18.3231^M - A_v \quad (281)$$

This is the value that needs to be subtracted from μ in order to determine m_b , assuming A_v is negligibly small. Obviously, that's not the case. The header of the text file contains important information, including two values for M_b . With it, we are able to determine A_v .

```
# alpha 0.121851859725
# beta 2.46569277393
# delta -0.0363405630486
# M(h=0.7, statistical only) -19.3182761161
# M(h=0.7, with systematics) -19.3081547178
```

The first three values could not be assigned. They obviously have to do with systematics. In any case, the relevant value for M_b is the last one (-19.3081547178^M). The value of A_v is at 0.9850875^m then.

It is almost one class of magnitude and amounts to a ratio of 2.47762 or 60% loss. The factor 0.4 in many expressions is derived therefrom too. During measurement, the luminosity is reduced (divided) by exactly this factor (2.47762). In [78] it's stated:

Thus, the atmospheric extinction increases with the zenith distance. At the zenith, it amounts to around 0.28 mag (23%) at sea level and is essentially caused in equal parts by Rayleigh scattering from air molecules and scattering from aerosol particles.

If we subtract the 0.28^m , the sum of interstellar and technical extinction is 0.705088^m or 48% then. To determine the proportionality factor **MaG[#]** with an increase of the magnitude m_b of #, I have defined the following function **MaG=Function[10[^](-0.4#)]**. The inverse function is **GaM=Function[-2.5 Log10[#]]**. Now we can also determine the m_b values and summarize them with the z values in the list form **SNList1={{z,mb},{0.015,15.0716180869},...}**; Then, the list can be imported into *Mathematica* via clipboard or text file and displayed with the following program:

```
new1={}; (* High-z-SN-Data *)
y=Length[SNList1];
For[i=0,<K>y,i++,all=Part[SNList1,i+1];AppendTo[new1,{Log10[Part[all,1]],Part[all,2]}]
bb=ListPlot[new1,ImageSize->Full,LabelStyle->{FontFamily->"Chicago",12,Black},
PlotRange->{{-2,1},{14,43}},PlotStyle->{PointSize[Medium],Red},AxesOrigin->{1,14};
Show[bb,Graphics[Line[{{0,0},{0,60}}]]] (282)
```

The result (Figure 36) is an overlay file already superimposed the existing Figure 162 of [29]. The objects with $z > 0.9$ are to the right of the left vertical line. As you can see, there are many more measured values and they fit the solution (278) exactly. Even the increasing attenuation in the range $0.1 \leq z \leq 1.414$ can be seen very clearly now. This was not really to be expected, as the blue curve (278) is based on my SN-Ia brightness of $L_{\text{Ia}} = 6.40949 \cdot 10^{35} \text{ W}$, while PERLMUTTER et. al. probably used a different value. It is not specified anywhere, but we can calculate it.

The blue curve is described by the function $m_b(z)$. There are no more parameters. First let's have a look which partial expression of (278) may change with constant z and where the brightness L_{Ia} is contained at all. Only the first expression, the 23.3734, remains, because the 5 and the \log_{10} -logarithm in the second expression are stipulated by the definition of the magnitude class. The 0.5429 in the third expression is owed to the conversion of the e -function in the damping expression into the exponential function $e^{-\tau/R} = 10^{-\tau/R \cdot \lg e}$ and therefore also invariable. The factor $\frac{1}{2}$ follows from (240) and is counted among the z -expression.

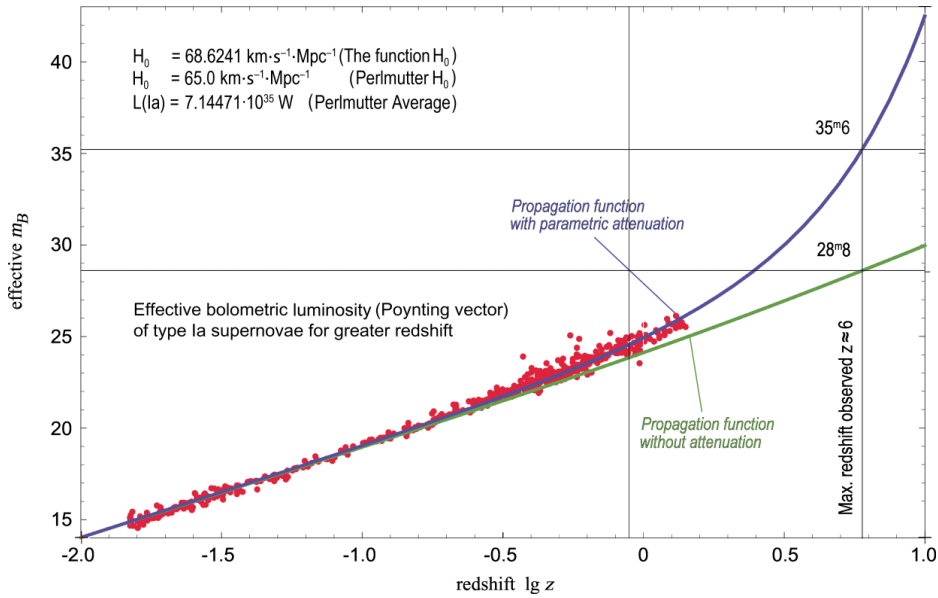


Figure 36: Calculated Effective Bolometric Luminosity for the Project Data with Solution (257) of the HUBBLE-Parameter for more Distant SNæ-Ia

But if the measured data validate my function, that means nothing other than, that the 23.3734 does not change, even though it contains L_{Ia} . The reason is, PERLMUTTER simultaneously works with a different L_{Ia} , but also with a different H_0 of 65 instead of $68,6241 \text{ km s}^{-1} \text{ Mpc}^{-1}$. Since the value 23.3734 doesn't change, we should analyse where it comes from. If we substitute r for (240) in (271), we obtain:

$$m_b = -2.5 \lg \left(\frac{1}{4\pi r^2} \frac{L_{Ia}}{F_0} \right) = -2.5 \lg \left(\frac{\pi^{-1} L_{Ia}}{\tilde{R}^2 F_0} \frac{1}{((z+1)^{4/3}-1)^2} \right) = -2.5 \lg \left(\frac{\tilde{H}_0^2 L_{Ia}}{\pi c^2 F_0} \dots \right) \quad (283)$$

The right-hand expression without the ... amounts to the wanted 23.3735. Analogous for L'_{Ia} , and \tilde{H}'_0 . Since π , c and F_0 are constants, $m_b = m'_b$ and we are using the same measured values, we can equate both expressions obtaining for $L'_{Ia} = L_{Ia} (\tilde{H}_0/\tilde{H}'_0)^2$ a value of $7.14414 \cdot 10^{35} \text{ W}$ resp. -18.40998^m . The negative sign indicates that the objects are very very bright. The average L_{Ia} value I determined is not quite as bright and is equal to $6.40949 \cdot 10^{35} \text{ W}$ resp. -18.2922^m . Then, we obtain the absolute brightnesses (at a distance of 10 pc):

$$L_{Ia} = 6.40949 \cdot 10^{35} \text{ W} = -18.2922^m \quad L_{Ia} = 7.14414 \cdot 10^{35} \text{ W} = -18.410^m$$

$$F_{Ia} = \frac{L_{Ia}}{400\pi \text{ pc}^2} = 0.535674 \text{ W m}^{-2} \quad F_{Ia} = -2.5 \lg \left(\frac{1}{400\pi \text{ pc}^2} \frac{L_{Ia}}{F_0} \right) = -18.323^m \quad [117.289 \text{ dB}_{\text{pWm}^{-2}}] \quad (284)$$

$$F'_{Ia} = \frac{L'_{Ia}}{400\pi \text{ pc}^2} = 0.597073 \text{ W m}^{-2} \quad F'_{Ia} = -2.5 \lg \left(\frac{1}{400\pi \text{ pc}^2} \frac{L'_{Ia}}{F_0} \right) = -18.441^m \quad [117.760 \text{ dB}_{\text{pWm}^{-2}}]$$

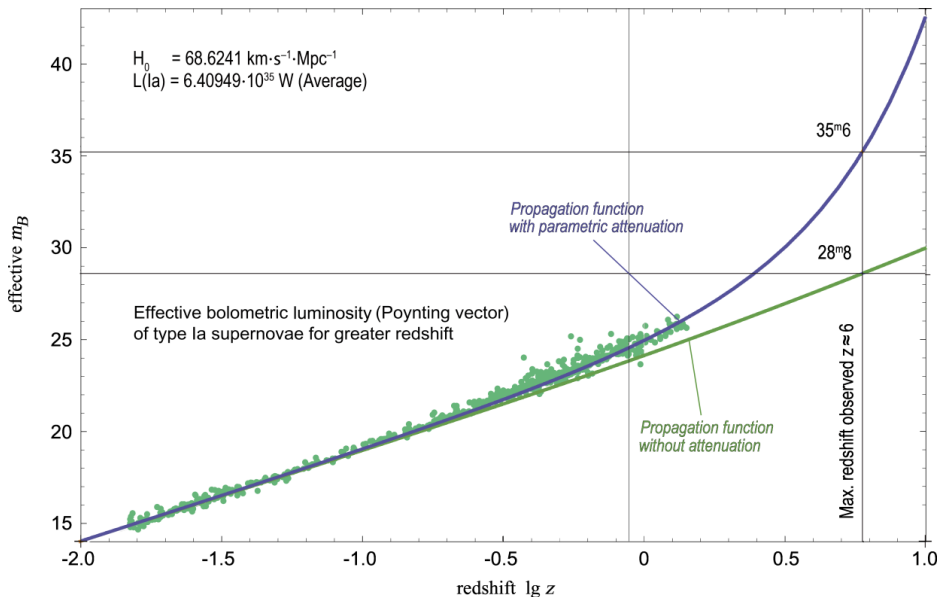


Figure 37: Calculated Effective Bolometric Luminosity for the MLE-Model with Solution (257) of the HUBBLE-Parameter for more Distant SNæ-Ia

There is a slight difference in flux between the two values in the order of magnitude of $\Delta F_{Ia} = F_{Ia} - F'_{Ia} = 0.117817^m$. This corresponds to a 10.2833% lower level for my model, i.e. since my mean bolometric SN-Ia-brightness is slightly lower, the absolute bolometric bright-ness at 10 pc distance is slightly lower too. As the 10 pc always remain the same, regardless of how large H_0 , a different value of H_0 does not affect the measured values, only the model. Therefore, the data does not need to be corrected for the MLE model. For $H_0=68.6241\text{kms}^{-1}\text{Mpc}^{-1}$ we obtain the same presentation as in Figure 36.

The following user-friendly functions are defined for calculations even with a different H_0 :

```

P0= H0; (* or 65*1000/Mpc *);
P1=SetPrecision[-2.5Log10[P0^2/c^2L1a/Pi/F0] - 0.4515449878350246, 30]; → See thereto (294)
P2=SetPrecision[1.25Log10[E],30]; (* -2.5(-1/2*Log10[E]) *)
Mby=Function[P1+5Log10[(((#+1)^(4/3)-1)]];
Mbz=Function[P1+5Log10[(((#+1)^(4/3)-1)]+P2((#+1)^(4/3)-1)];
Mbq=Function[P1+5Log10[2# P0/c];
MbQ=Function[P1+5Log10[2#];
Mbr=Function[P1+5Log10[2# P0/c]+P2*2# P0/c];
MBr=Function[P1+5Log10[2#]+P2*2# ];

```

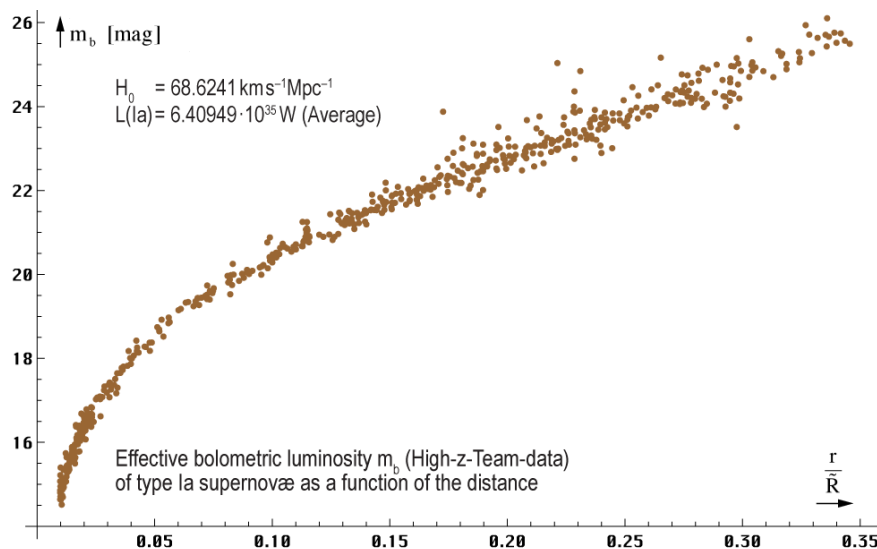


Figure 38:
Effective Bolometric Luminosity of the High-z-SN-Ia Measured Data as a Function of Linear Distance (286)

The function $m_b(r)$ is interesting too. From (240) follows the substitution $((z+1)^{4/3}-1) = \frac{2r}{\tilde{R}}$

```

y=Length[SNList1]; SNList2={}; new2={};
For[i=0,<y,i++,all=Part[SNList1,i+1];AppendTo[SNList2,
{N[.5(1-(1+Part[all,1])^(-4/3))],Part[all,2]}]]
aa=ListPlot[SNList2,ImageSize->Full,PlotRange->{{-.005,.359},{13.7,26.3}},AxesOrigin->{0,14},
LabelStyle->{FontFamily->"Chicago",12,Black},PlotStyle->{PointSize[Medium],Brown}]

```

Figure 38 clearly shows the area covered by the observation data. It should be noted that because of the definition of the radiation cosmos, $R=2cT$ applies. The x-axis then naturally runs up to $0.7cT$. The logarithmic view in Figure 39 provides further information about the course. It was displayed with the following program:

```

new2={};
For[i=0,<y,i++,all=Part[SNList2,i+1];AppendTo[new2,{Log10[(((Part[all,1]+1)^(4/3)-1)],Part[all,2]}]]

bb = Plot[{MbQ[10^y],MbX[10^y],Mbr[10^y]}, {y, Log10[10 pc/R] - .1, 0}, ImageSize -> Full,
PlotRange -> {{-8.8, 0.1}, {-21, 31}}, LabelStyle -> {FontFamily -> "Chicago", 12, Black},
PlotStyle -> {{Thickness[0.0035],Brown},{Thickness[0.0035],Blue},{Thickness[0.0035],Red}}];

cc=ListPlot[new2,ImageSize->Full,LabelStyle->{FontFamily->"Chicago",12,Black},
AxesOrigin->{0,0},PlotRange->{{-8.8,0.1},{-21,31}},
PlotStyle->{PointSize[Medium],CMYKColor[.4,.2,1,0]}];

Show[cc,bb,Graphics[Line[{{{-10,26.102},{1,26.102}},{{-10,Mbr[10 pc]},
{1,Mbr[10 pc]}},{{Log10[10pc/R],-21},{Log10[10pc/R](*-8.3*),31}},{{-0.295,-21},
{-0.295,31}},{{-1.885,-21},{-1.885,31}},{{-10,14.516},{1,14.516}}]]]]

```

I have taken the boundaries for the display from the High-z file. Interestingly enough, the measured values from a distance of approx. $0.1R$ on are distributed in a totally different manner than generally assumed. They are darker

(higher magnitude) than calculated by the previous relations. Neither the function (275) substituted by (240) [brown], nor the substituted function (278) [red] are tracing the distribution accurately enough:

$$m_b = 23.3734 + 5 \lg \frac{2r}{R} \quad \text{Average geometric only} \quad (288)$$

$$m_b = 23.3734 + 5 \lg \frac{2r}{R} + 0.54295 \frac{2r}{R} \quad \text{Average geometric+parametric} \quad (289)$$

It looks as if an additional damping occurs from $0.1R$ on. At this point, however, another effect comes into play. In Section 4.5.2.3. of [29] I stated that the value of H already increases from $r \geq 0.01 R$ on, so that it reaches a value of $H_1 = 3/2 H_0$ at the world radius, at $r=R/2=cT$. The distance r (to the SN) is here the constant wave count vector r_k and not the zero vector of the radiation of the observed SN.

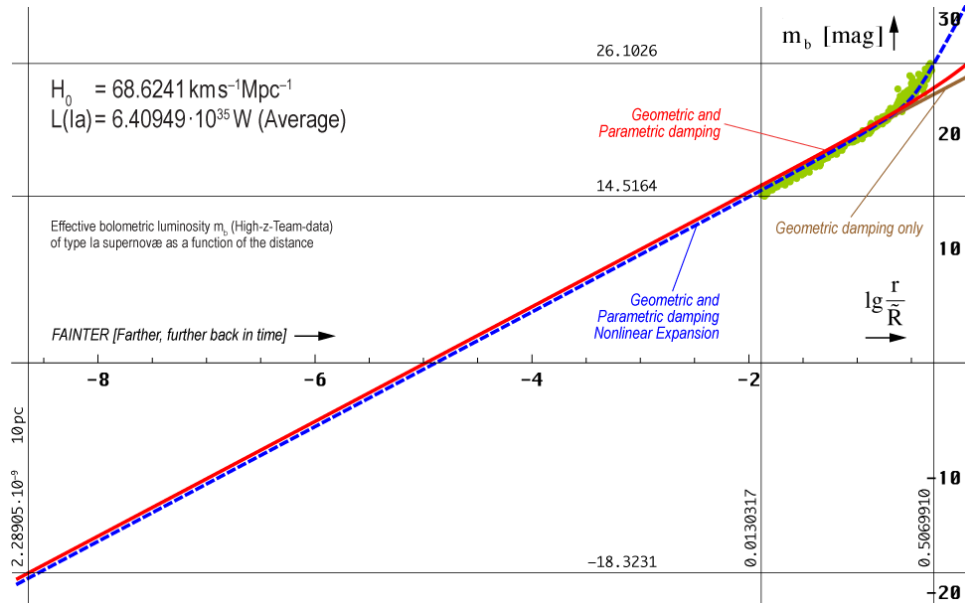


Figure 39: Effective Bolometric Luminosity of the High-z-SN-Ia as a Function of Distance Logarithmic Coarse

Functions (288), (289), (290)

That means, the expansion velocity $v=Hr$ over the entire length increases above $r > 0.1 R$. This can clearly be seen in Figure 43 of [29]. However, if the expansion rate increases at greater distances, it was greater in the past, not later in the future. It's said *Fainter [farther, further back in time]*. However, this also means, *the expansion rate does not increase, but decreases over time!* Indeed, the objects are really further away than calculated. But that's only because H_0 used to be much greater in the old days. At large distances, expansion speed and H along the total distance r aren't uniform everywhere. This can be neglected for $r \leq 0.1R$, but not for $r > 0.1R$. Then you have to calculate the integral over the entire distance, as I did in Section 4.5.2.3. of [29]. The blue curve in Figure 39 shows the probable function (291). But it's displaced (lighter in colour) compared to the brown and red function.

For a better overview and to determine the complete function, a section of the data area is shown in Figure 40. On the right you will find a smaller version of Figure 43 of [29].

The relevant function (green) is described by $v=Hr = r m/T$ with $H=m/T$ (345). The parameter m is the Taylor series for the solution of the implicit function (339). We choose the third, most accurate variant of (344 [29]) with $r = r/R$

$$m \approx 0.5001002 + 0.598206r - 3.45991r^2 + 18.3227r^3 - 42.69950r^4 + 38.0733r^5$$

The exact derivation can be found in [29].

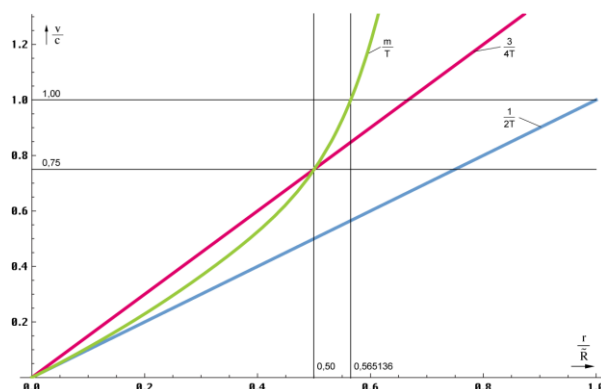


Figure 43 [29]: Expansion-Velocity as a Function of the Distance for $t=0$, the Values $r > 0.5R$ Are Extrapolated

The value of m for $r=0$ is denoted as m_0 . But how the »strange behaviour of the real measured values« can be mapped correctly in our formula? The fact is that it's about an additional damping but not a parametric, but a geometric one. This is caused by the fact that the objects are further away than the calculation with a constant $H = H_0$

would have us believe. All expressions containing R or H are relevant. If it contains R^\uparrow , \tilde{R}^\uparrow , H_0 or \tilde{H}_0 , we must compensate for the dependency on the total length/distance using a correction factor. Because of $m_0=1/2$, $H=m/T$ applies $H \sim m$ and $H/H_0 = m/m_0 = 2m$. In (283) R_0 resp. H_0 occurs exactly once and that in the square. Substituted in (289) gives the following:

$$m_b = 23.3734 + 51g \frac{m^2}{m_0^2} \frac{2r}{\tilde{R}^\uparrow} + \frac{0.54}{1/2} \frac{2r}{\tilde{R}^\uparrow} = 23.3734 + 51g \frac{2r}{\tilde{R}^\uparrow} + 51g 2m + 1.08 \frac{2r}{\tilde{R}^\uparrow} \quad (290)$$

Now the added parametric part also contains \tilde{R}^\uparrow . The question is, do we have to correct this too? No, as the universe expands, r and \tilde{R}^\uparrow are changing in the same way. But the damping factor α is always $-1/R$, regardless of the size of R . Since the parametric damping does not depend on $2r/\tilde{R}^\uparrow$, but on r/\tilde{R}^\uparrow , a different correction is necessary here. We have to divide by a factor 2, which has turned into $1/2$ due to the sign change of the product $-2.5 \lg 10^{(-1/2 \lg e)}$. The $-1/2$ actually belongs to the z -bracket expression, but it »disappeared« in the coefficient $0.54\dots$. This way, the initially higher expansion rate also had had an influence on the parametric share. I would like to call the whole concept *non-linear expansion*. Then, after rounding, we get the final expression, re-sorted:

$$m_b = 23.3734 + \frac{2r}{\tilde{R}^\uparrow} + 51g \frac{2r}{\tilde{R}^\uparrow} + 1.51g m \left(\frac{2r}{\tilde{R}^\uparrow} \right) \quad \text{Exactly, geometric and parametric, nonlinear expansion} \quad (291)$$

The factors of the second [1.08574] and fourth [1.50515] expression are rounded. The course of function (291) is already shown as a dashed line in Figure 39. As you can see, the measurement data was hit correctly. At smaller distances, however, the curve runs permanently below the geometric and parametric function. The gap down to the 10 pc limit (F_{Ia}) is -0.451545^m (brighter). Actually, we should have to correct L_{Ia} as well. Since the $m_b(z)$ functions are correct, but (288) and (289) too dark, it is more appropriate to correct them. Why? If you examine the overall course, both describe exactly the course of the statistical mean value of the measured data without taking the shape into account. But the given systematic target value $M_b = -19.3081547178^m$ is also a statistical mean. Therefore, it's no wonder that the curve deviates from the form-fit function (291). Therefore, for use as an exact function in the range $r \leq 0.1 \tilde{R}^\uparrow$, we correct as follows:

$$m_b = 22.922 + 5 \lg \frac{2r}{\tilde{R}^\uparrow} \quad r \leq 0.1 \tilde{R}^\uparrow \quad \text{Exactly, geometric only} \quad (292)$$

$$m_b = 22.922 + 5 \lg \frac{2r}{\tilde{R}^\uparrow} + 0.54295 \frac{2r}{\tilde{R}^\uparrow} \quad r \leq 0.1 \tilde{R}^\uparrow \quad \text{Exactly, geometric+parametric} \quad (293)$$

Adding the green addition to P1 in (285) changes the functions (288) and (289) into (292) and (293). Figure 40 shows the exact functions (291), (292), (293). Here still the functions for the calculation of m (Hm_0) and the blue line (MbX).

$$\begin{aligned} Hm_0 &= (0.5+0.598206 \# - 3.45991 \#^2 + 18.3227 \#^3 - 42.6995 \#^4 + 38.0733 \#^5) \& ; \\ MbX &= \text{Function}[P1+2\#+5\text{Log}10[2\#+1.5\text{Log}10[Hm0[2\#]]]; \end{aligned} \quad (294)$$

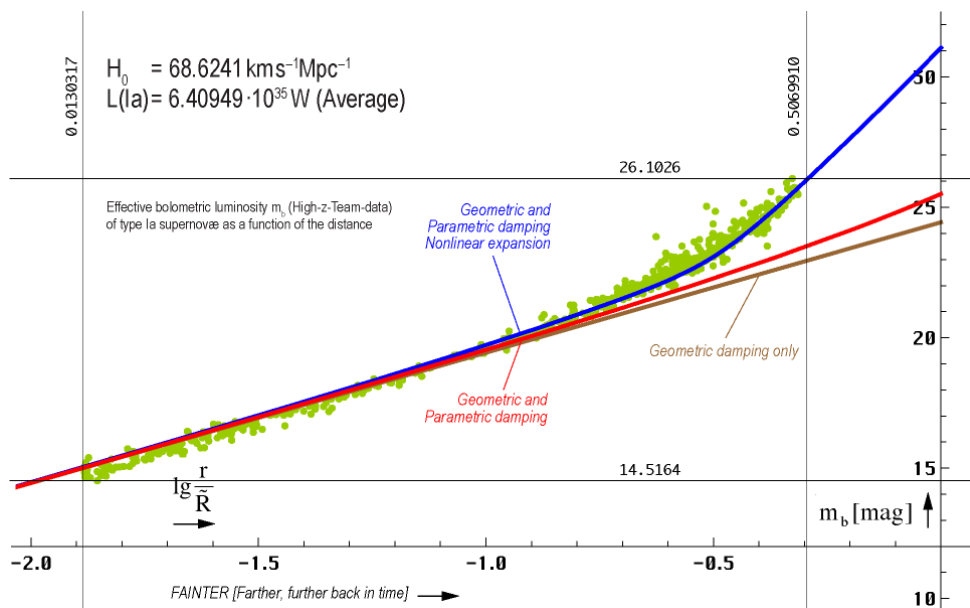


Figure 40: Effective Bolometric Luminosity of the High-z-SN-Ia as a Function of Distance Logarithmic Fine

Functions (291), (292), (293)

6. Conclusion

When comparing the observed (maximum) brightness m_b of the SN-Ia with the respective value $m_b(z)$ calculated from L_{Ia} using z in the SN-Ia cosmology project, it was found at that time that the measured brightness was slightly lower, i.e. the SN were dimmer than calculated. The difference is visible from approx. $z=0.1$ on continuing to increase beyond this point. It was therefore assumed that the objects are further away than expected, which should lead to a stronger geometric attenuation. It was also assumed that this was caused by an *increasing expansion* ($H_0 \sim T^{n>1}$) instead of the previously supposed decreasing one ($H_0 \sim T^{-1}$).

At the beginning of this paper it was found that this *increasing expansion* is a fallacy resulting from contradictory, i.e. inconsistent, premises. These are mainly the geometric damping with and the wave propagation without expansion. It has been shown that the predominant propagation function for electromagnetic waves ($\square \mathbf{E}=0$) is suitable for local applications, but not for processes on a cosmic scale. The reason for this is that MAXWELL's equations and their solution do not take into account, imply or condition the expansion of the universe.

As a result, a complete, alternative propagation function with expansion (237) was developed, based on the MLE model developed by me which behaves like the classical MAXWELL solution in the first approximation for $z \leq 0.1$. Using this function, the successful comparison with the observational data of the SN-Ia cosmology project, first conducted in [29], has been repeated and extended in order to include the High- z -SN-Ia data. In this context, the 580 SCPUnion2.1 records have been graphically displayed and overlaid the previously published prediction graph (Figure 162 [29]) for SN-Ia with $z \geq 1$, confirming the MLE model for this range as well. The originally postulated discrepancy in brightness has been resolved. If we apply consistent premises we also get a consistent result.

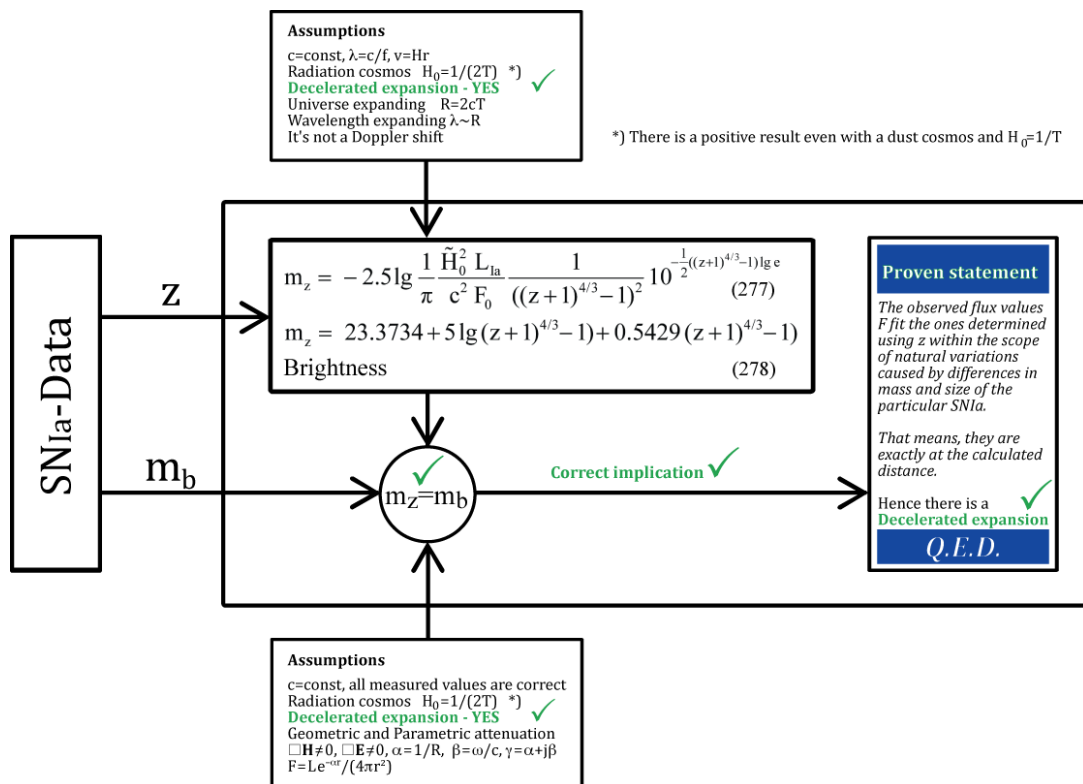


Figure 41: Successful data analysis of the Supernova-Ia-Cosmology Project

Using the MLE model consistently, I carried out a further evaluation $m_b(r)$ in addition to the project's own data evaluation $m_b(z)$. This revealed a new deviation in the converted project data of $r \geq 0,1R$, even not expected by me. Surprisingly, these are darker than calculated (magnitude \uparrow). This deviation could be attributed to the fact that the HUBBLE-parameter is time- and distance-dependent due to $H = 1/(2T)$ [29]. Sections that are further away expand faster than those that are closer. The greater the distance, the greater the value of H and the expansion speed $v = Hr$. This made it possible to create a function $m_b(r)$ which correctly traces the deviant distribution. At the same time, it's the *proof that the expansion rate decreases with time and does not increase*, as falsely claimed. Thus all contradictions have been resolved.

7. The Concerted International System of Units

A variety of formulas for the calculation of various variables and graphics are specified in the course of this work. These in turn access certain values and natural constants whose meaning or values are not shown in the text, but which are required to carry out the calculations correctly.

Using the MLE model of [29] it has been possible to calculate a series of natural constants associated with the electron, the proton and the ^1H atom via their relation to the reference frame Q_0 and that exactly. The model is based on the basic variables of the subspace, which are fixed values, independent of the reference system. It is sufficient to define only five genuine constants (μ_0 , c , κ_0 , \hbar_1 and k) as base variables plus a so-called *Magic value*, in this case m_e to specify the reference system Q_0 . All values are related via Q_0 ; if one value changes, they all change. If an influence is added, it is yet another reference system. With it, all values except for the fixed ones form a so-called canonical ensemble, the *Concerted System of Units*.

The program that makes these basic constants and functions available can be found in the appendix. It can also be used in other of my publications. The numerical values calculated with it, in comparison with the corresponding CODATA₂₀₁₈-values are shown in Table 3. When preparing the table, I added further values to the system that are simply dependent on those already defined, including σ_e , a_e , g_e , γ_e , μ_e , μ_N , Φ_0 , G_0 , K_J and R_K . Except for r_e , whose definition is misstated in all editions, I used the expressions and symbols from the CODATA₂₀₁₈-document [63] for the other values. Please find the definition of the formula symbols from there.

8. Notes to the appendix

The basic formulas and definitions used in this work, are shown in the appendix. It's about the source code for *Mathematica*. The data from the .pdf may be converted into a text file (UTF8), which can be opened directly. Data is presented as a single cell then. However, it is not advantageous to evaluate the entire source code in one single cell. To split, use the Cell/Divide Cell function (*Ctrl/Shift/d*). However, with this procedure there may be problems with special characters, not correctly transferred (e.g. ε , ϵ) or even lead to the conversion being aborted. It is more advantageous to copy and paste data page by page into the text file via clipboard. However, then each line is present as a separate cell. With the command Cell/Merge (*Ctrl/Shift/m*) the cells belonging together can be merged, ideally in blocks between the headings. Then, the values shown in the »Variable« column are available for own calculations.

Symbol	Variable	Calculated (CA)	Source	CODATA ₂₀₁₈ (CD) © COBE Data	± Accuracy	Δy (CA/CD-1)	Unit
c	c	$2.99792458 \cdot 10^8$	S	$2.99792458 \cdot 10^8$	defined	defined	m s^{-1}
ε_0	ep0	$8.854187817620390 \cdot 10^{-12}$	S	$8.854187817620390 \cdot 10^{-12}$	defined	defined	$\text{As V}^{-1}\text{m}^{-1}$
κ_0	ka0	$1.369777663190222 \cdot 10^{93}$	S	n.a.	n.a.	defined	$\text{A V}^{-1}\text{m}^{-1}$
μ_0	my0	$1.256637061435917 \cdot 10^{-6}$	S	$1.256637061435917 \cdot 10^{-6}$	exactly	exactly	$\text{Vs A}^{-1}\text{m}^{-1}$
k	k	$1.3806485279 \cdot 10^{-23}$	S	$1.380649 \cdot 10^{-23}$	statistic	$+3.41941 \cdot 10^{-7}$	J K^{-1}
\hbar_1	hb1	$8.795625796565460 \cdot 10^{26}$	S	n.a.	n.a.	defined	J s
\hbar	hb0	$1.054571817000010 \cdot 10^{-34}$	C	$1.054571817 \cdot 10^{-34}$	defined	$+8.88178 \cdot 10^{-15}$	J s
Q_0	Q0	$8.340471132242850 \cdot 10^{60}$	C	$8.3415 \cdot 10^{60}$ ©	$3.3742 \cdot 10^{-2}$	$-1.23343 \cdot 10^{-4}$	1
Z_0	Z0	376.7303134617700	F	376.73031366857	$1.5 \cdot 10^{-10}$	$-5.48932 \cdot 10^{-10}$	Ω
G	G0	$6.674301499999827 \cdot 10^{-11}$	C	$6.674301499999999 \cdot 10^{-11}$	$2.2 \cdot 10^{-5}$	$-5.48932 \cdot 10^{-10}$	$\text{m}^3\text{kg}^{-1}\text{s}^{-2}$
G_1	G1	$9.594550966819210 \cdot 10^{-133}$	C	n.a.	n.a.	unusual	$\text{m}^3\text{kg}^{-1}\text{s}^{-2}$
G_2	G2	$1.150360790738584 \cdot 10^{-193}$	F	n.a.	n.a.	unusual	$\text{m}^3\text{kg}^{-1}\text{s}^{-2}$
m_e/m_p	mep	$5.446170214846793 \cdot 10^{-4}$	F	$5.4461702148733 \cdot 10^{-4}$	$6.0 \cdot 10^{-11}$	$-4.867 \cdot 10^{-12}$	1
M_2	M2	$1.514002834704114 \cdot 10^{114}$	F	n.a.	n.a.	unusual	kg
M_1	M1	$1.815248576128075 \cdot 10^{53}$	C	n.a.	n.a.	unusual	kg
m_p	mp	$1.6726219236951 \cdot 10^{-27}$	C	$1.6726219236951 \cdot 10^{-27}$	$1.1 \cdot 10^{-5}$	$-2.22045 \cdot 10^{-16}$	kg
m_e	me	$9.109383701528 \cdot 10^{-31}$	M	$9.109383701528 \cdot 10^{-31}$	$3.0 \cdot 10^{-10}$	magic ± 0	kg
m_0	m0	$2.176434097482374 \cdot 10^{-8}$	C	$2.176434097482336 \cdot 10^{-8}$	calculated	$+1.70974 \cdot 10^{-14}$	kg
M_H	MH	$2.609485798792167 \cdot 10^{-69}$	C	n.a.	n.a.	unusual	kg
T_{p2}	Tp2	$9.855642915740690 \cdot 10^{153}$	C	n.a.	n.a.	unusual	K
T_{p1}	Tp1	$1.181665011421291 \cdot 10^{93}$	C	n.a.	n.a.	unusual	K
T_{p0}	Tp0	$1.416784486973613 \cdot 10^{32}$	C	$1.416784486973588 \cdot 10^{32}$	$1.1 \cdot 10^{-5}$	$+1.75415 \cdot 10^{-14}$	K
T_{k1}	Tk1	$5.475357175411492 \cdot 10^{152}$	C	n.a.	n.a.	unusual	K
T_{k0}	Tk0	2.725436049425770	C	2.72548 ©	$4.3951 \cdot 10^{-5}$	$-1.61258 \cdot 10^{-5}$	K

Symbol	Variable	Calculated (CA)	Source	CODATA ₂₀₁₈ (CD) © COBE Data	± Accuracy	Δy (CA/CD-1)	Unit
r ₁	r1	1.937846411698606·10 ⁻⁹⁶	F	n.a.	n.a.	unusual	m
r ₀	r0	1.616255205549261·10 ⁻³⁵	C	1.616255205549274·10 ⁻³⁵	calculated	-8.21565·10 ⁻¹⁵	m
r _e	re	2.817940324662071·10 ⁻¹⁵	C	2.817940326213 ·10 ⁻¹⁵	4.5·10 ⁻¹⁰	-5.50377·10 ⁻¹⁰	m
λ _C	λbarC	3.861592677230890·10 ⁻¹³	C	3.861592679612 ·10 ⁻¹³	3.0·10 ⁻¹⁰	-6.16614·10 ⁻¹⁰	m
λ _C	λC	2.426310237188940·10 ⁻¹²	C	2.4263102386773 ·10 ⁻¹²	3.0·10 ⁻¹⁰	-6.13425·10 ⁻¹⁰	m
a ₀	a0	5.291772105440689·10 ⁻¹¹	C	5.291772109038 ·10 ⁻¹¹	1.5·10 ⁻¹⁰	-6.79793·10 ⁻¹⁰	m
R	R	1.348032988422084·10 ²⁶	C	n.a.	at issue	at issue	m
R	RR	4.368617335409830	C	n.a.	at issue	at issue	Gpc
t ₁	2 t1	6.463959849512312·10 ⁻¹⁰⁵	F	n.a.	n.a.	unusual	s
t ₀	2 t0	5.391247052483426·10 ⁻⁴⁴	C	5.391247052483470·10 ⁻⁴⁴	calculated	-8.43769·10 ⁻¹⁵	s
T	2 T	4.496554040802734·10 ¹⁷	C	4.497663485280829·10 ¹⁷	1.1385·10 ⁻³	-2.46671·10 ⁻⁴	s
T	2 T	1.424902426903056·10 ¹⁰	C	1.425253996152531·10 ¹⁰	1.1385·10 ⁻³	-2.46671·10 ⁻⁴	a
R _∞	R∞	1.097373157632934·10 ⁷	C	1.097373156816021·10 ⁷	1.9·10 ⁻¹²	+7.44426·10 ⁻¹⁰	m ⁻¹
ω ₁	Om1	1.547039312249824·10 ¹⁰⁴	F	n.a.	n.a.	unusual	s ⁻¹
ω ₀	Om0	1.854858421929227·10 ⁴³	C	1.854858421929212·10 ⁴³	calculated	+8.65974·10 ⁻¹⁵	s ⁻¹
ω _{R∞}	OmR∞	2.067068668297942·10 ¹⁶	C	2.067068666759112·10 ¹⁶	1.9·10 ⁻¹²	+7.44451·10 ⁻¹⁰	s ⁻¹
cR _∞	cR∞	3.289841962699988·10 ¹⁵	C	3.289841960250864·10 ¹⁵	1.9·10 ⁻¹²	+7.44450·10 ⁻¹⁰	Hz
H ₀	H0	2.223925234581364·10 ⁻¹⁸	C	2.223376656062923·10 ⁻¹⁸	1.1385·10 ⁻³	+2.46732·10 ⁻⁴	s ⁻¹
H ₀	HPC[Q0]	68.62410574852400	C	68.60717815146482←↑⊙	1.1385·10 ⁻³	+2.46732·10 ⁻⁴	kms ⁻¹ Mpc ⁻¹
q ₁	q1	1.527981474087040·10 ¹²	F	n.a.	n.a.	unusual	As
q ₀	q0	5.290817689717126·10 ⁻¹⁹	C	5.2908176897171 ·10 ⁻¹⁹	calculated	+4.44089·10 ⁻¹⁵	As
e	qe	1.602176634000007·10 ⁻¹⁹	C	1.602176634 ·10 ⁻¹⁹	exactly	+4.44089·10 ⁻¹⁵	As
U ₁	U1	8.698608435529670·10 ⁸⁷	F	n.a.	n.a.	unusual	V
U ₀	U0	1.042939697003725·10 ²⁷	C	1.042939697286845·10 ²⁷	calculated	-2.71463·10 ⁻¹⁰	V
W ₁	W1	1.360717888312544·10 ¹³¹	F	n.a.	n.a.	unusual	W
W ₀	W0	1.956081416291675·10 ⁹	C	1.956081416291641·10 ⁹	calculated	+1.73195·10 ⁻¹⁴	W
S ₁	S1	5.605711433987692·10 ⁴²⁶	F	n.a.	n.a.	unusual	Wm ⁻²
S ₀	S0	1.388921881877266·10 ¹²²	C	n.a.	n.a.	unusual	Wm ⁻²
σ _e	σe	6.652458724888907·10 ⁻²⁹	C	6.6524587321600 ·10 ⁻²⁹	9.1·10 ⁻¹⁰	-1.09299·10 ⁻⁹	m ²
a _e	ae	1.159652181281556·10 ⁻³	C	1.1596521812818 ·10 ⁻³	1.5·10 ⁻¹⁰	-2.10054·10 ⁻¹³	1
g _e	ge	-2.00231930436256	C	-2.00231930436256	1.7·10 ⁻¹³	-2.22045·10 ⁻¹⁶	1
γ _e	γe	1.760859630228709·10 ¹¹	C	1.7608596302353 ·10 ¹¹	3.0·10 ⁻¹⁰	-3.74278·10 ⁻¹²	s ⁻¹ T ⁻¹
μ _e	μe	-9.28476469866128·10 ⁻²⁴	C	-9.284764704328 ·10 ⁻²⁴	3.0·10 ⁻¹⁰	-6.10325·10 ⁻¹⁰	JT ⁻¹
μ _B	μB	-9.27401007265130·10 ⁻²⁴	C	-9.274010078328 ·10 ⁻²⁴	3.0·10 ⁻¹⁰	-6.12109·10 ⁻¹⁰	JT ⁻¹
μ _N	μN	5.050783742986264·10 ⁻²⁷	C	5.0507837461150 ·10 ⁻²⁷	3.1·10 ⁻¹⁰	-6.19456·10 ⁻¹⁰	JT ⁻¹
Φ ₀	φ0	2.067833847194937·10 ⁻¹⁵	C	2.067833848 ·10 ⁻¹⁵	exactly	-3.89327·10 ⁻¹⁰	Wb
G ₀	GQ0	7.748091734611053·10 ⁻⁵	C	7.748091729000002·10 ⁻⁵	exactly	+7.24185·10 ⁻¹⁰	S
K _J	KJ	4.835978487132911·10 ¹⁴	C	4.835978484 ·10 ¹⁴	exactly	+6.47834·10 ⁻¹⁰	HzV ⁻¹
R _K	RK	2.581280744348851·10 ⁴	C	2.581280745 ·10 ⁴	exactly	-2.52258·10 ⁻¹⁰	Ω
α	alpha	7.297352569776440·10 ⁻³	F	7.297352569311 ·10 ⁻³	1.5·10 ⁻¹⁰	+6.37821·10 ⁻¹¹	1
δ	delta	9.378551014802563·10 ⁻¹	F	9.378551009654370·10 ⁻¹	1.5·10 ⁻¹⁰	+5.48932·10 ⁻¹⁰	1
χ	xtilde	2.821439372122070`	F	2.821439372	exactly	exactly	1
σ	σ	5.670366673885495·10 ⁻⁸	C	5.670366673885496·10 ⁻⁸	exactly	exactly	Wm ⁻² K ⁻⁴

S Subspace value (const) M Magic value MachinePrecision → ±2.22045·10⁻¹⁶
F Fixed value (invariable) C Calculated (calculated)

Table 3:
Concerted International
System of Units

9. Definition of basic constants and functions

Declarations

```
Off[General::spell]
Off[General::spell1]
Off[InterpolatingFunction::dmval]
Off[FindMaximum::lstol]
Off[FindRoot::nlnum]
```

Units

```
km = 1000;
pc = 3.08572*10^16;
Mpc = 3.08572*10^19 km;
minute = 60;
hour = 60 minute;
day = 24*hour;
year = 365.24219879*day;
Mo = 1.98840*10^30 (*Sun mass kg*);
Ro = 6.96342*10^8 (*Sun radius m*);
ME = 5.9722*10^24 (*Earth mass kg*);
RE = 6.371000785*10^6 (*Earth radius m*);
F0 = 2.51*10^-8 (*Zero flux brightness Wm^-2*);
L0 = 3.09*10^28 (*Zero luminosity W*);
L1a= 6.40949*10^35 (*Standard candle SNIa W*);
```

Basic Values

```
c=2.99792458*10^8; (*Speed of light*);
my0=4 Pi 10^-7; (*Permeability of vacuum*);
ka0=1.3697776631902217*10^93; (*Conductivity of vacuum*);
hb1=8.795625796565464*10^26; (*Planck constant slashed init*);
k=1.3806485279*10^-23; (*Boltzmann constant*);
me=9.109383701528*10^-31; (*Electron rest mass with Q0 Magic value 1*);
mp=1.6726219236951*10^-27; (*Proton rest mass Magic value 2*);
```

Auxilliary Values

```
mep=SetPrecision[me/mp,20]; (*Mass ratio e/p*);
ma=1822.8884862171988 me; (*Atomic mass unit*);
ϵ=ArcSin[0.3028221208819742993334500624769134447]-3Pi/4; (*RnB angle ϵ null(fix)*);
γ=Pi/4-ϵ; (*RnB angle γ nullvector*);
ζ=1/(36Pi^3) (3Sqrt[2])^(-1/3)/mep; (*re-correction factor*);
xtilde=xtilde=3+N[ProductLog[-3E^-3]]; (*Wien displacement law constant (v)*);
alpha=Sin[Pi/4-\[Epsilon]]^2/(4Pi); (*Correction factor QED \[Alpha](Q0)*);
delta=4Pi/alpha*mep; (*Correction factor QED \[Delta](Q0)*);
(*Q0=(9Pi^2 Sqrt[2]delta me/my0/ka0/hb0SI)^(-3/4) (*Phase Q0=2ω0t during calibration*);*)
Q0=(9 Pi^2 Sqrt[2]delta me/my0/ka0/hb1)^(-3/7); (*Phase Q0=2ω0t after calibration*);
```

Composed Expressions

```
Z0=my0 c; (*Field wave impedance of vacuum*);
ep0=1/(my0 c^2) (* Permittivity of vacuum*);
R∞=1/(72 Pi^3)/r1 Sqrt[2] alpha^2 /delta Q0^(-4/3); (*Rydberg constant*);
Om1=ka0/ep0; (*Cutoff frequency of subspace*);
Om0=Om1/Q0; (*Planck's frequency*);
OmR∞=2 Pi c R∞; (*Rydberg angular frequency*);
cR∞=c R∞; (*Rydberg frequency*);
H0=Om1/Q0^2; (*Hubble parameter local*);
H1=3/2*H0; (*Hubble parameter whole universe*);
r1=1/(ka0 Z0); (*Planck's length subspace*);
a0=9Pi^2 r1 Sqrt[2] delta/alpha Q0^(4/3); (*Bohr radius*);
ΛbarC=a0 alpha; (*Reduced Compton wavelength*);
ΛC=2 Pi ΛbarC; (*Compton wavelength electron*);
re= r1 (2/3)^(1/3)/ζ Q0^(4/3); (*Classic electron radius*);
r0= r1 Q0; (*Planck's length vac*);
R= r1 Q0^2; (*World radius*);
RR=R/Mpc/1000; (*World radius Gpc*);
```

```

t1=1/(2 Om1); (*Planck time subspace*);
t0=1/(2 Om0); (*Planck time vacuum*);
T=1/(2 H0); (*World time constant*);
TT=2T/year; (*The Age*);
hb0=hb1/Q0; (*Planck constant slashed*);
h0=2Pi*hb0; (*Planck constant unslashed*);
q1=Sqrt[hb1/Z0]; (*Universe charge*);
q0=Sqrt[hb1/Q0/Z0]; (*or qe/Sin[pi/4-ε] Planck charge*);
qe=q0 Sin[Pi/4-ε]; (*Elementary charge e*);
M2=my0 ka0 hb1; (*Total mass with Q=1*);
M1=M2/Q0; (*Mach mass*);
m0=M2/Q0^2; (*Planck mass downwardly*);
(*m0=(9Pi^2Sqrt[2]*delta*me)^.75*(my0*ka0*hb0SI)^.25; (*Planck mass upwardly*);*)
mp=4Pi me/alpha/delta; (*Proton rest mass with Q0*);
(*me=Sqrt[hb1/Q0/Z0]*Sin[Pi/4-ε]; (*if using Q0 as Magic value*);*)
MH=M2/Q0^3; (*Hubble mass*);
G0=c^2*r0/m0; (*hb0*c/m0^2*); (*Gravity constant local*);
G1=G0/Q0^2; (*Gravity constant Mach*);
G2=G0/Q0^3; (*Gravity constant Init*);
U0=Sqrt[c^4/4/Pi/ep0/G0]; (*Planck voltage generic*);
U1=U0*Q0; (*Planck voltage Mach*);
W1=Sqrt[hb1 c^5/G2]; (*Energy with Q=1*);
W0=W1/Q0^2; (*Planck energy*);
S1=hb1 Om1^2/r1^2; (*Poynting vector metric with Q=1*);
S0=S1/Q0^5; (*Poynting vector metric actual*);
Sk1=4Pi^2*E^2/18^4/60*hb1*Om1^2/r1^2; (*Poyntingvec CMBR initial*);
Sk0=Sk1/Q0^4/Q0^3/E^2; (*Poyntingvec CMBR actual*);
wk1=Sk1/c; (*Energy density CMBR initial*);
wk0=Sk0/c; (*Energy density CMBR actual*);
Wk1=wk1*r1^3; (*Energy CMBR initial*);
μB=-9/2Pi^2 Sqrt[2 hb1/Z0]delta Sin[γ]/my0/ka0 Q0^(5/6); (*Bohr magneton*);
μN=-μB*mep; (*Nuclear magneton*);
μe=1.0011596521812818 μB (*Electron magnetic moment*);
Tk1=hb1 Om1/18/k; (*CMBR-temperature Q=1*);
Tk0=Tk1/Q0^(5/2); (*CMBR-temperature*);
Tp0=Sqrt[hb0 c^5/G0]/k; Tp1=Tp0*Q0; Tp2=Tp0*Q0^2; (*Planck-temperature*);
ϕ0=Pi Sqrt[hb1 Z0/Q0 ]/Sin[Pi/4-ε]; (*Magnetic flux quantum Pi h/e*);
GQ0=1/Pi/Z0*Sin[Pi/4-ε]^2; (*Conductance quantum e^2/Pi h*);
KJ=2q0 Sin[Pi/4-ε]/h0; (*Josephson constant 2e/h*);
RK=.5 my0 c/alpha; (*von Klitzing constant μ0c/2α*);
oe=8Pi/3 re^2; (*Thomson cross section (8Pi/3)re^2*);
ae=SetPrecision[μe/μB,20]-1; (*Electron magnetic moment anomaly*);
ge=-2(1+ae); (*electron g-factor*);
ye=2 Q0 Abs[μe]/hb1; (*electron gyromagnetic ratio*);
σ1=SetPrecision[Pi^2/60 k^4/c^2/hb1^3, 16]; (*Stefan-Boltzmann constant initial*);
σ=σ1*Q0^3; (*Stefan-Boltzmann constant*);

```

Basic Functions

```

cMc=Function[-2 I/#/Sqrt[1-(HankelH1[2,#]/HankelH1[0,#])^2]];
Qr=Function[#1/Q0/2/#2];
PhiQ=Function[If[#>10^4,-Pi/4-3/4/#,
Arg[1/Sqrt[1-(HankelH1[2,#]/HankelH1[0,#])^2]]-Pi/2]]; (*Angle of c arg θ(Q)*);
PhiR=Function[PhiQ[Qr[#1,#2]]];
RhoQ=Function[If[#<10^4,N[2/#/Abs[Sqrt[1-
(HankelH1[2,#]/HankelH1[0,#])^2]]],1/Sqrt[#]];
RhoR=Function[RhoQ[Qr[#1,#2]]];
AlphaQ=Function[Pi/4-PhiQ[#]]; (*Angle α*);
AlphaR=Function[N[Pi/4-PhiR[#1,#2]]];
BetaQ=Function[Sqrt[#1]*((#2)^2+#1^2*(1-(#2)^2)^2)^(-.25)];
GammaPQ=Function[N[PhiQ[#]+ArcCos[RhoQ[#]*Sin[AlphaQ[#]]]+Pi/4]];
HPC=Function[Om1/#^2/km*Mpc]; (*H0=f(Q0) [km*s-1*Mpc-1]*);
rq={0,0};
For[x=-8;i=0,x<4,++i,x+=.01;AppendTo[rq,{10^x,N[10^x*RhoQ[10^x]]}]];
RhoQ1=Interpolation[rq];
RhoQQ1=Function[If[#<10^3,RhoQ1[#],Sqrt[#]]]; (*Interpolation RhoQ*);
Rk=Function[If[#<10^5,3/2*Sqrt[#]*NIntegrate[RhoQQ1[x],{x,0,#}],6#]];
Rn=Function[Abs[3/2*Sqrt[#]*NIntegrate[RhoQQ1[x]*Exp[I*(PhiQ[x])],{x,0,#}]]];
RnB=Function[Arg[NIntegrate[RhoQQ1[x]*Exp[I*(PhiQ[x])],{x,0,#}]]];
alphaF=Function[Sin[Pi/2+ε-(*RNBP*)RnB[#]]^2/(4Pi)]; (*RNBP def further below*);
deltaF=Function[4Pi/alphaF[#]*mep]; (*Correction factor QED ΔQ*);

```

End of Metric System Definition

```
rnb={"Insert output from below"};
rn={};
For[d=-6.01; i=0,d<6.01, (++i), d+=.05; AppendTo[rn, {d, RnB[10^d]/Pi}]]
RNB1=Interpolation[rnb]; (*RnB angle ε nullvector from Q*)
RNB=Function[If[#<10^-8, Null, If[#<10^6, RNB1[Log10[#]], -.25]]];
RNBP=Function[If[#<10^-8, Null, If[#<10^6, Pi RNB1[Log10[#]], -Pi/4]]];
alphaF=Function[Sin[Pi/2+ε-RNBP[#]]^2/(4Pi)]; (*Redfinition for faster calculation*);
```

```
rs={"Insert output from below"};
rs={};
For[x=(-3); i=0,x<3, (++i), x+=.025;
AppendTo[rs, {10^x, NIntegrate[RhoQQ1[z], {z, 0, 10^x}]/Abs[NIntegrate[RhoQQ1[z]*
Exp[I/2*ArgThetaQ[z]], {z, 0, 10^x}]]]}];
rs
RS=Interpolation[rs]; (*Relation rk/rn*);
RS1=Function[1/RS[#]];
```

```
qq1={"Insert output from below"};
qq1={};
For[xy=(-17); i=0,xy<5, (++i), xy+=.05; AppendTo[qq1, {10^xy, N[Sin[(Pi/2-
RnB[10^xy]+ε)]]}]]];
qq1
QQ0=Interpolation[qq1]; (*Relation qe/q0*);
QQ=Function[If[#<10^5, QQ0[#], 0.3028223504900885]]];
QQ1=Function[If[#<10^5, 1/QQ0[#], 3.3022661582990733]]];
```

```
inb={"Insert output from below"};
inb={};
For[d=-6.01; i=0,d<6.01, (++i), d+=.05; AppendTo[inb, {RnB[10^d]/Pi, d}]]];
inb
INB1=Interpolation[inb]; (*InvRnB Q from angle ε nullvector*);
INB=Function[Which[-1<#<0, INB1[#], #==0, 3/2Pi Q0^.25, #>0, Null]]];
INBP=Function[Which[-Pi<#<0, INB1[#/Pi], #==0, 3/2 Q0^.25, #>0, Null]]];
```

End of Optional Metric System Definition

Functions Used for Calculations in Articles

```
P0= H0; (* or e.g. 65*1000/Mpc *);
P1=SetPrecision[-2.5Log10[P0^2/c^2L1a/Pi/F0]-0.4515449878350246, 30];
P2=SetPrecision[1.25Log10[E], 30]; (* -2.5(-1/2*Log10[E]) *)
Hm0 = (0.5+0.598206 # - 3.45991 #^2 + 18.3227 #^3 - 42.6995 #^4 + 38.0733 #^5) &;
Mby=Function[P1+5Log10[((#+1)^(4/3)-1)]];
Mbz=Function[P1+5Log10[((#+1)^(4/3)-1)]+P2((#+1)^(4/3)-1)];
Mby=Function[P1+5Log10[2# P0/c]];
MbQ=Function[P1+5Log10[2#]];
Mbr=Function[P1+5Log10[2# P0/c]+P2*2# P0/c];
Mbr=Function[P1+5Log10[2#]+P2*2# ];
MbX=Function[P1+2#+5Log10[2#]+1.5Log10[Hm0[2#]]];
MaG=Function[10^(-0.4 #)];
GaM=Function[-2.5 Log10[#]];
TpSQ = M2*(c^2/k/#1^2) &;
TpST = hb1/2/k/#1 &;
TkSQ = hb1*(Om1/18/k/#1^2.5) &;
TkST = hb1*Om1*(t1^1.25/18/k/#1^1.25) &;
```

Your own Calculations...

References

1. Treder, H. J. (Ed.). (1979). *Gravitationstheorie und Theorie der Elementarteilchen: Wiederabdruck ausgewählter Beiträge des Einstein-Symposiums 1965 in Berlin*. Akademie-Verlag.
2. Georg Dautcourt. (1972). Relativistische Astrophysik.
3. Michail Wolkenstein. (1990). Entropie und Information.
4. Gernot Neugebauer. (1980). Relativistische Thermodynamik.
5. Brockhaus ABC Physik. (1972). *F.A. Brockhaus-Verlag Leipzig*.
6. Braginski, Polnarjow. (1989). Der Schwerkraft auf der Spur, *BSB B.G. Teubner Verlagsgesellschaft Leipzig*.
7. Spiering, C. (1986). *Auf der Suche nach der Urkraft*. Deutsch.
8. I.D. Nowikow. (1982). Evolution des Universums, *BSB B.G. Teubner Verlagsgesellschaft Leipzig*.
9. Felix Klein. (1933). Vorlesungen über die hypergeometrische Funktion, Berlin.
10. W. Maak, Fastperiodische Funktionen, Die Grundlehren der mathematischen Wissenschaften in Einzeldarstellungen Bd. 61 *Springer-Verlag*.
11. Srivastava, H. M., & Karlsson, P. W. (1985). Multiple Gaussian hypergeometric series. *Halsted Press Chichester*.
12. Harold Exton. (1983). q Hypergeometric Functions and Applications, *Chichester*.
13. Exton, H. (1978). Handbook of hypergeometric integrals: theory, applications, tables, computer programs.
14. Exton, H. (1976). Multiple hypergeometric functions and applications.
15. Mathai, A. M., Saxena, R. K. (1976). Generalized Hypergeometric Functions with Applications in Statistics & Physical Sciences.
16. Wilhelm Maak. (1971). Zur hypergeometrischen Differentialgleichung über Banachalgebren, *Seminarbericht 30 (Burmam) Göttingen*. Reading room of the Mathematical Faculty UNI Göttingen
17. Slater, L. J. (1966). Generalized hypergeometric functions.
18. Felix Klein. (1894). Über die hypergeometrische Funktion, *Göttingen*. Reading room of the Mathematical Faculty UNI Göttingen.
19. Buchholz, H. (2013). *Die Konfluente Hypergeometrische Funktion: Mit Besonderer Berücksichtigung ihrer Anwendung*. Springer-Verlag.
20. Lectoral Notes. Theoretical Electrotechnics. Ingenieurhochschule für Seefahrt (Hochschule für Seefahrt) Warnemünde/Wustrow.
21. Bartsch, H. J. (1977). Mathematische Formeln Fachbuchverlag Leipzig, 16.
22. Bronstein, I. N., & Semendjajew, K. A. (1979). Taschenbuch der Mathematik, BSB BG.
23. Sieber, Sebastian. (1977). Spezielle Funktionen, Mathematik für Ingenieure, Naturwissenschaftler, Ökonomen und Landwirte, Band 12 *BSB B. G. Teubner Verlagsgesellschaft, Leipzig*.
24. Weller, Winkler. (1979). Elektrodynamik, Mathematisch-Naturwissenschaftliche Bibliothek, Band 69, *BSB B.G. Teubner Verlagsgesellschaft Leipzig*.
25. Lectoral notes. Analog Systems. Ingenieurhochschule für Seefahrt (Hochschule für Seefahrt) Warnemünde/Wustrow.
26. Prof. Dr. sc. techn. Dr. techn. h.c. Eugen Philippow. (1977). TH Ilmenau Taschenbuch der Elektrotechnik, Band 2, Grundlagen der Informationstechnik *Verlag Technik Berlin*.
27. Weißmantel, C., et al. (1970). Hrsg. Kleine Enzyklopädie Atom Struktur der Materie *VEB Bibliographisches Institut Leipzig, 1. Auflage*.
28. Danos, M., & Rafelski, J. (1984). Pocketbook of mathematical functions.

-
29. Pommerenke, G. (2023). *The Metric Universe*, 2nd edition Augsburg.
 30. d’Inverno, R. (1995). *Einführung in die Relativitätstheorie*, VCH mbH.
 31. Amoroso, R. L., Hunter, G., Kafatos, M., & Vigier, J. P. (Eds.). (2002). *Gravitation and cosmology: from the Hubble radius to the Planck scale: proceedings of a symposium in honour of the 80th birthday of Jean-Pierre Vigier* (Vol. 126). Springer Science & Business Media.
 32. v. Borzeszkowski, H. H., Einstein, R. W. (1982). Laboratorium für Theoretische Physik der AdW der DDR, Potsdam Eddingtons Zahlen und die Einheit der physikalischen Welt *Wissenschaft und Fortschritt Heft*.
 33. Eddington, A. S. (1923). *Raum, Zeit und Schwere*, Ein Umriß der allgemeinen Relativitätstheorie; übers. u. hrsg. von W.
 34. Eddington, A. S. (1935). *Naturwissenschaft auf neuen Bahnen*; übers. u. hrsg. v. W. Westphal, Braunschweig.
 35. Eddington, A. S. (1949). *Philosophie der Naturwissenschaft*; Bern.
 36. Eddington, A. S. (1948). *Fundamental Theory*; Cambridge.
 37. Dirac, P. A. M. (1937). The Cosmological Constants, *Nature*, 139, S. 32.
 38. Treder, H. J. (1981). Eddingtons Zahlen, Einsteins Kriterium und Rydbergs rationelles Dimensionssystem. *Astronomische Nachrichten*, 302(3), 115-125.
 39. Assis, A. K., & Neves, M. C. (1995). History of the 2.7 K temperature prior to Penzias and Wilson. *Apeiron*, 2(3), 79-84.
 40. Amoroso, R. L., Hunter, G., Kafatos, M., & Vigier, J. P. (Eds.). (2002). *Gravitation and cosmology: from the Hubble radius to the Planck scale: proceedings of a symposium in honour of the 80th birthday of Jean-Pierre Vigier* (Vol. 126). Springer Science & Business Media.
 - 40.1. Sisirroy, Datta, S. Physics & Applied Mathematics Unit, Indian Statistical Institute, Calcutta 700035, India, sisir@isical.ac.in, res9428@isical.ac.in published in 40. Multiple scattering theory in Wolf’s mechanism and implications in QSO redshift.
 41. Marti, O. (2015). Institut für Experimentelle Physik Universität Ulm.
 42. Marcus Herrmann. RWTH Aachen Promotionsvortrag (lecture of graduation).
 43. Thomas Hebbeker, RWTH Aachen Die Entwicklung des Universums.
 44. Hüttemeister, S. Ruhr-Uni Bochum (3) Meßgrößen: Helligkeiten, Farben, Temperaturen Abstract: Wir blicken zum Himmel und sehen Sterne:.. Was unterscheidet sie? Helligkeit und Farbe.
 45. Saul Perlmutter, et al. (2023). High Redshift Supernova Search, Home Page of the Supernova Cosmology Project. Lawrence Berkeley Laboratory 50-232, University of California, Berkeley, CA 94720.
 46. Pommerenke, G. Is the Course of the Planck’s Radiation-Function the Result of the Existence of an Upper Cut-Off Frequency of the Vacuum?.
 47. Seite, Grauer Körper, G. (2018). In: Wikipedia, Die freie Enzyklopädie. Bearbeitungsstand.
 48. [Wegener, T. \(2021\). Symmetry, Crystal Systems and Bravais Lattices Bearbeitungsstand.](#)
 49. Pommerenke, G. (2023). The Electron and Weak Points of the Metric System.
 50. Zollner, M. (2017). Negative Laufzeit–gibt’s die wirklich?.
 51. [Hornung, H. \(2019\). A solar eclipse illuminates physics.](#)
 52. Pommerenke, G. Expansion, Topology and Entropy.

-
53. Huntemann, N., Lipphardt, B., Tamm, C., Gerginov, V., Weyers, S., & Peik, E. (2014). Improved limit on a temporal variation of mp/me from comparisons of Yb⁺ and Cs atomic clocks. *Physical review letters*, 113(21), 210802.
 54. Unzicker, A. (2012). Auf dem Holzweg durchs Universum. *Warum sich die Physik verlaufen hat*. München: Hanser.
 55. Seite. (2021). Planck-Einheiten. In: Wikipedia – Die freie Enzyklopädie. Bearbeitungsstand.
 56. Seite. (2021). Raketengrundgleichung“. In: Wikipedia – Die freie Enzyklopädie. Bearbeitungsstand.
 57. Bislin, W. (2021). Grenzen einer Reise mit Antimaterie-Photonen-Antrieb Bearbeitungsstand.
 58. Einstein, A. (1905). Zur elektrodynamik bewegter körper. *Annalen der physik*, 17(10), 891-921.
 59. [Wikipedia contributors. Cosmic microwave background. Wikipedia. The Free Encyclopedia.](#)
 60. [Seite. \(2021\). Compton-Effekt“. In: Wikipedia – Die freie Enzyklopädie. Bearbeitungsstand.](#)
 61. [Seite. \(2021\). Rydberg-Konstante. In: Wikipedia – Die freie Enzyklopädie. Bearbeitungsstand. Seite, Bohrsches.](#)
 62. [Magnetron. \(2021\). In: Wikipedia – Die freie Enzyklopädie. Bearbeitungsstand.](#)
 63. [Fundamental Physical Constants — Extensive Listing.](#)
 64. [Seite. \(2022\). Apsidendrehung. In: Wikipedia – Die freie Enzyklopädie. Bearbeitungsstand](#)
 65. [Cosmic microwave background. Wikipedia.](#)
 66. [Seite. \(2022\). Plancksches Strahlungsgesetz. In: Wikipedia – Die freie Enzyklopädie. Bearbeitungsstand.](#)
 67. [Seite. \(2022\). Wiensches Verschiebungsgesetz. In: Wikipedia – Die freie Enzyklopädie. Bearbeitungsstand.](#)
 68. [tec-science. Different forms of Planck’s law.](#)
 69. [Seite. \(2023\). Logische Fehlschlüsse. Portal Wissenschaftliches Schreiben“.Bearbeitungsstand.](#)
 70. [Seite. \(2022\). Ex falso quodlibet“. In: Wikipedia – Die freie Enzyklopädie. Bearbeitungsstand.](#)
 71. [Seite. \(2024\). Rotverschiebung. In: Wikipedia – Die freie Enzyklopädie. Bearbeitungsstand.](#)
 72. [Seite. \(2022\). Supernova Cosmology Project“. In: Wikipedia – Die freie Enzyklopädie. Bearbeitungsstand.](#)
 73. [Seite. \(2022\). High-Z Supernova Search Team“. In: Wikipedia – Die freie Enzyklopädie. Bearbeitungsstand.](#)
 74. [Seite. \(2023\). Supernova vom Typ Ia. In: Wikipedia – Die freie Enzyklopädie. Bearbeitungsstand.](#)
 75. Pommerenke, G. (2021). The Shape of the Universe, Augsburg. 6th revised edition, please update older editions + Corrigendum.
 76. [User Geek3: File. \(2010\). VFpt charges plus minus.svg“. In: Wikimedia Commons, Processing status. Image file was reworked and supplemented according to Creative Commons Attribution-Share Alike 3.0 Unported license©.](#)
 77. [Seite. \(2023\). Absolute Helligkeit. In: Wikipedia – Die freie Enzyklopädie. Bearbeitungsstand.](#)
 78. [Suite. \(2022\). Extinction \(Astronomy\). In: Wikipedia – Die free Enzyklopädie. Bearbeitungsstand.](#)